

Can Curcumin improve the Methotrexate based treatment for Rheumatoid Arthritis?

By

Ashish Sahadev Darekar

A thesis submitted at the University of Central Lancashire in partial
fulfilment of the requirements for the degree of Doctor of Philosophy.

November 2016

DECLARATION

I declare that while registered as a candidate for the research degree, I have not been a registered candidate or enrolled student for another award of the University or other academic or professional institution. I declare that no material contained in the thesis has been used in any other submission for an academic award and is solely my own work

Signed

Ashish S Darekar

Type of Award Doctor of Philosophy (PhD)

School Pharmacy and Biomedical Sciences

ABSTRACT

Rheumatoid arthritis (RA) is an autoimmune disorder characterised by its varied and unpredictable origin, eventual destruction of cartilage and bone and the perpetual length of treatment involved. Even though significant developments have taken place over the past couple of decades in the treatment, the efficacy of drugs for RA is a major concern due to the side effects involved. Methotrexate (MTX) is currently used as first line treatment due to its ability to modify the rheumatic conditions so that disease progression can be prevented. However, at the same time prolonged exposure to MTX can lead to severe side effects such as lung fibrosis and hepatotoxicity. Recent research has focused on developing an alternative to MTX with similar efficacy but with reduced adverse effects. One such promising option is curcumin, an active compound extracted from Indian spice Turmeric. Various studies have indicated the synergistic properties exhibited by curcumin and its ability to modulate the underlying inflammatory pathways involved in RA. However, no previous studies have been reported with regards to using a combination of MTX and curcumin for the treatment of RA. A novel RP-HPLC stability indicating method was developed in order to establish the compatibility of the two compounds. The method was developed using Waters Reverse Phase (XBridge™ Shield RP18 4.6x250 mm, 5 µM) column. A gradient system, consisting of two mobile phases with acetonitrile concentrations of 35% and 60% respectively, was designed to optimise the separation of the two compounds while taking into consideration the difference in hydrophobicity. The wavelengths for detection were 305 nm and 430 nm for MTX and curcumin, respectively. The retention time for MTX and curcumin was 4.8 ± 0.10 min and 12.3 ± 0.10 min, respectively. The

total run time of analysis was 25 minutes. The developed method was validated for parameters such as accuracy, precision, linearity, limit of detection and lower limit of quantification. The system was tested through intraday and interday repeatability and reproducibility. The method was used to analyse the MTX and curcumin under different stress conditions such as pH, UV radiation, temperature and humidity to establish their compatibility. The degradation products are successfully separated and therefore, the method can be effectively used as stability indicating method.

Gene expression profiling was performed using HFLS-RA cells treated with MTX and curcumin separately and concurrently. The DNA microarray data identified 53 genes that were downregulated and 21 genes that were upregulated in all the treated samples using both stringent and non-stringent filtering. The total of 13 genes were selected based on the fold change obtained in the microarray data and their potential as therapeutic biomarkers based on previous research. The gene validation using qRT-PCR confirmed the higher efficacy of curcumin in the inhibition of the pro-inflammatory genes such as *ANGPTL7*, *CD248*, *CH25H*, *COL14A1*, *CXCL12*, *CYTL1*, *IFITM1* and *IL7*. Curcumin was found to also increase the expression levels of genes associated with anti-inflammatory roles, namely *BCAR4*, *CD274*, *HSPA6*, *OTP* and *RELT*. The increased gene expression in samples treated with both MTX and curcumin confirmed the possible synergistic activity which is encouraging, taking in to account the fact that these compounds are compatible according to the stability studies carried out and thus could be used in combination for the treatment of RA. This could improve the current treatment by reducing the severity of side-effects attributed to MTX while maintaining the efficacy of the treatment due to the ability of curcumin to modulate specific therapeutic biomarkers involved in the RA pathogenesis.

TABLE OF CONTENTS

DECLARATION.....	2
ABSTRACT.....	3
TABLE OF CONTENTS.....	5
LIST OF FIGURES.....	10
LIST OF TABLES.....	12
ACKNOWLEDGEMENTS.....	15
ABBREVIATIONS.....	16
CHAPTER 1 INTRODUCTION.....	27
1.1. Rheumatoid arthritis.....	28
1.2. Risk factors for rheumatoid arthritis.....	28
1.3. Pathophysiology of RA.....	29
1.3.1. Effector cells involved in the pathogenesis of RA.....	31
1.3.2. Cytokines and the impact on effector cells.....	32
1.3.3. Role of IL6 signalling in RA pathophysiology.....	32
1.3.4. Role of cytokines in RA bone and cartilage degeneration.....	33
1.3.5. Acute-phase protein production.....	34
1.4. Treatment for Rheumatoid Arthritis.....	35
1.4.1. Non-Steroidal Anti-Inflammatory Drugs (NSAIDs).....	35
1.4.2. Disease-Modifying Anti-Rheumatic Drugs (DMARDs).....	36

1.5.	Methotrexate (MTX).....	38
1.5.1.	Mechanism of action.....	39
1.5.2.	Inhibiting NF- κ B activation in RA.....	40
1.5.3.	Side effects.....	42
1.6.	Curcumin	45
1.6.1.	Effects on the NF- κ B Pathway.....	46
1.6.2.	Induction of Apoptotic Signalling Cascade.....	47
1.7.	Efficacy and synergistic activity of concurrent MTX –Curcumin treatment	48
1.7.1.	Cardiovascular disorders in RA	48
1.7.2.	Hepatotoxicity.....	49
1.7.3.	Nephrotoxicity.....	49
1.7.4.	Increased activity in folate receptors.....	49
1.8.	Simultaneous stability analysis of MTX and curcumin	50
1.8.1.	High-Performance Liquid Chromatography (HPLC)	50
1.8.2.	Forced degradation and validated Stability-indicating method	52
1.9.	Comparative analysis of the mechanisms of actions of both MTX and curcumin.....	54
1.9.1.	DNA microarray.....	54
1.9.2.	Data analysis	54
1.10.	AIM OF THE RESEARCH	56
CHAPTER 2	MATERIALS AND METHODS	58

2.1.	HPLC analysis	59
2.1.1.	Chemicals and materials	59
2.1.1.	Standard solutions	59
2.1.2.	Preparation of the mobile phase	59
2.1.3.	Apparatus and chromatographic conditions	59
2.1.4.	Analytical method validation	62
2.1.5.	Forced degradation studies	63
2.2.	Cell culture.....	65
2.2.1.	Resuscitation of the cells	67
2.2.2.	Subculture and cell library maintenance	67
2.2.3.	Quantification of cells using haemocytometer.....	68
2.2.4.	Cell viability assay.....	70
2.3.	Gene expression analysis	71
2.3.1.	Drug treatment for microarray analysis	71
2.3.2.	Total RNA isolation.....	71
2.3.3.	Determination of RNA concentration and Purity	72
2.3.4.	RNA integrity control	72
2.3.5.	Preparation of Cyanine-3 labelled cRNA.....	74
2.3.6.	Quantification and quality control of labelled cRNA samples.....	77
2.3.7.	Microarray hybridisation.....	78
2.3.8.	Bioinformatics data analysis	80

2.3.9.	Statistical analysis of microarray data	81
2.4.	Gene transcription technique	82
2.4.1.	The mRNA isolation.....	82
2.4.2.	The mRNA Quantification using NanoDrop spectrometer	85
2.4.3.	Complimentary DNA (cDNA) synthesis	86
2.4.4.	Gene sequence and Primer design	88
2.4.5.	Primer preparation.....	88
2.4.6.	Quantitative real time polymerase chain reaction (qRT-PCR).....	91
2.4.7.	Copy Number Quantification	94
2.4.8.	Analysis of RT-PCR amplicons using agarose gel electrophoresis	98
2.5.	Quantitation of IL6 protein.....	99
2.5.1.	Assay principle.....	99
CHAPTER 3	RESULTS.....	101
3.1.	RP-HPLC stability indicating studies	102
3.1.1.	Analytical Method Validation	102
3.1.2.	Forced Degradation Studies.....	105
3.2.	Inhibitory concentration (IC ₅₀) of MTX and curcumin in HFLS-RA	115
3.3.	Gene Expression Profiling.....	117
3.3.1.	Total RNA concentration, purity and integrity.....	117
3.3.2.	Quantification and quality control of labeled cRNA	120
3.3.3.	Microarray quality control	121

3.3.4.	Effects of Quantile normalisation	121
3.3.5.	Correlation analysis.....	122
3.3.6.	Differential gene expression	125
3.3.7.	Analysis and validation of expression of significantly regulated Genes .	134
3.4.	Interleukin-6 (IL6) Activity	138
CHAPTER 4	DISCUSSION	139
CHAPTER 5	CONCLUSION AND FUTURE WORK	159
5.1.	Conclusion	160
5.2.	Future work	161
CHAPTER 6	REFERENCES	162
CHAPTER 7	APPENDIX	186

LIST OF FIGURES

Figure 1-1 Pathophysiology of RA.....	30
Figure 1-2 Chemical structure of folic acid and its structural analogue Methotrexate.	39
Figure 1-3 Molecular structure of Curcumin.	45
Figure 2-1 Pictorial representation of the gradient system used for degradation analysis of Curcumin and Methotrexate.	61
Figure 2-2 Diagram showing haemocytometer grid under microscope.	69
Figure 2-3 Schematic representation of the isolation of total RNA.	72
Figure 2-4 Typical electropherograms representing eukaryotic total RNA degradation analysed on 2100 Bioanalyzer.	74
Figure 2-5 Schematic representation cRNA amplification procedure.	76
Figure 2-6 Example electropherograms of cyanine-3 cRNA analysed on 2100 Bioanalyzer.....	77
Figure 2-7 Workflow of sample preparation and microarray processing.....	79
Figure 2-8 Experimental protocol for the mRNA isolation technique.....	83
Figure 2-9 Standard to calculate the copy number of the targeted gene.	97
Figure 3-1 Chromatograms showing elution of 50 µg/ml MTX (at 305 nm) and 50 µg/ml Curcumin (at 430 nm) under different conditions.....	105
Figure 3-2 Possible degradation products of MTX.....	113
Figure 3-3 Possible degradation products of curcumin.....	114
Figure 3-4 Dose-dependent inhibitory effects on cell viability employing different concentrations (0 – 0.1µM) of MTX on HFLS-RA cells.....	115

Figure 3-5 Dose-dependent inhibitory effects on cell viability employing different concentrations (0 – 25µM) of curcumin on HFLS-RA cells.....	116
Figure 3-6 Original electrophoresis gel for assessing RNA integrity.	118
Figure 3-7 Original chart recordings showing electropherograms for RNA integrity in HFLS-RA cells	119
Figure 3-8 BoxWhisker plot after quantile normalisation.....	121
Figure 3-9 Bar charts showing Gene transcription levels of selected genes.....	137
Figure 7-1 Agarose gel electrophoresis of validated 13 genes.	192

LIST OF TABLES

Table 2-1 Reagents and supplements used for cell lines.....	66
Table 2-2 Reagents and buffers used for mRNA isolation.....	84
Table 2-3 Volumes of reagents and buffer used for mRNA isolation of 2×10^6 cells. .	84
Table 2-4 Reagents used in first strand cDNA synthesis for one sample.	87
Table 2-5 Primer design parameters.....	88
Table 2-6 Primer sequence, annealing temperatures and amplicon size for all the 13 genes used in qRT-PCR.....	89
Table 2-7 Components required for LightCycler® FastStart DNA Master PLUS SYBR Green I kit sample preparation for qRT-PCR primer mastermix.....	92
Table 2-8 Applied Biosystems 7500 Real Time PCR system thermal profile for qRT-PCR	93
Table 2-9 Genomic DNA correspondence to its average Ct values and equivalent copy number.	96
Table 3-1 Linearity Data.	102
Table 3-2 LOD and LLOQ concentrations.....	103
Table 3-3 Intraday and Interday precision for HPLC analysis of MTX and curcumin.	104
Table 3-4 Acid Degradation for stability indicating method.....	107
Table 3-5 Base Degradation for stability indicating method.	108
Table 3-6 Oxidation Degradation for stability indicating method.	110
Table 3-7 Photolysis Data for stability indicating method.	111
Table 3-8 Heat/Humidity exposure Data.	112

Table 3-9 Table showing quality control results for the total RNA samples for HFLS-RA cells.....	118
Table 3-10 NanoDrop ND-1000 quality control parameters for all labeled cRNA samples.....	120
Table 3-11 Correlation coefficient (r) values between and within the treatment samples with corresponding heat-map.	123
Table 3-12 Number and percentage of <i>ProbeNames</i> detected in each HFLS-RA sample	124
Table 3-13 The list of genes identified to be differentially expressed in sampled treated with MTX.	126
Table 3-14 Fold change of the selected genes in Microarray data in pairwise comparison	134
Table 3-15 The copy numbers obtained from qRT-PCR validation of gene expression analysis of selected genes.....	136
Table 3-16 IL6 concentration in cell culture supernatant from treated HFLS-RA cells.	138
Table 7-1 Primer design of <i>ANGPTL7</i> gene using PrimerBlast.	187
Table 7-2 Primer design of <i>CD248</i> gene using PrimerBlast.....	187
Table 7-3 Primer design of <i>CH25H</i> gene using PrimerBlast.	187
Table 7-4 Primer design of <i>CXCL12</i> gene using PrimerBlast.	188
Table 7-5 Primer design of <i>CYTL1</i> gene using PrimerBlast.	188
Table 7-6 Primer design of <i>IFITM1</i> gene using PrimerBlast.....	188
Table 7-7 Primer design of <i>IL7</i> gene using PrimerBlast.	189
Table 7-8 Primer design of <i>COL14A1</i> gene using PrimerBlast.....	189
Table 7-9 Primer design of <i>BCAR4</i> gene using PrimerBlast.	189

Table 7-10 Primer design of <i>CD274</i> gene using PrimerBlast.....	190
Table 7-11 Primer design of <i>RELT</i> gene using PrimerBlast.	190
Table 7-12 Primer design of <i>HSPA6</i> gene using PrimerBlast.	190
Table 7-13 Primer design of <i>OTP</i> gene using PrimerBlast.	191

ACKNOWLEDGEMENTS

I wish express eternal gratitude to my Gurus, Dr Leroy Shervington and Dr Amal Shervington, for their colossal patience, constant guidance, continual encouragement and careful supervision in past three years. Not only did they make me a better researcher; but also, taught me to be a better person and to make the most of every opportunity. For giving me chance to work under your supervision, I thank you both.

I wish to thank my RDT Professor Jaipaul Singh for his support and guidance. I appreciate the contribution from all of my colleagues and staff from School of Pharmacy and Biomedical Sciences, UCLan as they have helped maintain lively environment throughout the research.

My sincere regards to all the persons in my life who have made this research possible by supporting me in more ways than I can count.

I wish to specially thank my partner Dr Harshada Patil for her invaluable support both academically and emotionally.

Finally, my earnest gratitude to my family, my parents, Mrs Supriya Darekar and Mr Sahadev Darekar and my brother Amey, for everything they have done for me. Thank you, for believing in me every moment.

ABBREVIATIONS

Note: All protein names are written in uppercase such as ANGPTL7 while the gene names are italicised such as *ANGPTL7*.

ACN	Acetonitrile
ACR	American College Of Rheumatology
ADAMTSL2	ADAMTS-Like 2
AGE	Agarose Gel Electrophoresis
AICAR	5-Aminoimidazole-4-Carboamide Ribonucleotide
AKD1	Adenylate Kinase 1
AMP	Adenosine Monophosphate
AMV	Avian Myeloblastosis Virus
ANGPTL7	Angiopoietin like-7
ANKRD1	Ankyrin Repeat Domain 1
ANOVA	Analysis Of Variance
APLN	Apelin
APR	Acute Phase Response
ARHGAP32	Rho Gtpase Activating Protein 32
BCAR1	Breast Cancer Anti-Estrogen Resistance 1
BCAR4	Breast Cancer Anti-Estrogen Resistance 4
BCL2	B Cell Lymphoma 2
bp	Base Pair
CA	Citric Acid
CCD	Charged Coupled Device

CCDC81	Coiled-Coil Domain Containing 81
CCL2	Chemokine (C-C Motif) Ligand 2
CCL5	Chemokine (C-C Motif) Ligand 5
CCP	Cyclic Citrullinated Peptide
CCR2	C-C Motif Receptor 2
CCRN4L	CCR4 Carbon Catabolite Repression 4-Like
CD20	Cluster Of Differentiation 20
CD22	Cluster Of Differentiation 22
CD225	Cluster Of Differentiation 225
CD248	Cluster Of Differentiation 248
CD274	Cluster Of Differentiation 274
CD300A	Cluster Of Differentiation 300A
CD4	Cluster Of Differentiation 4
CD40	Cluster Of Differentiation 40
CD68	Cluster Of Differentiation 68
cDNA	Complementary DNA
CH25H	Cholesterol 25-Hydroxylase
CHI3L2	Chitinase 3-Like 2
COL14A1	Collagen, Type XIV, Alpha 1
COX	Cyclooxygenase
COX1	Cyclooxygenase-1
COX2	Cyclooxygenase-2
CP	Ceruloplasmin

c-REL	Avian Reticuloendotheliosis
CRHR2	Corticotropin Releasing Hormone Receptor 2 (CRHR2)
cRNA	Complementary RNA
CRP	C-Reactive Protein
CRTAC1	Cartilage Acidic Protein 1
CRTAM	Cytotoxic And Regulatory T Cell Molecule
Ct	Threshold Cycle
CTLA4	Cytotoxic T-Lymphocyte Antigen 4
CVD	Cardiovascular Diseases
CXCL12	Chemokine (C-X-C Motif) Ligand 12
Cy3	Cyanine-3
CYTL1	Cytokine-Like-1
D	Detected
DDIT4L	DNA-Damage-Inducible Transcript 4-Like
DHFR	Dihydrofolate Reductase
DIO2	Deiodinase Iodothyronine, Type II
DIO3	Deiodinase Iodothyronine, Type III
DMARD	Disease Modifying Anti-Rheumatic Drug
DMSO	Dimethyl Sulfoxide
DNA	Deoxynucleic Acid
DNAH10	Dynein, Axonemal, Heavy Chain 10
DNA-PKcs	DNA-Dependent Protein Kinase catalytic subunit
DTT	Dithiothreitol

ECACC	European Collection Of Authenticated Cell Cultures
EDTA	Ethylenediaminetetraacetic Acid
ERVK13-1	Endogenous Retrovirus Group K13, Member 1
ERVMER34-1	Endogenous Retrovirus Group MER34, Member 1
EtBR	Ethidium Bromide
FACIT	Fibril-Associated Collagens With Interrupted Helices
FAM20A	Family With Sequence Similarity 20, Member A
FBS	Foetal Bovine Serum
FC	Fold Change
FCS	Foetal Calf Serum
FDR	False Discovery Rate
FGFBP2	Fibroblast Growth Factor Binding Protein 2
FLJ45950	FLJ45950 Gene
FR β	Folate Receptor Beta
GAPDH	Glyceraldehyde 3-Phosphate Dehydrogenase
GC	Guanine Cytosine
GJB2	Gap Junction Protein, Beta 2
GLUT3	Glucose Transporters
GM-CSF	Granulocyte Macrophage Colony-Stimulating Factor
GP130	Glycoprotein 130
GPR88	G Protein-Coupled Receptor 88
H ₂ SO ₄	Sulphuric Acid
HCl	Hydrochloric Acid

HD	Homeodomain
HEATR7B1	HEAT Repeat Containing 7B1 (Predicted)
HEPES	(4-(2-Hydroxyethyl)-1-Piperazineethanesulfonic Acid
HFLS-RA	Human Fibroblast-Like Synoviocytes-RA
HK2	Hexokinase 2
HLA	Human Leucocyte Antigen
HLA-DRB1	HLA Class II, DR Beta 1
HLF	Hepatic Leukemia Factor
HPLC	High Performance Liquid Chromatography
HSPA6	Heat Shock 70kda Protein 6 (HSP70B')
IC ₅₀	Inhibitory Concentration (50%)
ICAM-1	Intercellular Adhesion Molecule 1
IFITM1	Interferon Induced Transmembrane Protein 1
IFN-g	Interferon Gamma
IGFN1	Immunoglobulin-Like And Fibronectin Type III Domain Containing 1
IIK	Inhibitor Of Nuclear Factor Kappa
IL1	Interleukin 1
IL17	Interleukin 17
IL1B	Interleukin 1b
IL2	Interleukin 2
IL21	Interleukin 21
IL23	Interleukin 23
IL36A	Interleukin 36, Alpha

IL6	Interleukin 6 (Interferon, Beta 2)
IL6R	Interleukin 6 Receptor
IL7	Interleukin 7, Transcript Variant 1
IL8	Interleukin 8
IMP	Inosine Monophosphate
lncRNA	Long Non-Coding RNA
JNK	C-Jun Amino-Terminal Kinases
KCL	Potassium Chloride
KMNO ₄	Potassium Permanganate
LAMTOR3	Late Endosomal/Lysosomal Adaptor, MAPK And MTOR Activator 3
LGALS8-AS1	LGALS8 Antisense RNA 1 (Non-Protein Coding)
lincRNA	Long Intervening Non-Coding RNA
LLOQ	Lower Limit Of Quantification
LOD	Limit Of Detection
M	Molarity
MAFB	V-Maf Musculoaponeurotic Fibrosarcoma Oncogene Homolog B (Avian)
MAPK	Mitogen Activate Protein Kinase
MCHR1	Melanin-Concentrating Hormone Receptor 1
MCP-1	Monocyte Chemoattractant Protein-1
MCSF	Macrophage Colony-Stimulating Factor
MDM-2	Mouse Double Minute 2 Homolog / E3 Ubiquitin-Protein Ligase
MDM-4	Mouse Double Minute 4 Homolog / P53-Binding Regulator
MHC	Major Histocompatibility Complex

MIR17HG	Mir-17-92 Cluster Host Gene (Non-Protein Coding)
miRNA	Micro RNA
MMP	Matrix Metalloproteinases
MMP1	Matrix Metalloproteinase 1
MMP13	Matrix Metalloproteinase 13
MMP9	Matrix Metalloproteinases 9
mRNA	Messenger RNA
MSMP	Microseminoprotein
MTX	Methotrexate
NaOH	Sodium Hydroxide
NCBI	National Center For Biotechnology Information
ND	Not Detected
NF- κ B	Necrosis Factor κ B
NHLH1	Nascent Helix Loop Helix 1
NIK	NF- κ B Inducing Kinase
npcRNA	Non-Protein Coding RNA
NPPC	Natriuretic Peptide C
NR3C2	Nuclear Receptor Subfamily 3, Group C, Member 2
Nrf2	Nf-E2-Related Factor-2
NSAID	Non-Steroidal Anti-Inflammatory Drugs
OA	Osteoarthritis
OTP	Orthopedia Homeobox
p53	Protein 53

PADI4	Peptidyl Arginine Deiminase, Type Iv
PARK2	Parkinson Protein 2, E3 Ubiquitin Protein Ligase (Parkin)
PBS	Phosphate Buffer Saline
PCR	Polymerase Chain Reaction
PDA	Photodiode Array
PD-L1	Programmed Death Ligand-1
PG	Prostaglandin
PGE2	Prostaglandin E2
PLA2	Phospholipase A2
PPE	Personal Protective Equipment
PRKCQ	Protein Kinase C Theta Type
PTPN22	Protein Tyrosine Phosphatase Non-Receptor, Type 22
PUMA	P53 Upregulated Modulator Of Apoptosis
qRT-PCR	Quantitative RT-PCR
RA	Rheumatoid Arthritis
RANK	Receptor Activator Of Nuclear Factor κ B
RANKL	RANK Ligand
RAS	Rat Sarcoma Viral Oncogene Homolog
RBM47	RNA Binding Motif Protein 47 (RBM47)
REL1	Relaxin-1
RelB	V-Rel Avian Reticuloendotheliosis Viral Oncogene Homolog B
RELT	Receptor Expressed In Lymphoid Tissues
RIN	RNA Integrity Number

RLT	Buffer RLT
RLU	Relative Luminescence Unit
RNA	Ribonucleic Acid
RND1	Rho Family Gtpase 1
RPE	RPE Buffer
RPGR	Retinitis Pigmentosa Gtpase Regulator, Transcript Variant C
RP-HPLC	Reversed Phase HPLC
RPM	Rotation Per Minute
RPMI-1640	Roswell Park Memorial Institute Culture Medium-1640
rRNA	Ribosomal RNA
RSD	Relative Standard Deviation
RT	Room Temperature
RT-IVT	Reverse Transcription In Vitro Transcription
SAM	S-Adenosylmethionine
SD	Standard Deviation
SDF-1	Stromal Cell-Derived Factor-1
SDS	Sodium Dodecyl Sulphate
sIL6	Soluble Interleukin 6
siRNA	Small Interference RNA
SLC2A5	Solute Carrier Family 2 (Facilitated Glucose/Fructose Transporter)-5
SMAD2	Mothers Against Dpp Homolog 2
SMP	Streptavidin Magnetic Particles
SNOMAD	Standardisation And Normalisation Of Microarray Data

SNORD103A	Small Nucleolar RNA, C/D Box 103A
SNP	Single Nucleotide Polymorphisms
SPDYE3	Speedy Homolog E3 (Xenopus Laevis)
SSZ	Sulphasalazine
STAT4	Signal Transducer And Activator Of Transcription 4
TAE	Tris-Acetate Acid-EDTA
TBAA	Tetrabutylammonium Acetate
TCTEX1D1	Tctex1 Domain Containing 1
TGF-B	Tumour Growth Factor-B
TGIF	TGF-B Induced Factor
TH17	T Helper 17
TLR2	Toll-Like Receptor 2
TMCO2	Transmembrane And Coiled-Coil Domains 2
TNF- α	Tumour Necrosis Factor Alpha
TNF-AIP3	TNF Alpha-Induced Protein 3
TNFRSF19	TNF Receptor Superfamily Member 19I
TNFSF10	TNF (Ligand) Superfamily, Member 10
TRAF	TNF Receptor Associated Factor
TRAF1	TNF Receptor-Associated Factor 1
TRAF1-C5	TNF Receptor Associated Factor 1 Encoding Complement Component 5
TREM1	Triggering Receptor Expressed On Myeloid Cells 1
TRIML2	Tripartite Motif Family-Like 2
tRNA	Transfer RNA

TRPA1	Transient Receptor Potential Cation Channel, Subfamily A, Member 1
UND	Undulin Gene
UV	Ultraviolet
VAV3	Vav 3 Guanine Nucleotide Exchange Factor
VCAM-1	Vascular Cell Adhesion Molecule 1
VEGF	Vascular Endothelial Growth Factor
WDR33	WD Repeat Domain 33, Transcript Variant 1
WDR66	WD Repeat Domain 66, Transcript Variant 1
XIAP	X-Linked Inhibitor Of Apoptosis

CHAPTER 1

INTRODUCTION

1.1. Rheumatoid arthritis

Rheumatoid arthritis (RA) is a chronic inflammatory disorder that affects approximately 1% of the adult population. Being predominantly genetic in nature, once the onset has occurred, there is no cure for the disorder, however it is possible to attempt remission through optimal well-timed treatment. It is a systemic autoimmune disease with predominant joint involvement and typically involves small joints of the hands and feet which when untreated has been associated with increased morbidity and mortality. Early intervention in particular has proven to be the best mode of action in RA treatment so as to prevent functional impairment that may occur and to preserve structural integrity. Over the past decade, early intensive treatment has also been proven to change the course of later RA and therefore, the aim should be to treat RA early and continuously until remission is present. Despite the new criteria developed in 2010 by American College of Rheumatology (ACR) for classification of RA making a correct diagnosis of RA (especially early RA) remains a challenge due to large number of differential diagnoses (Funovits *et al.* 2010, Neogi *et al.* 2010).

1.2. Risk factors for rheumatoid arthritis

Smoking is the only environmental factor that has been widely established as a risk factor, particularly in people who have HLA-DRB1 shared epitope alleles (Linn-Rasker *et al.* 2007). The risk of RA cannot increase dramatically by a single risk factor since more than 100 genetic risk factors for RA have been identified with varying allele frequency; several of which are frequently present in the population. Several of the identified genes are present in the same pathway. For example, HLA class II histocompatibility antigen DRB1-9 beta chain (HLA-DRB1), protein tyrosine phosphatase non-receptor type 22 (PTPN22), signal transducer and activator of

transcription 4 (STAT4), cluster of differentiation 40 (CD40), cytotoxic T-lymphocyte antigen 4 (CTLA4), interleukin (IL) 2, IL21 and protein kinase C theta type (PRKCQ) are all involved in T-cell activation, while CD40, CTLA4, IL 2, IL21, PRKCQ, PTPN22, STAT4, tumour necrosis factor alpha-induced protein 3 (TNF-AIP3) and tumour necrosis factor receptor-associated factor 1 (TRAF1) are involved in cell-cycle regulation (Aletaha *et al.* 2010).

1.3. Pathophysiology of RA

RA is a chronic, progressive, inflammatory autoimmune disease associated with articular, extra-articular and systemic effects (Staud 2009). The synovial lining, usually two cell layers thick, becomes inflamed. The pannus that subsequently develops erodes cartilage and bone, resulting in joint destruction. T cells, B cells and the subsequent interaction involving pro-inflammatory cytokines play primal roles in the pathophysiology of RA. The cytokines most directly implicated in this process are TNF- α , IL6, IL1 and IL17 (Smolen and Aletaha 2015).

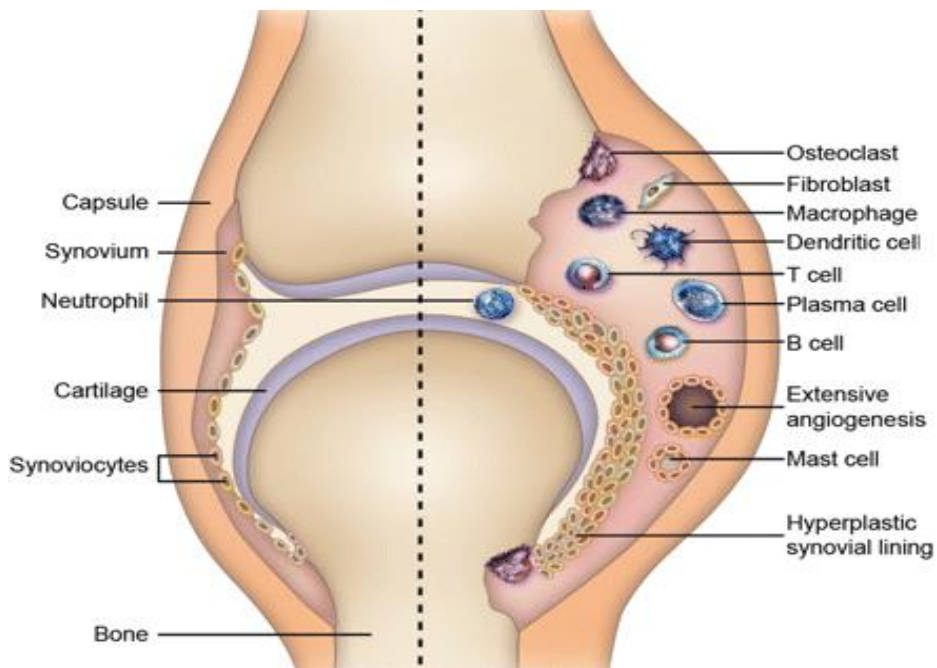


Figure 1-1 Pathophysiology of RA. (Anatomical difference between normal vs arthritic joint) (Adapted from Majithia and Geraci 2007)

More than 80% of patients carry the epitope of the HLA-DRB1*04 cluster and patients expressing two HLA-DRB1*04 alleles are at increased risk for major organ involvement and joint destruction (Jiang *et al.* 2013). Single-nucleotide polymorphism genotyping across the MHC has been identified to be related to RA, including those found on the conserved HLA multigene haplotype and those near the HLA-DPB1 gene. Other RA-associated loci are PTPN22, PADI4, STAT4, TRAF1-C5 and TNF-AIP3, although non-MHC risk alleles may represent only 35% of the genetic burden of RA (Descalzo *et al.* 2012). Numerous immune-regulators including cytokines and signalling pathways have been confirmed to be involved in the pathophysiology of RA. The complex interaction of immune modulators is responsible for the joint damage that begins at the synovial membrane and covers most intra-articular structures. Synovitis is caused by the influx or local activation or both of mononuclear cells as well as angiogenesis. The synovial lining becomes hyperplastic and the synovial membrane expands forming villi. The osteoclast-rich portion of the synovial membrane, also known as pannus, destroys

bone whereas enzymes secreted by neutrophils, synoviocytes and chondrocytes degrade cartilage (Haidar *et al.* 2013). Systemic manifestations include acute-phase protein production, anaemia, cardiovascular disease (CVD), osteoporosis, fatigue and depression (Dayer and Choy 2009).

1.3.1. Effector cells involved in the pathogenesis of RA

The initial stage of RA pathogenesis involves activation of the innate immune response, including activation of dendritic cells by exogenous material and autologous antigens. Antigen-presenting cells, including dendritic cells, macrophages and activated B cells, present arthritis-associated antigens to T cells. At the same time, CD4⁺ T cells secrete IL2 and IFN- γ leading to penetration of the synovial membrane. These alleles share a homologous amino acid sequence on the HLA-DR b-chain that confers binding of specific peptides and affects antigen presentation to T-cell receptors. Disease-associated HLA-DR alleles may present arthritis-related peptides, leading to the stimulation and expansion of autoantigen-specific T cells in the joints and lymph nodes (Smolen *et al.* 2013).

The role of B cells in RA pathogenesis involves antigen presentation as well as the production of antibodies, autoantibodies and cytokines. B lymphocytes express cell surface proteins, including immunoglobulin and differentiation antigens such as CD20 and CD22. RF and anti-CCP autoantibodies are commonly found in serum from patients with RA. Autoantibodies can form larger immune complexes that can further stimulate the production of pro-inflammatory cytokines, including TNF- α , through complement and Fc-receptor activation (Smolen *et al.* 2010).

The activation of lymphocytes leads to increased production of cytokines and chemokines, leading to increased additional T-cell, macrophage and B-cell interactions.

Along with antigen presentation, macrophages are also involved in osteoclastogenesis and are a major source of cytokines, including TNF- α , IL1 and IL6. The inflamed synovial membrane has increased the number of activated fibroblast-like synoviocytes which also directly contributes to the destruction of cartilage and bone through increased production of inflammatory cytokines and Matrix Metalloproteinases (MMPs) which are secreted directly into the synovial fluid and by direct invasion into these tissues (Dayer and Choy 2009).

1.3.2. Cytokines and the impact on effector cells

The pro-inflammatory cytokines such as IL6 and TNF- α have been well established for their involvement in the pathogenesis of RA (McInnes and Schett 2011). Through various signal pathways, these cytokines activate genes associated with inflammatory responses, including additional cytokines and MMPs involved in tissue degradation. The CD4⁺ cells which secrete IL17 has a critical role in synovitis, thereby enabling pathogenesis in many cancers and inflammatory autoimmune disorders such as RA (Nalbandian *et al.* 2009). The presence of CD4⁺ cells in the synovial fluid and peripheral blood indicates the involvement of this potent pro-inflammatory cytokine in RA pathology (Guggino *et al.* 2014). Because almost all of fibroblasts, endothelial cells, epithelial cells and neutrophils ubiquitously exhibit IL17 receptors, it can be concluded that this cytokine has the potential to influence a number of pathways and effector cells involved in RA (Iwakura *et al.* 2011).

1.3.3. Role of IL6 signalling in RA pathophysiology

IL6 has emerged as biomarker in RA pathogenesis due to its ability to influence distant target cells by way of trans-signalling cascade through ubiquitously expressed receptors. The classic signalling mechanism is a protein complex that includes a

membrane-bound, non-signalling receptor unit (IL6R) and two signal-transducing glycoprotein 130 (gp130) subunits. On the other hand, IL6 trans-signalling involves a soluble receptor (sIL6R) without transmembrane and cytoplasmic components generated during synovitis through partial proteolysis of membrane-bound IL6R or by alternative mRNA splicing. As IL6R is constitutively expressed in relatively few cell types, trans-signalling increases the range of IL6-responsive cells. For example, endothelial cells and synoviocytes express gp130 but not IL6R, however, they can respond to IL6 when IL6R is present (Dayer and Choy 2009).

IL6 trans-signalling is a major factor in RA pathogenesis (Rabe *et al.* 2008). Furthermore, trans-signalling promotes T-cell recruitment by regulating chemokine secretion during inflammation (Fielding *et al.* 2008). Trans-signalling also regulates the B-cell development and plays a significant role in various inflammatory disorders through chemokine activation (Nowell *et al.* 2006). In humans, IL6 in combination with TNF- α , TGF- β , IL1 β , IL6, IL21 and IL23 is responsible for the differentiation of naive T cells into TH17 cells (Bettelli *et al.* 2006).

1.3.4. Role of cytokines in RA bone and cartilage degeneration

Osteoclasts are multinucleated cells formed by the fusion of mononuclear progenitors of the monocyte/macrophage family. RA pathogenesis involves increased concentration of these cells in the synovial membranes and on bone surface. Macrophage colony-stimulating factor (M-CSF) through interaction with receptor activator of nuclear factor κ B (RANK) and the RANK ligand (RANKL) induce osteoclastogenesis. RANKL expression is regulated by pro-inflammatory cytokines such as TNF- α , IL1, IL6 and IL17 (Lutzky *et al.* 2007). M-CSF, IL6 and IL11 can also support

human osteoclast formation from peripheral blood mononuclear cells by a RANKL-independent mechanism (Kudo *et al.* 2003).

The development of pannus at the juncture between cartilage and bone due to angiogenesis leads to bone erosion (Akhavani *et al.* 2009). The increased expression of pro-angiogenic factors in synovium increases the level of blood supply and nutrients that are required to sustain the pannus. IL6, IL1b and TNF- α induce the vascular endothelial growth factor (VEGF) production which is essential for the development of the new blood vessels. VEGF is both a selective endothelial cell mitogen and an inducer of vascular permeability. IL6, IL1b and TNF- α also activate synoviocytes, resulting in the secretion of MMPs into the synovial fluid while cytokines activate chondrocytes, leading to the direct release of additional MMPs into the cartilage which accelerate the degradation process (Nagai *et al.* 2014).

1.3.5. Acute-phase protein production

The acute-phase response (APR) is defined as a significant change in the concentration of certain plasma proteins, such as C-reactive protein (CRP), hepcidin, serum amyloid A, haptoglobin and fibrinogen, following alterations in protein synthesis within hepatocytes (Dayer and Choy 2009). IL6 has the greatest effect on acute-phase protein levels, although IL1, TNF- α , TGF-b1 and IFN-g are also contributing factors (Ganz 2003). Even though the APR generally do not have viability of more than a few days, some components may persist indefinitely as part of secondary immunity. Increased levels of CRP directly aggravate tissue damage and contribute to the development of further complications, such as cardiovascular diseases (Courvoisier *et al.* 2008, Panichi *et al.* 2000).

1.4. Treatment for Rheumatoid Arthritis

Therapy for RA consists of both non-pharmacological and pharmacological measures. The patients are usually recommended to follow multiple movement based courses by health professionals such as physiotherapy and occupational therapy in early stages of RA. The pharmaceutical treatment includes general therapies consisting of non-steroidal anti-inflammatory drugs (NSAIDs) and disease-modifying anti-rheumatic drugs (DMARDs).

1.4.1. Non-Steroidal Anti-Inflammatory Drugs (NSAIDs)

The NSAIDs are ubiquitously used as anti-inflammatory and analgesic agents in RA and osteoarthritis (OA) as well as in chronic musculo-skeletal pain and diverse forms of acute pain. Despite the different types, all NSAIDs inhibit production of prostaglandins by inhibiting the activity of the enzyme cyclooxygenase (COX).

NSAIDs are frequently used as first-line agents for the symptomatic relief of many different inflammatory conditions. The analgesic action of NSAIDs is due to inhibition of prostaglandins in peripheral tissues and in the central nervous system. COX exerts increased expression in central nervous system during inflammation. Centrally generated PG-E₂ activates spinal neurons and also microglia that contribute to neuropathic pain.

NSAIDs can inhibit both isoforms of COX, COX-1 and COX-2, which are expressed at different levels in different tissues and serve different biological functions. COX-1 is involved in maintenance of homeostasis and the biosynthesis of PG. COX-2 is highly expressed as part of inflammatory response. Inhibition of COX-2 by NSAIDs blocks PG production at sites of inflammation or other forms of tissue damage, however simultaneous inhibition of COX-1 in other tissues such as platelets and the

gastroduodenal mucosa can cause common adverse side-effects of NSAIDs such as bleeding and gastrointestinal ulceration.

1.4.2. Disease-Modifying Anti-Rheumatic Drugs (DMARDs)

1.1.1.1 Biological DMARDs

The TNF- α which is a central cytokine in the inflammatory cascade has pleiotropic effects in the immune response and plays a vital role in RA pathogenesis. The biological DMARDs with a specific ability to inhibit this cytokine are used in the treatment of RA include infliximab, adalimumab and certolizumab. These agents provide rapid control of inflammation and have proven efficacy both in terms of clinical outcomes and structural damage (Nam *et al.* 2010). These however, are significantly more expensive than traditional DMARDs and are generally used in case of unsuccessful treatment with synthetic DMARDs (Schoels *et al.* 2010).

1.1.1.2 Synthetic DMARDs

In terms of DMARD therapy, several important treatments have emerged. The first is that of early intervention with effective and appropriate treatment. The early initiation of DMARD therapy is essential in achieving good clinical outcomes and minimising subsequent bone damage (Finckh *et al.* 2006). Of the synthetic DMARDs, methotrexate (MTX) remains the most popular choice of treatment (Smolen and Aletaha, 2015). In recent years, the emergence of more targeted biological DMARDs have further improved outcomes in RA treatment, however, due to cost and availability, they are mainly reserved for patients who fail to respond to synthetic DMARDs (Quinn *et al.* 2005, Klarenbeek *et al.* 2011). Glucocorticoids are also used in the treatment of RA for

remission induction and are often used as bridging therapy and for management for disease flares (Boers *et al.* 1997).

Early treatment with DMARDS is one of the key principles in the treatment of early arthritis. Synthetic DMARDS have an effect on the disease process within weeks to months. MTX, sulphasalazine (SSZ) and leflunomide are commonly used DMARDS that have been shown to halt RA development and delay radiological progression. Of the synthetic DMARDS, MTX is considered the anchor drug and is generally used first for patients at risk of developing persistent disease or erosive disease because of its relatively beneficial clinical and radiological efficacy and its beneficial properties in combination treatment with biological DMARDS. Leflunomide and SSZ have similar clinical efficacy and are considered good alternatives (Nakashima and Takayanagi 2009).

1.5. Methotrexate (MTX)

Methotrexate is an antimetabolite that is a structural analogue to folic acid (Figure 1-2) which is essential for cellular division, due to its role in DNA and RNA synthesis. The methotrexate precursor Aminopterin, another folic acid analogue, was designed to reduce proliferation of cancerous cells via the inhibition of folate as one of the world's first chemotherapeutics (Cronstein 2007, Chabner and Roberts 2005).

Dihydrofolate reductase (DHFR) has been identified as the enzyme responsible for the reduction of folic acid to metabolically active tetrahydrofolate, required in *de novo* synthesis of DNA. Hence, DHFR has been established as a therapeutic target in cancer treatment. Isolation of this enzyme allowed for the development of potent inhibitors of DHFR such as MTX (Cronstein and Chan 2000). The anti-carcinogenic mechanism of action of MTX involves inhibition of DHFR enzyme to prevent conversion of folic acid to the active tetrahydrofolate required in the thymidine synthesis. Folic acid is also essential in the purine and pyrimidine base biosynthesis. Therefore by inhibiting DHFR MTX effectively inhibits the *de novo* synthesis of DNA, RNA, thymidylate and proteins.

While MTX features prominently in current treatment of large cell or high grade lymphomas, head and neck cancer, breast cancer, bladder cancer and osteogenic sarcoma, it is most effectively utilised in the treatment of RA at low doses compared to the treatment of cancer (Smolen and Aletaha, 2015). The MTX treatment shows improved prognosis within three months of starting the treatment by reducing pain and improving joint functionality (Angeles *et al.* 2014).

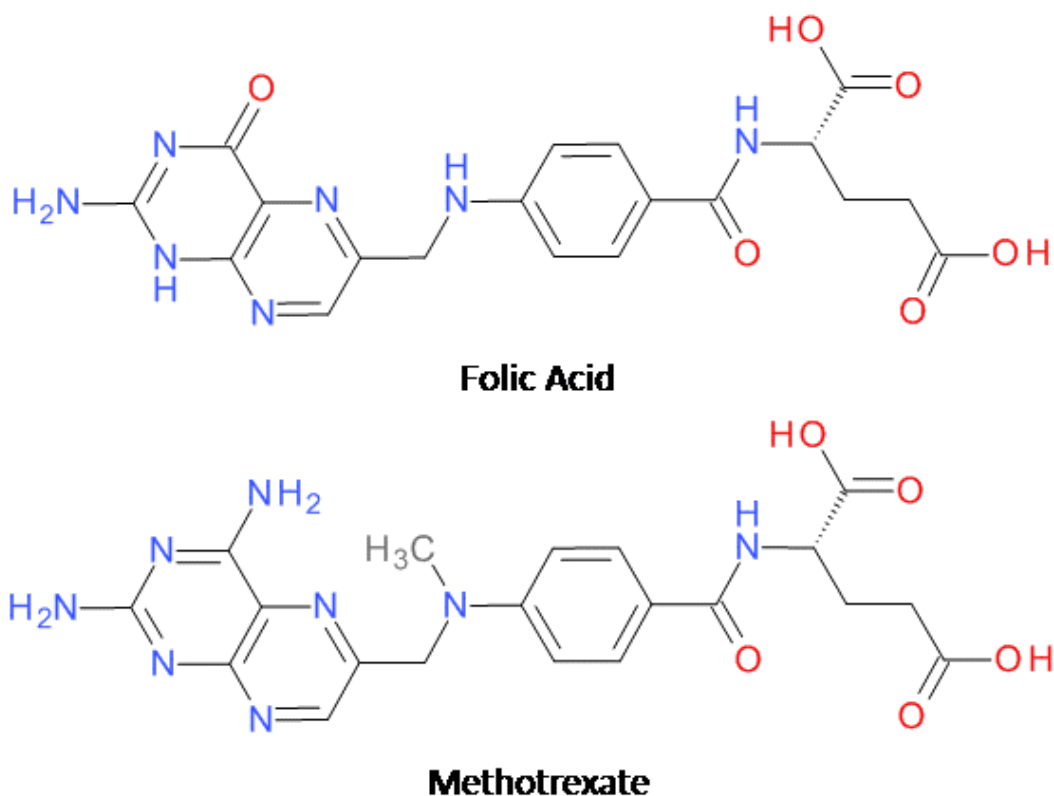


Figure 1-2 Chemical structure of folic acid and its structural analogue Methotrexate.

1.5.1. Mechanism of action

In the cancer treatment, MTX induces cell apoptosis by blocking the folate-dependent *de-novo* synthesis of DNA and RNA (Cronstein 2005, Chan and Cronstein 2013). However, in the treatment of RA the ability of MTX to modulate apoptotic pathways enables it to exert these anti-inflammatory properties (Stamp *et al.* 2011, Braun *et al.* 2007). MTX exerts its mechanism of action through induced release of adenosine to obstruct nucleotide synthesis. Reduced levels of methyl donors including tetrahydrofolate and methyl tetrahydrofolate through inhibition of DHFR blocks generation of lymphotoxic polyamines and inhibits chemotaxis in monocytes (van Dieren *et al.* 2006, Patel and Moreland 2009). The MTX metabolites are retained in tissues in the form of MTX polyglutamates, thus increasing the efficacy of MTX beyond its half-life in plasma.

The MTX polyglutamates increase intracellular levels of 5-Aminoimidazole-4-carboxamide ribonucleotide (AICAR) by inhibiting AICAR transformylase (Chan and Cronstein 2010). Increased AICAR levels inhibit adenosine monophosphate (AMP) and adenosine deaminases which are essential for conversion of adenosine to inosine monophosphate (IMP) and inosine. The adenosine accumulated in the tissues downregulates the macrophage activation (Chan and Cronstein 2013, Montesinos *et al.* 2007). MTX can also increase vasodilation leading to increased blood flow through inhibition of adenosine deamination (Ramakers *et al.* 2012).

The anti-inflammatory properties of MTX involve inhibition of T cell activation and alteration in the expression of T cell cytokines and adhesion molecules (Kooloos *et al.* 2010). The anti-inflammatory properties of MTX are critically dependent upon the ability to produce reactive oxygen species in both T cells and monocytes which ultimately lead to apoptosis (Johnston *et al.* 2005).

1.5.2. Inhibiting NF- κ B activation in RA

NF- κ B, a major therapeutic target, is a family of interrelated transcription factors that includes five genes: NF- κ B1 (p50/p105), NF- κ B2 (p52/p100), RelA (p65), c-Rel and RelB. Activation of NF- κ B may result from signalling pathways triggered by a variety of cytokines, growth factors and kinases. Various molecular mechanisms for NF- κ B activation have been proposed (Aggarwal and Harikumar 2009, Chakravarti *et al.* 2010).

MTX acts as a strong transcriptional activator which is achieved via activation of JNK. One other proteins induced by MTX is p53, a strong transcriptional activator through gene expression induction, influences many cellular functions such as cell cycle arrest and induction of apoptosis.

NF- κ B plays a crucial intermediary role between external inflammatory stimuli and pro-inflammatory molecules since genes that encode pro-inflammatory cytokines, chemokines and lymphocyte adhesion molecules require the activation through NF- κ B binding sites in their promoters. In T lymphocytes, MTX is a strong inhibitor of the activation of NF- κ B in response to various extracellular stimuli. In T cell tissue culture models, MTX inhibits activation of NF- κ B via JNK activation. Further, the inhibition of NF- κ B activity in T cells by MTX is dependent upon MTX-mediated induction of p53.

The RA progression is characterised by elevated activity of NF- κ B and depressed levels of the pro-apoptotic factor p53. The induction of p53 by MTX results in subsequent reduced NF- κ B activity in RA T helper cells.

The NF- κ B modulates the response to exogenous stimuli, whereas p53 modulates intrinsic stress responses through initiation of cell cycle arrest, apoptosis, or senescence, eliminating clones of cells with DNA damage and its resulting mutations. Generally, NF- κ B and p53 act as functional antagonistic due to the ability of NF- κ B as a pro-survival and pro-inflammatory transcription factor while p53 influences transcription factors in favour of anti-survival and anti-inflammatory cell-cycles. In a healthy cell DNA damage, hypoxia, or oncogene activation elicit p53 responses that activate cell cycle arrest, senescence or apoptosis, targeting genes that are pro-apoptotic such as PUMA, or induce cell cycle arrest proteins such as p21 (Ak and Levine 2010, Zhang *et al.* 2011). NF- κ B is activated via post-translational modifications via degradation of I κ B or MDM-2/MDM-4 in response to exogenous signals such as infectious agents, viruses, toll-like receptor agonists, antigen receptors or through inflammatory cytokines, such as TNF- α or interleukin-1 β . NF- κ B activation leads to transcription of mRNAs that encode inflammatory proteins such as cytokines, IL6, GM-

CSF; chemokines, IL8, MCP-1; enzymes, COX-2, PLA2 and adhesion molecules VCAM-1 and ICAM-1. The production of pro-inflammatory cytokines such as IL1 β and TNF- α creates an amplification loop that can lead to constitutive activation of the NF- κ B signalling pathway. Metabolic activation of NF- κ B enhances glycolysis and increases glucose transporters (GLUT3) leading to higher amounts of glucose uptake.

To induce cell cycle arrest or apoptosis, the transcriptional program activated by p53 is mediated by induction of the long non-coding RNAs (Hung *et al.* 2011). MTX contributes to MTX-dependent activation of NF- κ B in response to extracellular stimuli, such as TNF- α . Inhibition of DNA-PKcs, but not ATM, reverses MTX-dependent inhibition of TNF- α mediated NF- κ B activation. Furthermore, use of siRNAs to deplete either p53 mRNA or lincRNA-p21 reverses the ability of MTX to inhibit TNF- α mediated NF- κ B activation.

1.5.3. Side effects

Despite having relatively good safety profile MTX does exhibit adverse side effects. At low concentrations side-effects are limited, mild and preventable, however, with prolonged treatment they tend to escalate to more severe levels. The common toxicities relate to folate antagonism, anaemia, neutropenia, stomatitis and oral ulcer which can be improved with folic acid supplementation. However, the continuous folic acid supplements work to diminish the efficacy of methotrexate (Firestein 2010).

A major adverse effect of methotrexate is a hepatotoxicity, primarily in the form of fibrosis resulting from depletion of hepatic folate concentrates and their replacement with methotrexate polyglutamates in the liver (Nesher *et al.* 2003). As *de novo* synthesis prominently occurs in proliferating tissue such as hepatic cells and bone marrow, these areas are more prone to damage (De Lathouder *et al.* 2004).

Interstitial pneumonitis due to acute fibrosis in alveolar cavity is another prominent complication with common symptoms of cough or shortness of breath. Methotrexate pneumonitis may occur at any time during therapy and is not dose related. The RA patients are usually susceptible to chronic form of interstitial lung disease and fibrosis which can be aggravated with prolonged methotrexate medication. Myelosuppression (lowering of blood counts) can also develop over time due to methotrexate therapy.

Cancer risk with methotrexate is minimal even though cases of lymphoma associated with methotrexate therapy have been observed where the lymphoma resolved after discontinuing therapy. However, the correlation is not conclusive since rheumatoid arthritis itself presents an increased chance of developing lymphoma due to irregularities in autoimmune system (Keystone *et al.* 2004).

The MTX is classed as a teratogen, an agent that can cause malformation of an embryo and hence is classified as pregnancy category X drug (Ranganathan and Mcleod 2006). Several anecdotal instances indicate that MTX therapy may be related to congenital defects such as defects in coronal sutures, oxycephaly, hypertelorism, absence of digits and hypoplastic mandible. Therefore, it essential to strictly regulate the MTX therapy in patients who are either already pregnant or of child bearing potential (Levin and Almog 2015).

Due to the adverse effects involved in the prolonged use of MTX as primary therapeutic agent in RA treatment, it is important to identify and investigate other therapeutic agents, with similar or improved level of efficacy, which can be used as an alternative or as a supplement in RA treatment. This will reduce the amount of MTX

consumed thereby reducing the severity of the side-effects. One of the most promising candidate for such alternative treatment is curcumin.

1.6. Curcumin

Curcumin also called diferuloylmethane (Figure 1-3) is an active component of turmeric derived from the rhizome of the tropical plant *Curcuma longa*. Turmeric is used as a dietary spice and a colouring agent in the food and textile industry. It has been used for centuries in Ayurveda (the knowledge of long life) to treat biliary disorders, anorexia, cough, diabetic wounds, hepatic disorders, rheumatism and sinusitis. Several preclinical and clinical studies indicate that curcumin may exhibit preventive and therapeutic significance in cancer, atherosclerosis, aging, neurodegenerative disease, hepatic disorders, obesity, diabetes, AIDS, psoriasis and autoimmune diseases. Research over the past few decades have shown that curcumin targets multiple signalling pathways and regulates the expression of several transcription factors, inflammatory cytokines, enzymes, growth factors, receptors, adhesion molecules, anti-apoptotic proteins and cell cycle proteins (Aggarwal and Harikumar 2009).

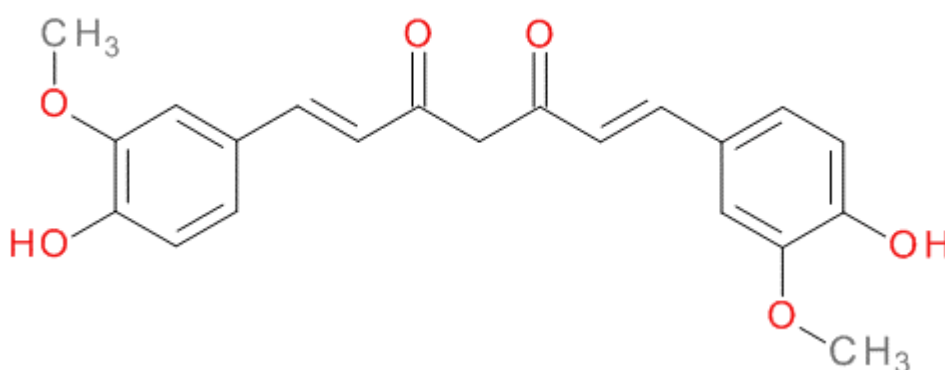


Figure 1-3 Molecular structure of Curcumin

Curcumin inhibits carcinogen activation, stimulates carcinogen detoxification and suppresses pro-inflammatory signalling, induction of cancer cell apoptosis, cell cycle arrest, inhibition of angiogenesis and metastasis and modulation of oncogenes and

tumour suppressor genes (Lin 2007). It regulates the expression of multiple genes involved in growth, metastasis, cell adhesion, cell invasion and apoptosis. Curcumin influences a wide range of molecular targets either by interacting physically with the target or by modulating the transcription factors, enzyme activity, or gene expression (Yan *et al.* 2012).

The effects of curcumin are mediated through intrinsic, extrinsic, p53, NF- κ B and NF- κ B-regulated gene expression of B cell lymphoma 2 (Bcl2), cyclin D1, cyclooxygenase-2 (COX-2), matrix metalloproteinase-9 (MMP-9), Akt, mitogen activate protein kinase (MAPK), NF-E2-related factor 2 (Nrf2), β -catenin and cell–cell adhesion. It has been reported that NF- κ B is regulated by several inflammatory cytokines including Notch signalling and that is highly activated in cases of human cancer. Curcumin has been shown to mediate anti-apoptotic effects through inhibition of NF- κ B and its related gene products (Anand *et al.* 2008, Hatcher *et al.* 2008, Strimpakos and Sharma 2008).

1.6.1. Effects on the NF- κ B Pathway

Curcumin inhibits activation of NF- κ B which in turn represses the expression of the COX-2 gene and TNF- α . Curcumin blocks tumour promoter-mediated NF- κ B transactivation by inhibiting the NF- κ B-inducing kinase (NIK)/IKK signalling complex at the level of IKK α /b (Shin *et al.* 2009, Hayden and Ghosh 2004). Curcumin can suppress IKK, inhibit both constitutive and inducible NF- κ B activation and promote the TNF- α -induced apoptosis (Bharti *et al.* 2003). Other signalling pathways, such as Ras/MAPK and phosphoinositide 3-kinase (PI3K)/Akt, are also involved in the activation of NF- κ B and curcumin has been reported to play an inhibitory role in these pathways (Khan *et al.* 2012).

1.6.2. Induction of Apoptotic Signalling Cascade

Curcumin can induce apoptosis by mediating both intrinsic (mitochondrial) as well as extrinsic cell signalling pathways. The mitochondrial apoptosis is mediated by members of the Bcl2 family of proteins as well as the tumour suppressor protein p53, which increases permeability in mitochondrial membrane and releases pro-apoptotic proteins into the cytosol (Li and Schwarz 2003, Ashkenazi *et al.* 2008).

The extrinsic signalling pathway for curcumin to induce apoptosis is mediated through transmembrane death receptors located on the cell surface which are members of the tumour necrosis factor- α (TNF- α) receptor gene superfamily, that are essential in apoptosis (Bush *et al.* 2001). Curcumin blocks NF- κ B mediated cell survival pathways and promotes the expression of pro-apoptotic proteins (Bax, Bim, Bak, Puma and Noxa) as well as inhibit the expression of anti-apoptotic proteins (BCL2, BCL-xL, survivin and IAP) (Shankar *et al.* 2007).

Curcumin has also been shown to induce apoptosis through inhibition of transforming growth factor-beta (TGF- β)-induced phosphorylation of Smad2, along with up-regulation of TGF- β induced factor (TGIF). TGIF has been reported to be a negative regulator of the TGF- β signalling pathway (Song *et al.* 2011).

1.7. Efficacy and synergistic activity of concurrent MTX – Curcumin treatment

Despite being highly effective anti-rheumatic agent, the severity of prolonged MTX therapy raises the question on overall efficacy of MTX as first line treatment. Even though MTX is administered in low doses in RA treatment, complications such as gastrointestinal, hepatic, nephrotic and haematological disturbances, due to sustained exposure to the drug cannot be ignored. Research in the field rheumatism focuses on the development of a viable candidate that can be utilised as a supplement, if not replaced, for effective treatment of RA.

The antioxidant and anti-inflammatory properties of curcumin are well documented (Picone *et al.* 2014). The pluripotent nature of the curcumin makes it a competitive option to enhance the therapeutic potency of MTX treatment.

1.7.1. Cardiovascular disorders in RA

The cardiovascular disorders are the most common cause of death in patients with RA (Symmons 2003). The increased occurrence of cardiovascular disorders in RA patients can be attributed to the active systemic inflammation which accelerates atherosclerosis (Sattar 2003). Several studies, although anecdotal, have linked the MTX therapy with the increased chances of developing cardiovascular risk. Through the inhibition of homocysteine-methionine pathway, long term low dose MTX can increase risk of hyper-homocystinaemia which leads to increased risk of cardiovascular manifestations, stroke and heart failure (De Bree *et al.* 2002). Curcumin has demonstrated the ability to reduce the CVD risk significantly (Weinblatt *et al.* 1999, Rosner *et al.* 2012). This process involves activation of Nrf2-dependent antioxidant response element (Pae *et al.* 2007). Curcumin also reduces the expression of TLR2,

MCP-1 and CD68 while improving the function of connexin-43 thereby improving heart contractility (Kim *et al.* 2012).

1.7.2. Hepatotoxicity

As an antioxidant the curcumin can counter MTX therapy induced the serum concentrations of reactive oxygen species and the transaminase enzymes. The cell membranes in hepatic tissue are rich in phospholipids and the reactive oxygen species can damage the cellular integrity. The anti-oxidant properties of curcumin reduce the oxidative stress and prevent the MTX induced formation of lipid peroxides. The MTX associated effects such as proliferation of kupffer cells, focal liver cell necrosis and fibrosis in hepatic cells are attenuated by curcumin (Banji *et al.* 2011).

1.7.3. Nephrotoxicity

The oxidative stress generated by MTX plays an important role in the development of the nephrotoxicity. The sustained oxidative stress stimulates transcription factors such as NF- κ B and induce nitric acid synthase. The curcumin treatment reduces the activity of antioxidant enzymes such as glutathione peroxidase and superoxide dismutase in renal tissues thereby increasing the efficacy of the treatment (Tapia *et al.* 2012).

1.7.4. Increased activity in folate receptors

The curcumin exhibits the synergistic activity by increasing the activity of folate receptors which increases cellular uptake of folic acid as well as MTX. The mechanism of action of curcumin involves up-regulation of folate receptor β mRNA and FR β protein. Therefore the addition of curcumin as supplement can significantly reduce the cytotoxicity of MTX (Dhanasekaran *et al.* 2013).

1.8. Simultaneous stability analysis of MTX and curcumin

The anti-inflammatory and anti-rheumatic activities of both MTX and curcumin have been extensively studied and established. However, a comparative analysis of both compounds is essential in order to establish their efficacy and the overall effectiveness of RA treatment involving MTX and curcumin. Chemical stability of pharmaceutical molecules plays a crucial role in safety and efficacy of the drug combination. In order to establish as a viable treatment the stability of the compounds in a formulation needs to be established so as to evade combined drug intoxication. The simultaneous forced degradation and stability measurement provides useful information regarding chemical interaction between two compounds and safety of the drug products which can be determined using HPLC.

1.8.1. High-Performance Liquid Chromatography (HPLC)

HPLC, also called high-pressure liquid chromatography, is the analytical technique used in chemistry and biochemistry to separate, identify and quantify each component in a mixture. HPLC analysis is used in wide range of fields such as legal, research, manufacturing and medical.

HPLC involves flowing pressurized liquid solvent containing the sample mixture through a column filled with a solid adsorbent material. Every component present in the sample interacts differently with the adsorbent material in the column, leading to different flow rates for the different components which leads to the separation of the components as they flow through the column. The active component of the column, the adsorbent, is typically a granular material made of solid particles. The pressurized liquid called the mobile phase which is composed of different solvents such as water, acetonitrile and/or methanol in varied composition. The buffering agents are used to

maintain constant ionic composition of the mobile phase. The composition and temperature of the mobile phase influences the interactions taking place between sample components and column. These interactions are physical in nature, such as hydrophobic, dipole–dipole and ionic, most often a combination.

Due to the small sample separated, typical column dimensions are 2.1–4.6 mm diameter and 30–250 mm length. The active component of the column is typically a granular materials made of solid adsorbent particles which are 2-50 micrometres in size. This provide HPLC higher resolution and the ability to distinguish between compounds when separating mixtures, which makes it a popular chromatographic technique.

The typical HPLC instrument setup includes a sampler, pump and a detector. The sampler brings the sample mixture into the mobile phase stream which carries it into the column. The pump delivers the desired flow and composition of the mobile phase through the column. The detector generates a signal proportional to the amount of sample component emerging from the column, hence allowing for quantitative analysis of the sample components. A digital microprocessor and user software control the HPLC instrument and provides data analysis. Some models of mechanical pumps can mix multiple solvents together in ratios changing in time, generating a composition gradient in the mobile phase. Various detectors are in common use, such as UV/VIS, photodiode array (PDA) or linked to a mass spectrometry.

1.8.1.1. Reverse-Phase HPLC (RP-HPLC)

RP-HPLC separates molecules on the basis of differences in their hydrophobicity. The components of the analyte mixture pass over stationary-phase particles bearing pores

large enough for them to enter, where interactions with the hydrophobic surface removes them from the flowing mobile-phase stream. The strength and nature of the interaction between the sample particles and the mobile phase, and the stationary phase depends on both hydrophobicity and polarity of the compounds. Since this elution depends on the precise distribution of hydrophobic residues in each species, each analyte elutes from the column at a characteristic time and the resulting peak can be used to confirm its identity and quantity.

1.8.2. Forced degradation and validated Stability-indicating method

A stability-indicating method is a validated stability profile of a compound. The validated method can be used to quantify the rate of degradation of the compound under different stress conditions. It can be used to accurately measure the changes in the active ingredients concentration without interference from other degradative products impurities and excipients. The validated stability indicating profile can also be used for the detailed analysis of the by-products obtained through the degradation of the compound. Usually reverse phase columns are used as stationary phase while different solvents and buffering agents are as mobile phase in different ratios for different stages of separation. The stability indicating method needs to be validated according to USP/ICH guidelines for linearity, accuracy, precision, limit of quantitation, limit of detection and robustness. Direct analysis of the elution of sample using the photo-diode array is required to establish specificity of the method. It is required to identify and quantitate the rate of degradation of the compounds due to stress inducing conditions.

Forced degradation analysis plays crucial role in the development process of formulations. The information regarding the stability of compounds in given

formulations under different stress conditions helps determine potential risk factors of the treatment involving formulation while also providing regulatory guidelines for manufacturing and storage conditions. In order to establish a viable concurrent treatment for RA, it is important to establish a stability indicating method for the simultaneous analysis of both MTX and curcumin under different stress conditions.

1.9. Comparative analysis of the mechanisms of actions of both MTX and curcumin

Gene expression profiling is the measurement of the simultaneous expression of the entire genome to establish overview of cellular activities. These profiles are an ideal way of establishing the difference between phenotypically distinct cells or to assess the effect of particular drugs on several cellular pathways. Gene expression profiling using DNA microarray is a powerful technique that can examine and compare the efficacy of MTX and curcumin in cells involved in RA pathogenesis.

1.9.1. DNA microarray

DNA microarray, introduced by Patrick O. Brown's group at Stanford University, allows one to quantify the expression of thousands genes in a single experiment. It consists of solid substrate usually attached to a microscopic glass slides consisting of thousands of DNA samples. These slides are probed with fluorescence tagged cDNA which is synthesised from mRNA isolated from sample cells. Each cDNA is tagged with a different fluorescent dye which allows the tracing of different population of cells. Different fluorescence dyes allow the determination of gene expression in various populations of cells in a single array thereby making it possible to determine the relative expression levels of genes by measuring the intensity of the fluorescence.

1.9.2. Data analysis

In order to analyse the data, statistical tools such as statistical package or Imaging software is used. The image processing is carried out using an imaging software package such as Spotfinder, ScanAnalyze, GenePix and QuantArray. These packages help process the images and enables adjusting the background, spotting and quantification. This will also involve statistical analysis of data for normalization to

reduce variation with the help of software known as SNOMAD (Standardization and Normalization of Microarray data). The identification of expressed genes, the quantification and analysis is carried out using ANOVA and paired-T Test utilising appropriate sets of gene data.

DNA microarray is time-efficient and cost-effective since it allows the quantitation of thousands of genes using small quantities of sample. This technology has numerous applications such as analysing the gene expression profile in malignant diseases, analysis of copy number variations, examining potential targets for drug discoveries and SNP chips detecting single nucleotide polymorphisms (SNPs), genotype tool for identifying inheritable markers and targeted sequences.

The data obtained from the DNA microarray following the treatment with MTX and curcumin should provide an insight in to the mechanism of action for both drugs. This should allow us to compare the efficacy of the two compounds and their concurrent potential use in improving RA treatment.

1.10. Aim of the research

The individual effectiveness of both MTX and Curcumin as anti-inflammatory agents have been extensively studied and established. Both MTX and curcumin have been demonstrated to be successful in modulating critical pathways in RA. However, the specific comparison of the mechanism of action and the quantified combined effect of them both are yet to be determined. In order to establish whether or not these two compounds could be used in combination in order to help improve RA treatment, it is important to establish the stability and safety of these two compounds using a validated stability-indicating RP-HPLC method. It is also important to perform a detailed analysis of their effect on specific biomarkers and critical cellular pathways involved in RA pathogenesis.

Therefore, the aim of the project is to first investigate the stability of MTX and curcumin, by developing a stability-indicating method, followed by carrying out a comparative analysis of the effects of both compounds on cellular functions.

The long term benefits of the current MTX therapy in RA treatment are restricted by the inevitable adversities which manifest over time. The safety profile and pleiotropic nature of curcumin makes it an ideal candidate to modulate these adversities. Therefore the aim of our project is to improve the efficacy of the RA treatment by providing comparative evidence to establish curcumin as a viable anti-rheumatic agent.

The first phase of our research focused on the development of a RP-HPLC stability indicating method to assess the compatibility and the stability of the compounds. The developed HPLC method enabled us to distinguish between the compounds and their forced degradation products and thus is a reliable method of monitoring the effects of

the active compounds when combined in different ratios. The compounds were found to be stable at room temperature when stored in acidic conditions. The validated stability profile indicated that the compounds could be administered simultaneously as part of RA treatment.

The second phase consisted of measuring the effectiveness of the two compounds in specific cell lines which concentrated on quantifying the inhibition of specific pro-inflammatory biomarkers. The cells were treated with IC_{50} concentrations of the compounds to measure the effect on the RA biomarkers.

The PhD phase of the project concentrated on understanding the effect of MTX and curcumin on gene expression profiling and their subsequent impact on different modulatory cell pathways in specific rheumatoid arthritis associated cells. A novel investigation of the combined effects of these two compounds using microarray technology was carried out. The bioinformatics data was used as a basis for further studies which involved specific gene analysis. The main aim of the research was to analyse the mechanism of action of MTX and curcumin to understand the mechanisms in which they influence different therapeutic biomarkers and whether they could exhibit synergistic behaviour which would play a crucial role in future treatment of RA.

CHAPTER 2

MATERIALS AND METHODS

2.1. HPLC analysis

2.1.1. Chemicals and materials

MTX and Curcumin required HPLC analysis were purchased from Tocris Bioscience, UK. Acetonitrile (ACN), Water, Dimethyl Sulfoxide (DMSO), Citric Acid (CA) and Sodium dodecyl sulphate (SDS) were purchased from Fisher Scientific, UK. Tetrabutylammonium acetate (TBAA) was purchased from Sigma Aldrich, UK. All purchased reagents were of analytical grade.

2.1.1. Standard solutions

Due to sparingly soluble nature of curcumin in water, stock standard solutions were prepared by first solubilising MTX and Curcumin in DMSO. These solutions were used to prepare final working concentration of 5 mg/ 100 ml each using DMSO: ACN: H₂O (3:35:62).

2.1.2. Preparation of the mobile phase

Gradient system comprised of two mobile phase with varying concentrations of acetonitrile (ACN). Mobile phase A consisted of 35% acetonitrile and 65% water with a final concentration of 10 mM TBAA, 10 mM SDS and 25 mM Citric Acid. Mobile phase B was made of 60% acetonitrile and 40% water with a final concentration of 10 mM TBAA, 10 mM SDS and 25 mM Citric Acid. The specific mobile phase concentrations have been previously developed by our research group (Shervington *et al.* 2005).

2.1.3. Apparatus and chromatographic conditions

Analysis was carried out on a Jasco HPLC system equipped with the multiwavelength detector (Jasco MD-1510), autosampler (Jasco AS-1555 intelligent sampler) and gradient pump (Jasco PU-2089 Plus) controlled by analysis software ChromNAV. The

column used was a Waters Reverse Phase Column (XBridge™ Shield RP18 4.6x250 mm Column, 5 μM).

The gradient elution program, as shown Figure 2-1 in as normally run for total of 25 min: 5.50 min Mobile phase A, followed by a gradient to Mobile phase B by 6.50 min, maintained until 17 min. After the analysis, the mobile phase was returned back to mobile phase A by 18 min and the column was re-equilibrated during 7 min at A. The flow rate was maintained at 1.0 ml/min until 5.50 min followed by an increase to 1.5 ml/min at 6.50 min. This was maintained until 23 min after which it was reverted back to 1.0 ml/min by the 24 min. The injection volume was 20 μl. Chromatography was performed at room temperature. Under these chromatographic conditions, the retention times achieved were 4.88 and 12.33 min for MTX and curcumin, respectively.

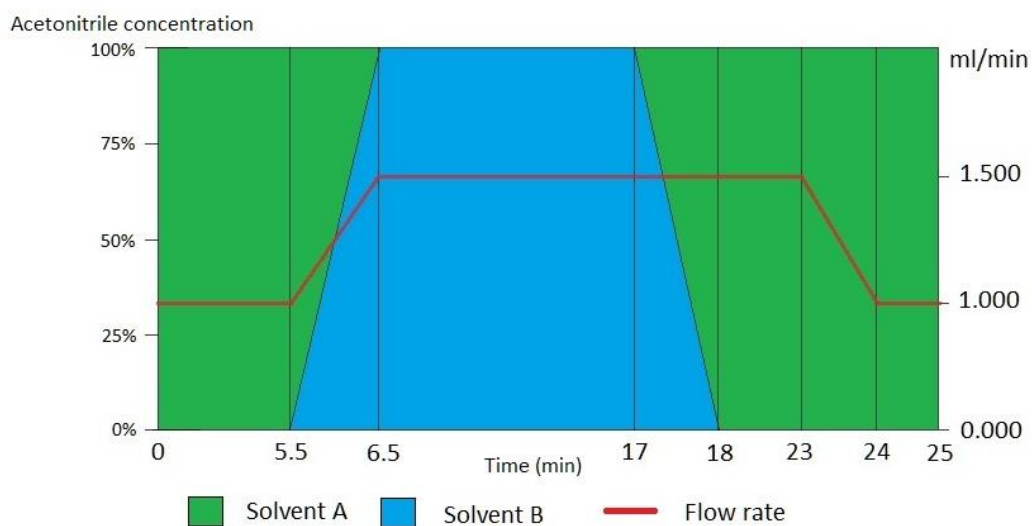


Figure 2-1 Pictorial representation of the gradient system used for degradation analysis of Curcumin and Methotrexate. (Solvent A contains 35% of acetonitrile and Solvent B contains 60% of acetonitrile)

2.1.4. Analytical method validation

2.1.4.1. Linearity

To determine the linearity, six concentrations of both MTX and curcumin were prepared separately and in mixtures at 20 µg/ml, 40 µg/ml, 50 µg/ml, 60 µg/ml, 80 µg/ml and 100 µg/ml for MTX and curcumin. The samples were analysed and the peak area was plotted against the concentration to determine the linearity.

2.1.4.2. Limit of Detection (LOD) and lower limit of quantification (LLOQ)

The 10 µg/ml concentrations of both compounds were serially diluted and analysed by HPLC to determine the limit of detection. The peak-to-peak noise was determined by injecting a blank (DMSO:CAN:Water 3:35:62). The concentration of the compounds with peak area three times the baseline noise was considered to be the LOD. The concentration of the compounds that could be quantitated without any interference from baseline noise and having RSD of less than 2% was considered to be LLOQ.

2.1.4.3. Intraday and interday method precision

The Intraday and interday method precision was tested through RSD of the recoveries for both compounds individually and as a mixture. Solutions of different concentrations 20 µg/ml, 50 µg/ml and 70 µg/ml MTX and Curcumin were analysed individually and as a mixture on the same day and on 3 different days. The recovery of the compound was determined by comparing concentrations of the solutions to the respective theoretical values.

2.1.5. Forced degradation studies

2.1.5.1. Acid degradation

The MTX, curcumin and their mixtures at a concentration of 50 µg/ml were subjected to 0.1 M hydrochloric acid (HCl) under three different temperatures: RT, 40°C and 70°C. The samples were withdrawn at regular intervals and analysed.

2.1.5.2. Base degradation

The MTX, Curcumin and their mixture at a concentration of 50 µg/ml were treated with 0.1 M Sodium hydroxide (NaOH) solution under similar temperatures: RT, 40°C and 70°C and the samples were analysed at regular intervals.

2.1.5.3. Oxidation

Both MTX and curcumin at a concentration of 50 µg/ml were treated with 3% hydrogen peroxide solution individually and as mixture at RT and 40°C. The samples were analysed at regular intervals.

An alternative oxidation method was used to for analysis. Both MTX and curcumin at a concentration of 50 µg/ml was treated with 0.1 mM potassium permanganate (KMnO₄) and 0.1 mM sulphuric acid (H₂SO₄) and heated to 90°C for an hour. The solution was then quenched using 10% (v/v) ethanol and sample recovery was determined.

2.1.5.4. Photolysis

A 50 µg/ml concentration of MTX and curcumin, both individually and as a mixture, were subjected to photolytic conditions using Ultraviolet C bulb (wavelength range:

100 nm- 280 nm). Samples were eluted and analysed every hour to determine recovery.

2.1.5.5. Dry heat and humidity

Samples of known weight were prepared for MTX, curcumin and the mixture (1:1) and subjected to two conditions, dry heat at 70°C and at 40°C at a relative humidity of 70-75%. The samples were removed at regular intervals and the theoretical concentrations of 50 µg/ml for MTX and curcumin were prepared and analysed.

2.2. Cell culture

The cell culture medium was prepared according to recommendations as shown in Table 2-1. Medium was stored at 4°C for 2-3 weeks within the stability period. The Human Fibroblast-Like Synoviocytes extracted from RA patients (HFLS-RA) were bought from Culture Collections, Public Health England. The cell line was cultured in RPMI-1640 supplemented with 5% Fetal calf serum (v/v) and 10 mM L-glutamine (Sigma, UK). According to standard procedures (recommended by company), cells were grown in 75 cm² tissue culture sterile polystyrene flasks (Sigma, UK) and maintained by incubating at 37°C in a humidified 5% CO₂ atmosphere.

Table 2-1 Reagents and supplements used for cell lines.

Reagents	Storage temperature (°C)	Components	Volume and Concentration	Suppliers
Roswell Park Memorial Institute, Culture Medium (RPMI-1640)	2-8	2.05 mM L-glutamine with 25 mM HEPES	1000 ml	Lonza,UK
Foetal calf serum (FCS)	-20	Heat inactivated FBS (5%)	55 ml	Sigma Aldrich,UK
L-glutamine	-20	8 mM L- glutamine	45 ml	Sigma Aldrich, UK
Phosphate buffer saline (1x)	2-8	8 g/l NaCl, 0.2 g/l KCl, 1.44 g/l Na ₂ HPO ₄ , 0.24 g/l KH ₂ PO ₄ , pH 7.4	2 ml	Fisher Chemicals, UK
Trypan blue	Room temperature	0.81% NaCl, 0.06% KH ₂ PO ₄		Sigma Aldrich, UK
Dimethyl Sulfoxide (DMSO)	Room temperature	99.5% DMSO, 0.81% NaCl		Sigma Aldrich, UK

2.2.1. Resuscitation of the cells

Each medium was pre-warmed at 37°C in a water bath for approximately 30 min before thawing the frozen ampoules of cells. These ampoules were stored in liquid nitrogen and appropriate Personal Protective Equipment (PPE) was used. Following the protocol of ECACC, ampoules of cell lines were partially opened in sterile conditions to release trapped nitrogen and then re-tightened. Cell lines were completely thawed at 37°C in a water bath for 1-2 min to minimise any damage to the cell membrane. Cells from cryotubes were resuspended in 2 ml of growth medium and centrifuged at 1000 rpm for 5 min. The supernatant was discarded and the pellet was resuspended in fresh medium. After determining the appropriate volume to attain seeding density, cells were resuspended in labelled 25 cm² flasks with the cell line name, passage number and date in a suitable volume of culture medium. The culture was mixed by shaking the flasks back and forth. These flasks were then incubated at 37°C with 5% CO₂ in filtered air and the medium was changed on alternate days. In order to maintain nutrient levels for slow growing cells, the medium was changed after every 48 hrs of incubation. Cells were observed under the light microscope with 10×magnification for monolayer growth of cells that were 70-80% confluent. Once they became 70-80% confluent, the cells were sub-cultured.

2.2.2. Subculture and cell library maintenance

After obtaining appropriate confluence of cells, the cell culture medium was aspirated and the cells were washed using 2-3 ml of PBS. 1-2 ml of trypsin solution provided by ECACC was added to partially detach the adhered cells from the flask bottom. Thereafter, cell scrapers were used to remove partially adhered cells from the walls of the flask. To ensure 95% cells detachment, the cells were observed under the

microscope. The media containing trypsin neutralising agent was added to the flask to deactivate the effect of trypsin. The media containing the cells was transferred to a centrifuge tube and centrifuged at 1000 rpm for 5 min to obtain the cell pellet. The supernatant media was discarded and the cell pellet was resuspended in 1 ml of fresh media.

2.2.3. Quantification of cells using haemocytometer

The 20 µl of cell suspension was aliquoted on a moistened haemocytometer. The cover slip was attached by applying pressure to obtain Newton refraction rings to ensure that the cover slip had affixed. The cell suspension was diluted by adding 0.4% trypan blue to stain the dead cells for determining the total number of live cells. The cell suspension mix was pipetted at the edge of the cover slip and was allowed to run under the cover slip. The stained cells were visualised under a light microscope in the haemocytometer grid using 20 × magnifications (Figure 2-2 shown below). Only cells from the middle square were counted and quantified. The cell count was recorded and calculations were carried out to determine the cell concentration per ml of cell suspension using the formula highlighted below:

$$X = Y \times df \times 10^4 \text{ cell/ml}$$

[Y is cell count in grid square, *df* is dilution factor]

df = 20: (total volume of Trypan blue + total volume of cell suspension)]

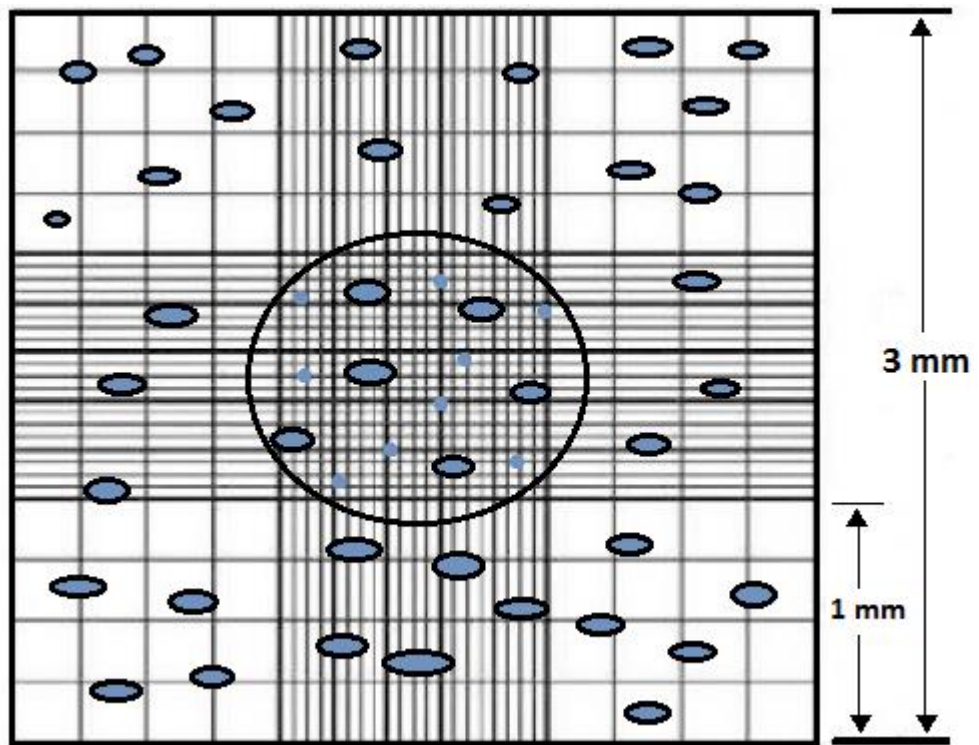


Figure 2-2 Diagram showing haemocytometer grid under microscope.

2.2.4. Cell viability assay

Methotrexate and Curcumin were dissolved in DMSO to provide a stock concentration of 10 mM and 20 mM, respectively. To calculate the inhibitory concentration (IC₅₀) of the drugs, the stock concentrations were further diluted in culture medium to achieve varying concentrations. These were added to cells and incubated for 72 hrs in order to determine the IC₅₀ and cell viability using HFLS-RA cells. CellTiter-Glo® Luminescent Cell Viability Assay determines the number of viable cells by quantifying ATP signals in the presence of metabolically active cells. Thus, cell viability was determined using CellTiter-Glo® Luminescent Cell Viability Assay (Promega, UK) according to the product protocol.

White flat clear bottom 96-well plates were seeded with 2×10^3 cells and incubated for 24 hrs. The cells were incubated for 72 hrs after treatment with increasing drug concentration. Each plate was allowed to equilibrate at room temperature for 30 min before the wells were emptied and 100 µl of fresh media and 100 µl of CellTiter-Glo reagent were added to each well and mixed for 2 min on an orbital shaker to induce cell lysis. The plates were then incubated at room temperature for 10 min to stabilize the luminescent signal before the luminescent signal was detected using Tecan GENios Pro® (Tecan, Austria) at an integration time of 0.25—1.00 second per well. The relative luminescence unit (RLU) emitted per cell was plotted against the concentrations.

2.3. Gene expression analysis

2.3.1. Drug treatment for microarray analysis

HFLS-RA cells were seeded in 75 cm² culture flasks 24 hrs prior to treatment. Cells were treated with IC₅₀ concentrations of MTX and Curcumin. The untreated cells (control) and drug treated cells were harvested after 48 hrs and stored in RNAprotect Cell reagent (Qiagen, UK) at -80°C. The cell samples were used for Gene expression analysis (IMGM Laboratories, Germany).

2.3.2. Total RNA isolation

RNeasy kit utilises selective binding properties of a silica-based membrane and speed micro spin technology. The specialised high-salt buffer system was used in this kit to obtain 100 µg of RNA. The biological sample was lysed and homogenised in the presence using guanidine-thiocyanate which prevents RNA degradation by inactivating RNases ensuring purification of intact RNA while ethanol is utilised to maintain appropriate binding conditions during the isolation process. Total RNA was isolated using the RNeasy Mini Kit (Qiagen) following the manufacturer's protocol described in Figure 2-3.

Cells were centrifuged at 300 × *g* for 5 min in order to remove cell medium. Buffer RLT and β-mercaptoethanol was added for cell lysis. Further, lysate was homogenised using QIAshredder spin column. 1 volume of 70% ethanol was added to the homogenised lysate and mixed well by pipetting. The sample (700 µl) was transferred to RNeasy spin column placed in 2 ml of collection tube and centrifuged for 15 s at 8000 × *g* (10,000 rpm). Buffer RW1 (700 µl) was added to the RNeasy spin column and centrifuged for 15 s at 8000 × *g* (10,000 rpm). RNeasy spin column was further washed by adding 500 µl RPE buffer and centrifuged for 15 s at 8000 × *g* (10,000 rpm). Buffer

RPE (500 μ l) was added to the RNeasy spin column and centrifuge for 2 min at $\geq 8000 \times g$ ($\geq 10,000$ rpm) to wash the spin column membrane. RNeasy spin column was transferred onto new 1.5 ml collection tube and RNase-free water (50 μ l) added directly on the spin column membrane. The lid was gently closed and centrifuged for 1 min at $8,000 \times g$ (10,000 rpm) and total RNA was eluted.

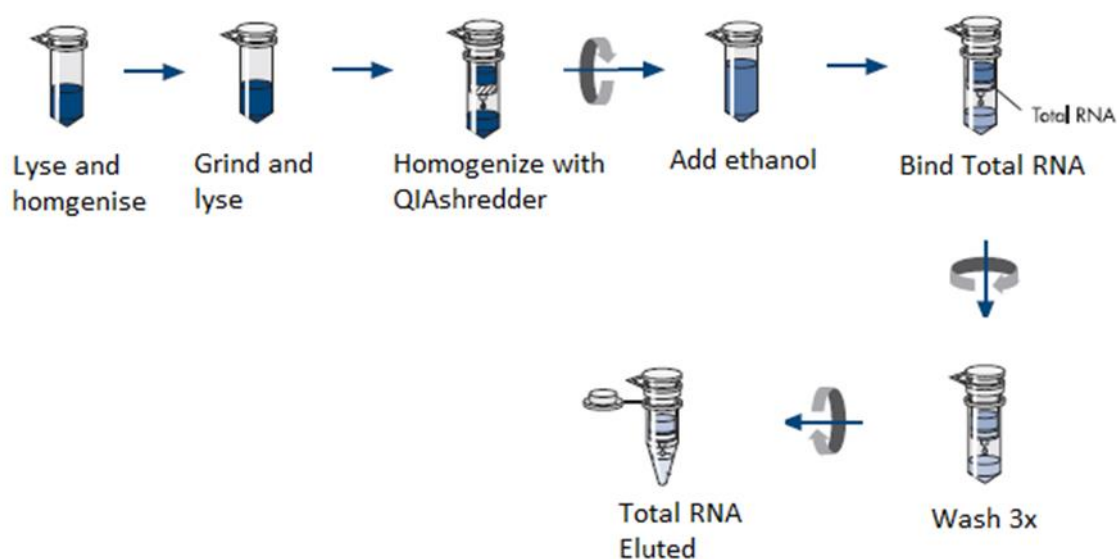


Figure 2-3 Schematic representation of the isolation of total RNA. (Adapted from Qiagen RNeasy protocol)

2.3.3. Determination of RNA concentration and Purity

The concentration and purity of RNA was determined by using NanoDrop ND-1000 spectral-photometer (peqLab). High quality Total RNA samples with A260/A280 ratio ≥ 1.9 and A260/A230 ratio of ≥ 1.0 were used for microarray analysis in order to eliminate contaminant interrupting data.

2.3.4. RNA integrity control

RNA integrity number (RIN) denotes quality of RNA samples. Total RNA samples was analysed using capillary electrophoresis to ensure quality of RNA. The 2100 Bioanalyzer

(Agilent Technologies) is microfluidic electrophoretic device which produces electropherograms by separating RNA according to fragment size and assesses the RNA quality (as shown in Figure 2-4). RIN integrity is calculated by measuring ribosomal-RNA ratio 28s /18s r-RNA along with the entire electrophoretic profile including the presence or absence of degradation products. RIN value is expressed ranging from 1 to 10 where 1 denotes high degradation and 10 indicates excellent RNA quality or intact RNA. As recommended by Agilent technologies, only total RNA samples with RIN values ≥ 7.5 were utilised for the labelling reaction to achieve high quality labelled RNA and evaluable microarray results. Also, samples with similar RIN values were used to assure data comparability.

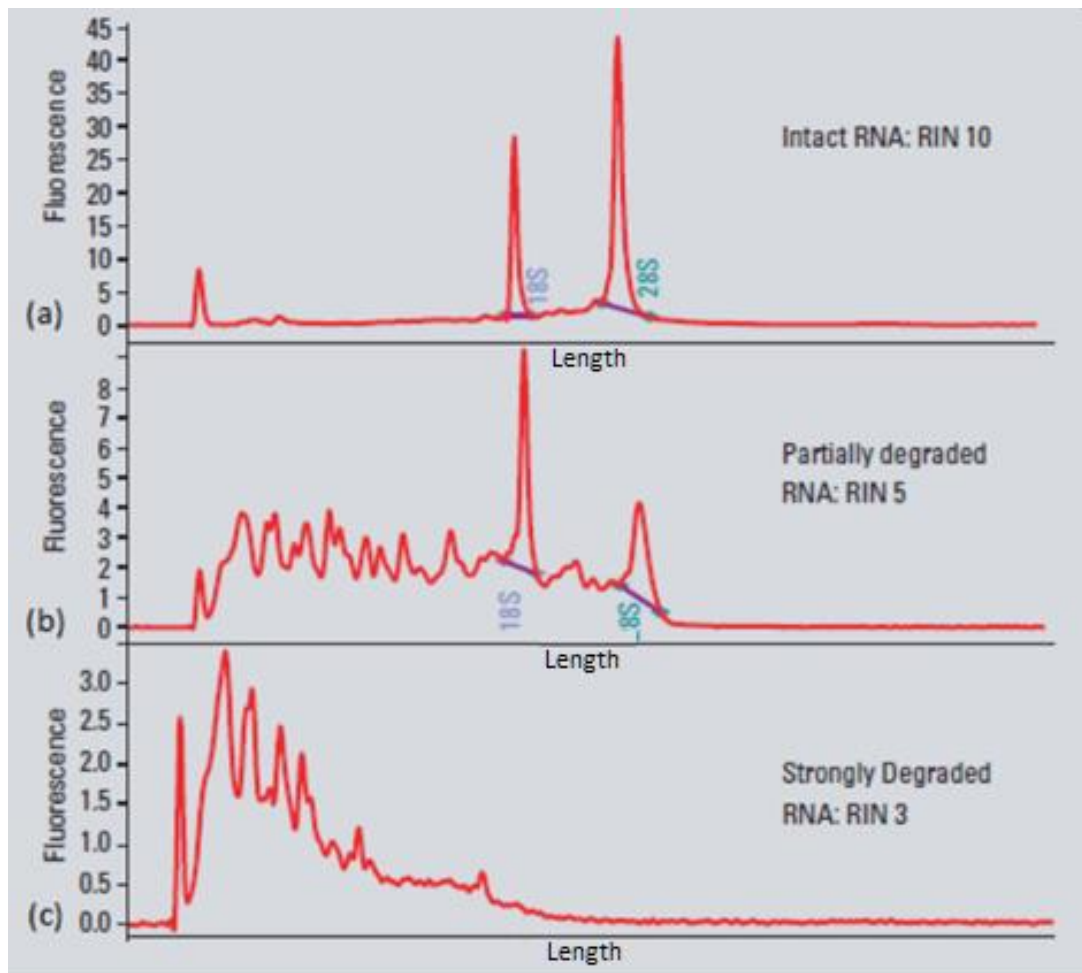


Figure 2-4 Typical electropherograms representing eukaryotic total RNA degradation analysed on 2100 Bioanalyzer (a) intact RNA (b) Partially degraded RNA (c) Degraded RNA (Adapted from Schroeder *et al.*, 2006)

2.3.5. Preparation of Cyanine-3 labelled cRNA

The Total RNA samples were spiked using One-color RNA Spike-in Mix (Product Number 5188-5282, Agilent Technologies) with *in vitro* synthesised polyadenylated transcripts to serve as positive controls for monitoring gene expression microarray flow from sample amplification and labelling to microarray processing and also to ensure linearity, sensitivity and accuracy throughout the experiments.

Further, the spiked total RNA (100 ng) was reverse transcribed into cDNA and then converted into Cyanine-3 labelled cRNA according to the manufacturer's instructions

Figure 2-5. Low input Quick Amp labelling kit (product no. 5190-2305, Agilent

technologies) was utilised for Reverse transcription *in vitro* transcription (RT-IVT). The method utilises T7 RNA Polymerase Blend for simultaneous amplification of target material and also incorporates Cyanine 3-CTP.

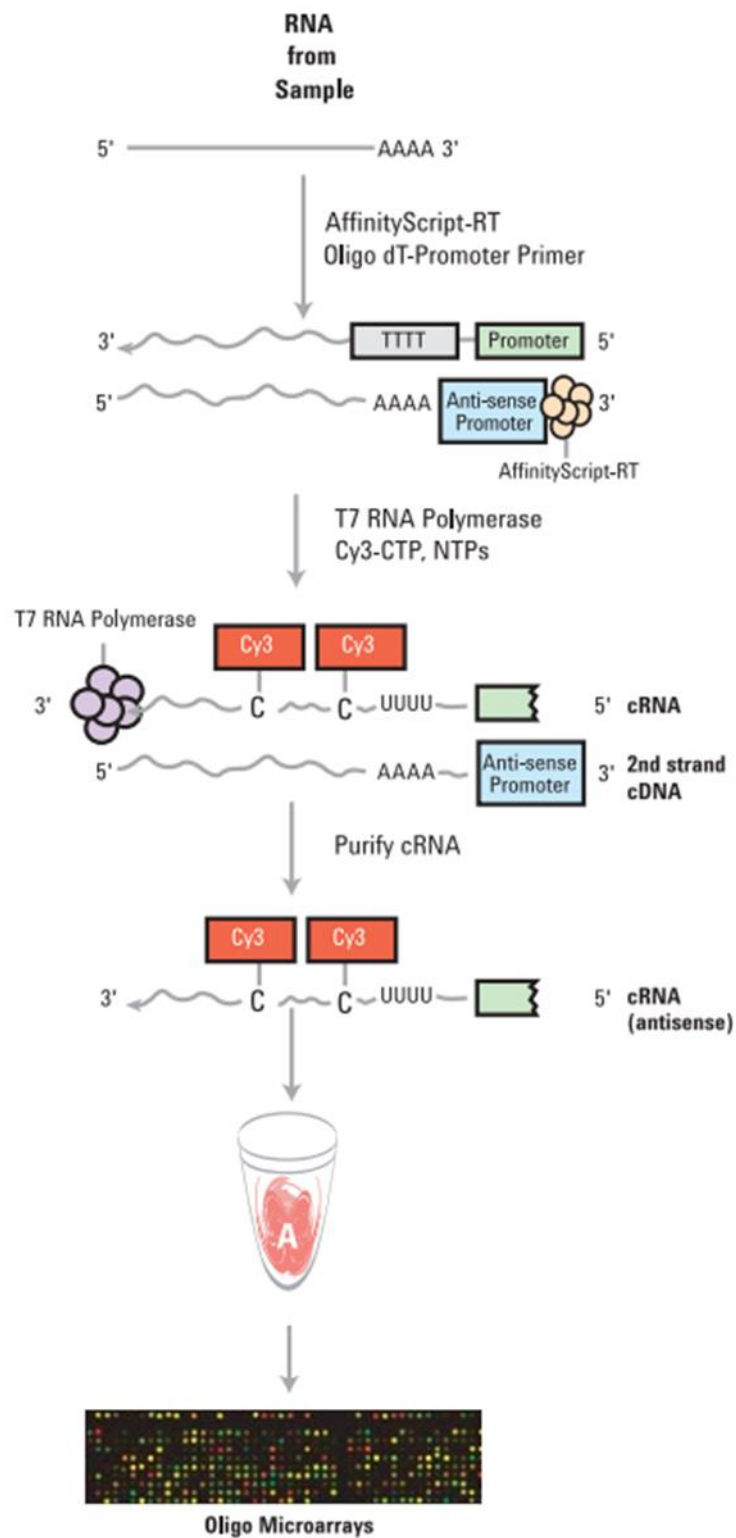


Figure 2-5 Schematic representation cRNA amplification procedure. (Adapted from Agilent technologies manual)

2.3.6. Quantification and quality control of labelled cRNA samples

The quality and integrity of Total RNA was assessed before producing cRNA. For the same reason, the integrity and quality of labelled non-fragmented cRNA was determined using RNA 6000 NanoChip kit (Agilent technologies) was used on the 2100 Bioanalyzer. Standard electropherograms for assessing cRNA have shown in Figure 2-6. A small initial hump followed by round curve with a few peaks indicates good quality of amplification and labelling.

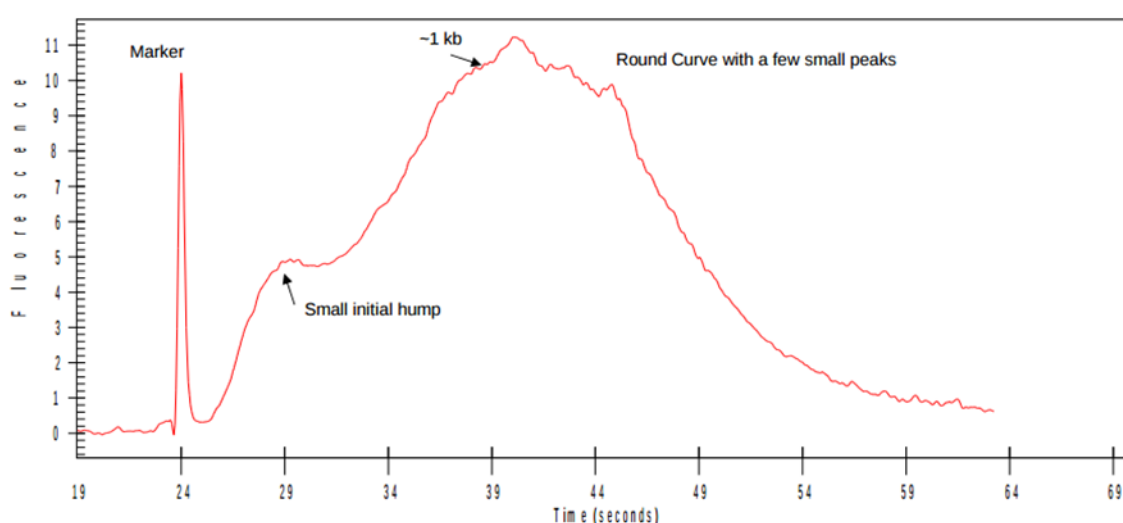


Figure 2-6 Example electropherograms of cyanine-3 cRNA analysed on 2100 Bioanalyzer

Further, cRNA concentration (ng/ μ l), RNA absorbance ratio (A260 nm: A280 nm) and Cyanine-3 (Cy3) dye concentration (pmol/ μ l) for each cRNA sample was determined and cRNA yield was measured based on the following calculation:

$$cRNA \text{ yield } (\mu\text{g}) = \text{concentration of cRNA (ng}/\mu\text{l}) * \text{volume of eluate}(\mu\text{l})/1000$$

The specific activity of dye incorporated in cRNA was calculated as described below:

$$\text{Specific activity (pmol}/\mu\text{l}) = \frac{\text{Concentration of cy3 (pmol}/\mu\text{l})}{\text{Concentration of cRNA (ng}/\mu\text{l})} * 1000$$

2.3.7. Microarray hybridisation

As recommended by Agilent technologies, samples with cRNA yields above 825 ng and specific activity above 6.0 pmol Cy3 per μg cRNA was used for 8 \times 60K arrays and hybridisation. This procedure was followed by the preparation of One-Color based hybridisation of the Cyanine-3-labelled cRNA sample. Cyanine-3-labeled cRNA sample (600 ng) was fragmented and prepared for One-color-based hybridisation. Following the manufacturer's protocol, samples were hybridised at 65°C for 17 hrs on separate Agilent SurePrint G3 Human Gene Expression version 2 8 \times 60K microarrays (AMADID 039494). Microarrays were washed with increasing stringency using Gene Expression Wash Buffers (Agilent Technologies) followed by stabilization and drying solution containing acetonitrile (SIGMA) to prevent ozone-related cyanine dye degradation affecting signal intensity. The fluorescent signal intensities were detected with Scan Control A.8.4.1. Software (Agilent Technologies) on the Agilent DNA microarray scanner and extracted from the images using Feature Extraction 10.7.3.1 software (Agilent Technologies) and the design file *039494_D_F_20140326*. Figure 2-7 describes the part of the work that was carried out by IMG M laboratories in Germany.

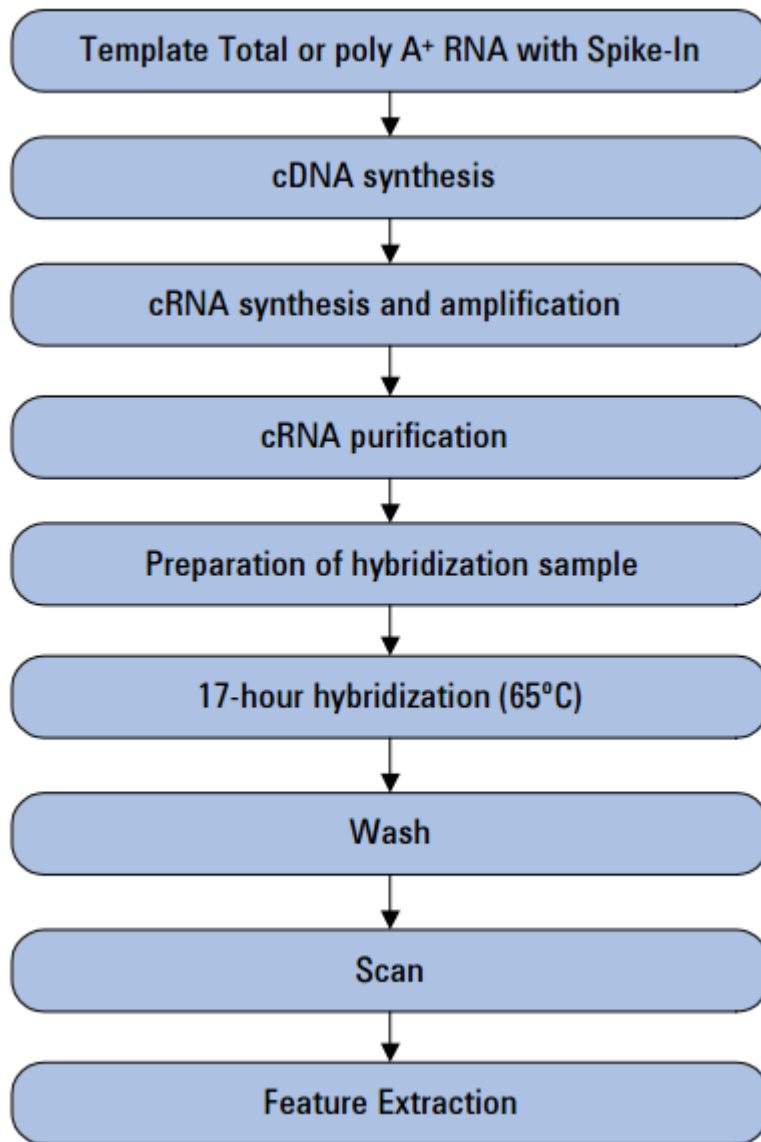


Figure 2-7 Workflow of sample preparation and microarray processing

2.3.8. Bioinformatics data analysis

This study used software tools Feature Extraction 10.7.3.1, GeneSpring GX 12.6.1 (Agilent Technologies), Excel 2010 (Microsoft) and the IMG/M internal tool marfin v1.9 for quality control, statistical data analysis, transcript annotation and visualization.

Quantile data normalization was applied to each data set in order to eliminate irregular noise and to maintain signal intensities to uniform levels enabling comparison of microarray for downstream analysis. After the application of quantile normalization the data was visualised as log₂ transformed manner (after normalization) or as raw data (before normalization).

After normalization, correlation between and within the sample groups was determined. Correlation analysis enabled analysing similarity between the samples. Pearson's correlation coefficients (r) were calculated for all biological replicates within the groups and for all pairwise comparisons of the samples in the experiment. In general, samples representing the same experimental conditions are expected to be similar but samples with different experimental conditions may not show similarity. Therefore, Correlation coefficient heat map were produced to demonstrate relation between different samples.

After normalization, the microarray probe data was filtered according to flag information provided by Feature Extraction 10.7.3.1 software and further classified as 'compromised' if probe was not significantly distinguishable or 'Not Detected' if it indicates unequal saturation/ non-uniformity.

The raw data was produced by calculating the average with replicated sample log₂ transformed data. Three pairwise sample comparisons were analysed. HFLS-RA untreated cells were used as a reference group and the gene expression data of

methotrexate-treated HFLS-RA, curcumin-treated HFLS-RA and HFLS-RA cells treated with both methotrexate and curcumin, respectively, were compared.

2.3.9. Statistical analysis of microarray data

Welch's approximate Student's t-test was applied to the comparison of different groups which produces a p-value (p). Benjamini and Hochberg False Discovery Rate (FDR) adjustment algorithm was applied to avoid multiple testing errors which could usually occur when there are more standard probes compared to analysed samples. The corrected p values were determined. Sample groups were then compared in pairwise manner in order to achieve the differential expressions between the groups by calculating fold change (FC). The ratio of raw values between the groups was calculated.

Using Feature Extraction 10.7.3.1 software robust differentially expressed probes were detected which screens only probes that are reliably detectable in at least one out of all samples of the two compared groups. Following statistical analysis, data sets were further filtered by applying different stringency levels:

a) Detection filtering in which a probe is only considered if it is reliably detected in at least 60% of the samples of one of the two compared groups.

b) Statistical significance in which a probe with a corrected p-value is ≤ 0.05 is only classified as induced if it has a Fold change value ≥ 2 or repressed if it has a Fold change value ≥ -2 .

The multiple testing errors were not taken into consideration while applying Non-stringent filtering.

2.4. Gene transcription technique

2.4.1. The mRNA isolation

The mRNA isolation kit (Roche-Diagnostics, Germany) used for isolation of mRNA from cultured cells utilises posttranscriptional polyadenylation. Length of the poly (A)⁺ tails shortens from 200 nucleotides (approximate initial size) to 40 – 65 adenylate residues during aging of mRNA. These poly (A)⁺ tails helps differentiate between polyadenylated RNA species from non-polyadenylated RNA (such as rRNA and tRNA). The Principle of this kit is described in Figure 2-8 and the reagents and buffers used in this study are listed in Table 2-2 - Table 2-3. The poly (A)⁺ tail of 3'-ends of the mRNA is hybridised to a biotin-labelled oligo (dT)₂₀ probe and captured using streptavidin-coated magnetic particles while non-adenylated RNA species bound weakly and easily washed off. The mRNA bound to streptavidin particles is eluted by lowering salt concentration.

Following the quantification of the cultured cells approximately 2×10^6 cells were pelleted and stored in RNA protect reagents to be used for mRNA isolation. The 200 μ l of ice cold PBS was used to wash thawed cells in order to remove excess reagents. Simultaneously in sterile eppendorf tube 50 μ l of thoroughly mixed Streptavidin Magnetic Particles (SMP) were aliquoted. The SMPs (50 μ l) were separated from the storage buffer using magnetic separator and storage buffer was discarded. The SMPs were washed in 70 μ l of lysis buffer and then separated to remove the buffer. Lysis buffer (500 μ l) was added to the cell samples and mechanically sheared six times using 21-gauge needle (1 ml). On the 6th time, samples was transferred to eppendorf tube containing SMPs. Biotin labelled oligo (dT)₂₀ (0.5 μ l) was added to these samples and incubated at 37°C in water bath for 5 min for immobilisation of the hybridisation mix. Samples were incubated at room temperature on magnetic separator and lysate was

discarded. Samples in SMPs were washed thrice with 200 μ l washing buffer and was placed on magnetic separator each time to discard washing buffer. Samples were centrifuged and placed on magnetic separator to remove remaining buffer. On addition of 10 μ l redistilled water, samples were incubated at 65°C for 2 min. The magnetic separator was used to elute mRNA by separating from the SMPs. mRNA was transferred to labelled eppendorf tube and then stored at -20°C.

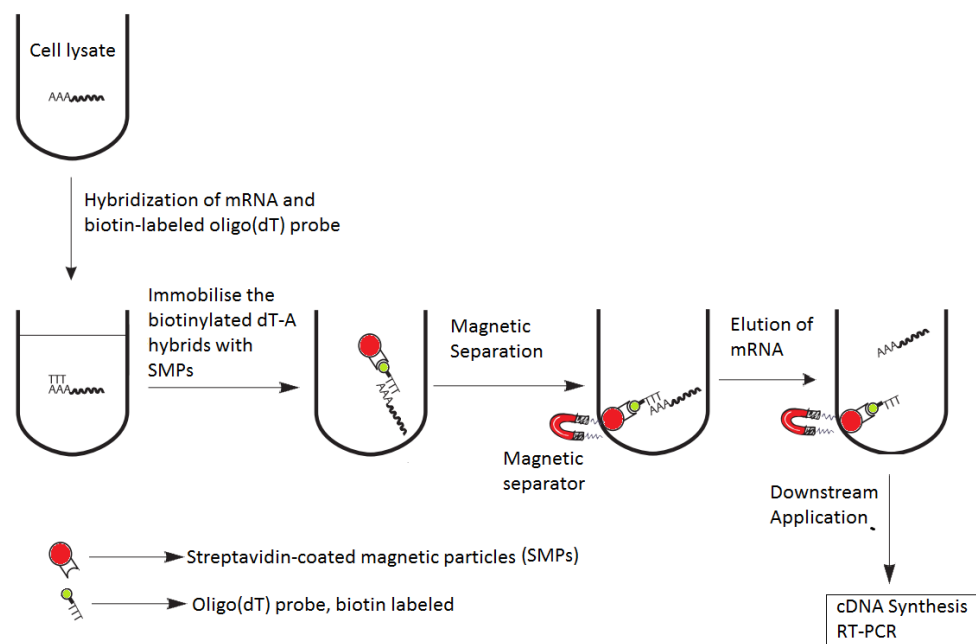


Figure 2-8 Experimental protocol for the mRNA isolation technique. The poly (A)⁺ tail of mRNA hybridized to a biotin-labelled oligo (dT)₂₀ probe and captured using streptavidin coated magnetic particles and these magnetic particles were removed using a magnetic separator. After washing with PBS, mRNA was eluted and incubated in redistilled water. (Taken from mRNA isolation kit manual Roche Applied Sciences, UK 2014).

Table 2-2 Reagents and buffers used for mRNA isolation (Roche applied sciences, UK)

Reagents	Contents
PBS	Ice cold, pH 7.4
Lysis Buffer	0.1 M Tris buffer, 0.3M LiCl, 10 mM EDTA, 1% lithium dodecylsulfate, 5mM DTT (dithiothreitol), pH 7.5
Biotin-labelled Oligo(dT) ₂₀ probe	100 pmol biotin-labeled Oligo(dT) ₂₀ per µl of redistilled water
Streptavidin Magnetic Particles (SMPs)	Suspension of 10 mg/ml in 50 nM Hepes, 0.1% BSA, 0.1% chloracetamide, 0.01% methylisothiasolone, pH 7.4
Washing Buffer	10 mM Tris buffer, 0.2 M LiCl and 1 mM EDTA, pH 7.5
Redistilled Water (PCR Grade)	RNase free
Storage buffer	10 mM Tris buffer, 0.1% chloracetamide, 0.01% methylisothiasolone, pH 7.5

Table 2-3 Volumes of reagents and buffer used for mRNA isolation of 2×10^6 cells.

Number of cells (2×10^6)	Volume (µl)
PBS	200
Lysis buffer	500
Biotin-labelled Oligo(dT) ₂₀ probe	0.5
Volume of SMPs	50
Lysis buffer (preparation of SMPs)	70
Washing buffer	200 (× 3)
Redistilled water	10

2.4.2. The mRNA Quantification using NanoDrop spectrometer

Thermo scientific NanoDrop 2000 Spectrophotometer was used to carry out the mRNA quantification and purity analysis. The instrument employs patented sample retention technology by utilising surface tension to hold sample in place and measure with high accuracy and reproducibility by utilising 1 μ l sample. Sample was loaded on pedestal with fibre optic cable (the receiving fibre) and second fibre optic cable (the source fibre) was closed to bridge the gap between the fibre optic ends allowing spectrophotometer to analyse light passing through the liquid sample. This instrument helped to eliminate the use of cuvettes and also limits contamination since it is easy to clean.

After cleaning NanoDrop, application module settings were changed from Nucleic acid to RNA and a volume of 1 μ l Distilled water was loaded on sampling arm between the receiving fibre and the source fibre was then brought into contact with the liquid sample causing the liquid to bridge the gap between the fibre optic ends. A spectrophotometer utilized linear CCD (Charged Coupled-Device) array to analyse light passing through the liquid sample and this was set as a blank. The mRNA sample was loaded to measure and 260:280 (nm) value and ng/ μ l was recorded to check purity of mRNA. The mRNA purity between 260:280 values must be in the range of 1.5-2.00 which signified good purity.

2.4.3. Complimentary DNA (cDNA) synthesis

The isolated mRNA was reverse transcribed using First strand cDNA synthesis kit. This kit utilised the AMV (Avian Myeloblastosis virus) enzymes isolated from Avian Myeloblastosis which synthesizes the new cDNA strand at the 3'-end of the poly (A)-mRNA where oligo dT was used as a primer. From the concentration of mRNA obtained, specific volume of the solution was determined which contained the 100 ng mRNA. The quantity of 100 ng was required to be maintained as a constant quantity for preparation of all samples.

The Protocol of Roche applied sciences was followed to synthesise first strand cDNA. All reagents and samples were maintained at room temperature while the RNase inhibitor and AMV reverse transcriptase were kept on ice during the experiment. In order to avoid contamination, all equipment used for the experiment were autoclaved. The master mix of 11.8 μ l was prepared using reagents provided in first cDNA synthesis kit (Roche applied sciences, UK) (Table 2-4). The quantified amount of mRNA (100 ng) was added, followed by the addition of sterile water to attain a final volume of 20 μ l in each sample and the mixture was briefly vortexed and centrifuged.

The experiment samples were first incubated at 25°C for 10 min for the primer to anneal to the mRNA template. During the second incubation at 42°C for 60 min, mRNA was reverse transcribed to cDNA and following incubation at 99°C for 5 min, AMV Reverse Transcriptase denatured on incubation. Sample was then cooled to 4°C for 5 min and stored at -20°C.

Table 2-4 Reagents used in first strand cDNA synthesis for one sample.

Reagents	Volume of reagents (μl)	Final concentration
10 \times Reaction buffer	2.0	1 \times
25 mM Magnesium Chloride	4.0	5 mM
Primer Oligo-p(dT) ₁₅	2.0	0.04 A ₂₆₀ units (0.06 μ g)
RNAse inhibitor	1.0	50 units
AMV-Reverse Transcriptase	0.8	\geq 20 units
Deoxynucleotide mix	2.0	1 mM

2.4.4. Gene sequence and Primer design

Using GeneCards database, gene locations were determined. The mRNA sequences for each of the 13 gene were obtained using NCBI database. In order to carry out a study of genes using polymerase chain reaction (PCR), the specific primer is required to amplify the gene replication. This primer was designed using the Primer-BLAST online software provided by NCBI. The Table 2-5 shows the parameters used while designing the primer for the specific mRNA sequence.

Table 2-5 Primer design parameters

Amplicon size	Less than 200 base pairs
Tm	57-63 (Tm difference less than 1)
Max Tm difference	1 >
Exon junction span	Primer spanning exon-exon junction where possible
Ending	C or G at the end of Primer
GC content	50-60%
Self-complementary	Less than 3.00

2.4.5. Primer preparation

Primers were synthesised by TIB MOLBIOL (Berlin, Germany). Each primer (sense and antisense) was dissolved in 250 µl of molecular biology grade water to obtain 20 µM stock solutions and stored at -20°C as recommended by the manufacturer. Annealing temperature of Primers were used using Primer-BLAST recommendations as mentioned in Table 2-6..

Table 2-6 Primer sequence, annealing temperatures and amplicon size for all the 13 genes used in qRT-PCR.

Gene	Primer sequence	Annealing Temperature (°C)	Amplicon size (base pair (bp))
ANGPTL7	Sense: 5' – GTGTAGAGATGGAGGACTGGG – 3' Antisense: 5' – AACTGGAGGGCGTCGTTC – 3'	58	137
CD248	Sense: 5' – CCATCAAATCTCTGTGCCTGC – 3' Antisense: 5' – GTCTGGTTAGTGGGGCTCTG – 3'	59	87
CH25H	Sense: 5' – CACCCTGACTTCTCGCCATC – 3' Antisense: 5' – CACGGGGAACACAAACATCAC – 3'	59	87
CXCL12	Sense: 5' – GACAAGTGTGCATTGACCCG – 3' Antisense: 5' – CTCATGGTTAAGGCCCCCTC – 3'	58	173
CYTL1	Sense: 5' – AGATCACCCGCGACTTCAAC – 3' Antisense: 5' – GTACAGCCTGGGCAGGTATC – 3'	58	77
IFITM1	Sense: 5' – CGCCAAGTGCCTGAACATC – 3' Antisense: 5' – GTCACAGAGCCGAATACCAGT – 3'	58	87
IL7	Sense: 5' – GTGACTATGGGCGGTGAGAG – 3' Antisense: 5' – GCTACTGGCAACAGAACAAGG – 3'	59	141
COL14A1	Sense: 5' – AGACGAGGTGGTGGTAGATG – 3' Antisense: 5' – AGCAGTGTGGGCATAGATTG – 3'	56	106

Gene	Primer sequence	Annealing Temperature (°C)	Amplicon size (base pair (bp))
<i>BCAR4</i>	Sense: 5' – ACCAGTGACCTTGAGTGAAC – 3' Antisense: 5' – CTTGGGTGGGGATAGTGATTG – 3'	57	84
<i>CD274</i>	Sense: 5' – CTATGGTGGTGCCGACTACA – 3' Antisense: 5' – AGGACTTGATGGTCACTGCT – 3'	56	174
<i>RELT</i>	Sense: 5' – AACTTGCGGTGTGAGGG – 3' Antisense: 5' – CATAAGGAAGCAGGACAGGG – 3'	53	139
<i>HSPA6</i>	Sense: 5' – AATCTGTCGCCCCATCTTCTC – 3' Antisense: 5' – GCCCATAGCATAGCCCTGAC – 3'	59	174
<i>OTP</i>	Sense: 5' – CTTGGTTGTTTTGTGGTGGTC – 3' Antisense: 5' – CAGGGTTGTAGATGTCCGAGTG – 3'	62	91

2.4.6. Quantitative real time polymerase chain reaction (qRT-PCR)

The qRT-PCR is a technique enabling consistent detection and quantification of products generated during each cycle of the PCR process. It exponentially amplified short DNA sequences (usually less than 200 bases) within a longer double stranded DNA molecule. Thus, it enabled detection of very low copies of the target-specific product amplification (Roche Applied Science, UK). The genes were amplified by performing qRT-PCR on the Applied Biosystems 7500 Real Time PCR system. The experiments were carried out using LightCycler® FastStart DNA Master PLUS SYBR Green I kit following the manufacturer's instructions. LightCycler reaction Master Mix was prepared by using the reagents from the kit provided that includes 1a (white cap) FastStart Enzyme and 1b (Green Cap) FastStart DNA Master^{PLUS} Reaction Mix. A volume of 14 µl of 1a was pipetted into 1b. The 1b was re-labelled as 1 to prepare the master mix which was stored at 4°C and protected from light.

The reagents and samples were thawed and kept on ice throughout the experiment. PCR enzyme master mix was made from components of the LightCycler® FastStart DNA Master PLUS SYBR Green I kit (Table 2-7) with the recommended volume for each sample. PCR master mix was briefly centrifuged. The reaction tubes with clear caps were placed on the adapter 2 µl cDNA sample was loaded in each tube. Reaction tubes were centrifuged for a minute and then transferred to the instrument.

Table 2-7 Components required for LightCycler® FastStart DNA Master PLUS SYBR Green I kit sample preparation for qRT-PCR primer mastermix.

Components	Volume (µl)
Molecular biology H ₂ O, PCR grade	12
PCR Primer mix (Left + Right Primer)	2 (1 µl + 1µl)
PCR enzyme master mix	4
cDNA template	2

Following the settings described in Table 2-8, the qRT-PCR run was carried out. This protocol involved several steps which played an important role. Pre-incubation, FastStart DNA polymerase was activated and DNA was denatured. This also increased PCR specificity and sensitivity by preventing non-specific elongations. Target DNA was amplified and melting provides melting curves for analysis of the PCR product. The final step involved cooling of the rotor and the thermal chamber where PCR product is placed.

Table 2-8 Applied Biosystems 7500 Real Time PCR system thermal profile for qRT-PCR

Stage		Temperature (°C)	Hold time	Repeat
Initiation		50	2:00	1
Pre-incubation		95	10:00	1
Amplification	Denaturation	95	0:10	45
	Annealing	Variable to (refer table primers)	0:10	
	Extension	72	0:45	
Dissociation		95	0:15	1
		60	1:00	
		95	0:15	
		60	0:15	

2.4.7. Copy Number Quantification

Copy number standard curve (Figure 2-9) was generated to calculate the copy numbers of the unknown samples by plotting the crossing point or Ct value against copy numbers. In a real time PCR a positive reaction is detected by accumulation of a fluorescent signal. The Ct (cycle threshold) is defined as the number of cycles required for the fluorescent signal to cross the threshold (clearly exceed background noise level). This standard curve was previously established in our laboratory.

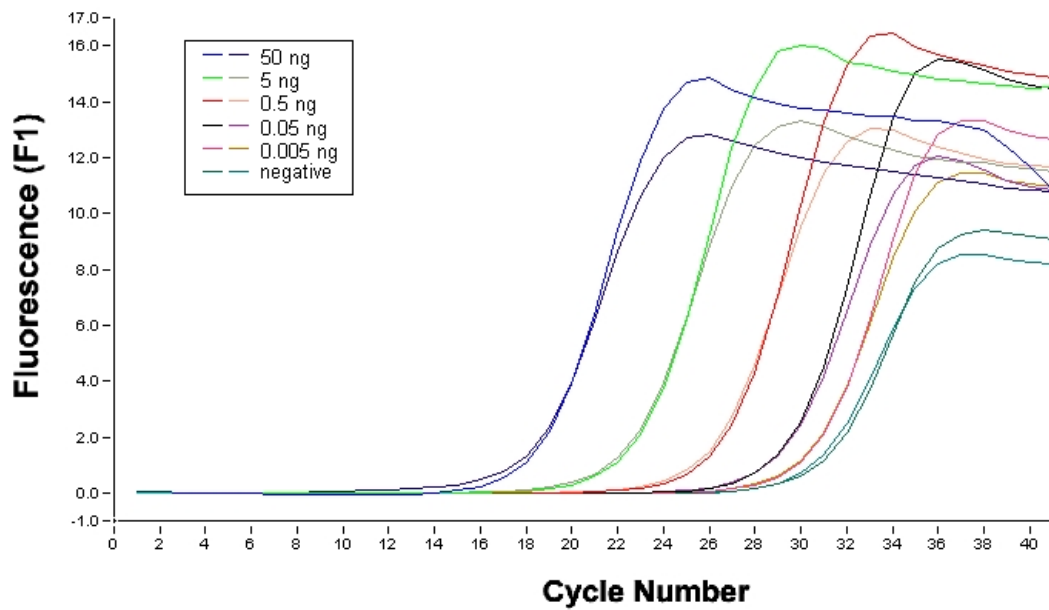
The external standard of known concentration or copy number was used to accurately determine amount of target amplicon. Previous experiments have established the quantification of copy numbers from the crossing point by using genomic DNA as a template. A standard curve was plotted for the quantitative method established on the Applied Biosystems 7500 Real Time PCR system. A standard genomic DNA (Qiagen, UK) with known concentration of 1 µg equivalent of 3.4×10^5 copies of a single gene was prepared using five concentrations (5 pg, 50 pg, 500 pg, 5 ng and 50 ng,

Table 2-9). Further amplification was achieved by using *GAPDH* reference gene with its threshold cycle (Ct) numbers in order to plot the standard curve. The reference genes are constitutively expressed genes which are necessary for the basic cellular function maintenance, and are expressed in all cells under normal and pathophysiological conditions. The equation generated ($y = -1.3124\ln(x) + 32.058$) from the standard graph was rearranged to $(=EXP \{Ct \text{ value}-32.058\}/-1.3124)$ to determine the copy numbers of the mRNA expression of all the genes used throughout the study.

Table 2-9 Genomic DNA correspondence to its average Ct values and equivalent copy number.

Genomic DNA concentration (ng)	Dilution factor	Average Crossing point (Ct)
50	17000	18.3
5	1700	22.6
0.5	170	26.42
0.05	17	29.12
0.005	1.7	30.15

(a)



(b)

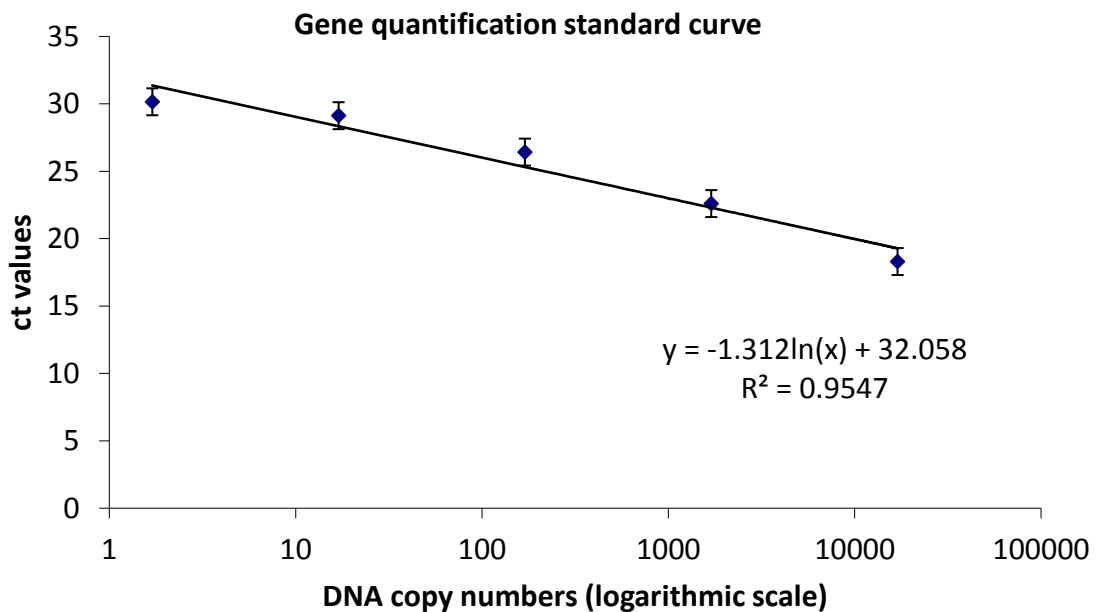


Figure 2-9 Standard to calculate the copy number of the targeted gene. (a) Light Cycler quantification curve generated with known concentration of genomic DNA amplified, showing that the higher the concentration of DNA the lower the Ct values. The negative control (Primer alone) shows no fluorescence acquisition until after 30 Ct (straight line). (b) The standard generated from the crossing points showing the relationship between Ct values and the copy numbers of the amplified genomic DNA using GAPDH as a reference gene (n=3).

2.4.8. Analysis of RT-PCR amplicons using agarose gel electrophoresis

Gene expression was determined by running PCR products of cDNA samples on 2% agarose gel electrophoresis (AGE). Agarose (0.8 g) was dissolved in 40 ml of 1× TAE buffer to obtain 2% agarose gel. This solution was heated in a domestic microwave at 700 W power for 2 min until agarose particles were thoroughly dissolved. The solution was then poured into casting tray set with comb and cooled for 45 min to set gel. The comb was removed after solidified of the agarose gel and was placed into electrophoresis gel tank. 1× TAE running buffer (300 ml) was poured into gel tank until the level to cover the gel. The loading sample contained 2 µl of loading dye and 5 µl of PCR products sample amplicons. A volume of 5 µl of 100 bp molecular marker was loaded along with samples to determine the molecular weight as standard at 50 V for approximately 1 h. The gel was stained with 0.5 µg/ml of Ethidium bromide (EtBr) for 30 min, followed by destaining in water for 20 min. The bandings patterns were observed using a GENE GENIUS Bioimaging system, UK and Gensnap software (Syngene, UK).

2.5. Quantitation of IL6 protein

2.5.1. Assay principle

IL6 ELISA kit employs the quantitative sandwich enzyme immunoassay technique to determine IL6 concentration in cell culture medium. A monoclonal antibody specific for human IL6 are pre-coated onto a microplate wells in order to capture IL6 present in standards and samples pipetted into the wells. After washing away unbound substances, an enzyme-linked polyclonal antibody specific to human IL6 is added which bound to the adhered IL6. The substrate solution which produces colour proportionate to the amount of IL6 was added to the well. The colour development is stopped using stop solution which develops end-point colour. The intensity of colour is measured at 450 nm using microplate reader. The cells were treated with respective drugs for 48 hrs and supernatant was obtained for IL6 ELISA. The particulates were removed by centrifugation and sample aliquots were stored at ≤ -20 °C.

All reagents and working standards were prepared according to manufacturer's protocol. 100 μ L of Assay Diluent RD1W was added to each well. 100 μ L of Standard, sample and control were added to appropriate wells. Wells were covered with the adhesive strips provided. The plates were incubated for 2 hours at room temperature. Each well was aspirated and washed four times by filling each well with 400 μ L of Wash Buffer. Any remaining Wash Buffer was removed by decanting wells and by inverting the plate and blotting it against clean paper towels. 200 μ L of Human IL6 Conjugate was added to each well and then covered with a new adhesive strip. The wells were further incubate for 2 hours at room temperature. Washing was repeated as before and 200 μ L of Substrate Solution was added to each well. Wells were covered and incubated for 20 minutes at room temperature while protecting them from light. 50 μ L

of Stop Solution was added to each well which turned the colour in the wells blue to yellow. The plates were gently tapped to ensure thorough mixing. The optical density was measured using a microplate reader set to 450 nm with correction wavelength set to 570 nm.

The standard curve fit was created using the optical density obtained from standards. The standard curve generated equation which was used to determine the concentration of IL6 protein in untreated/treated samples.

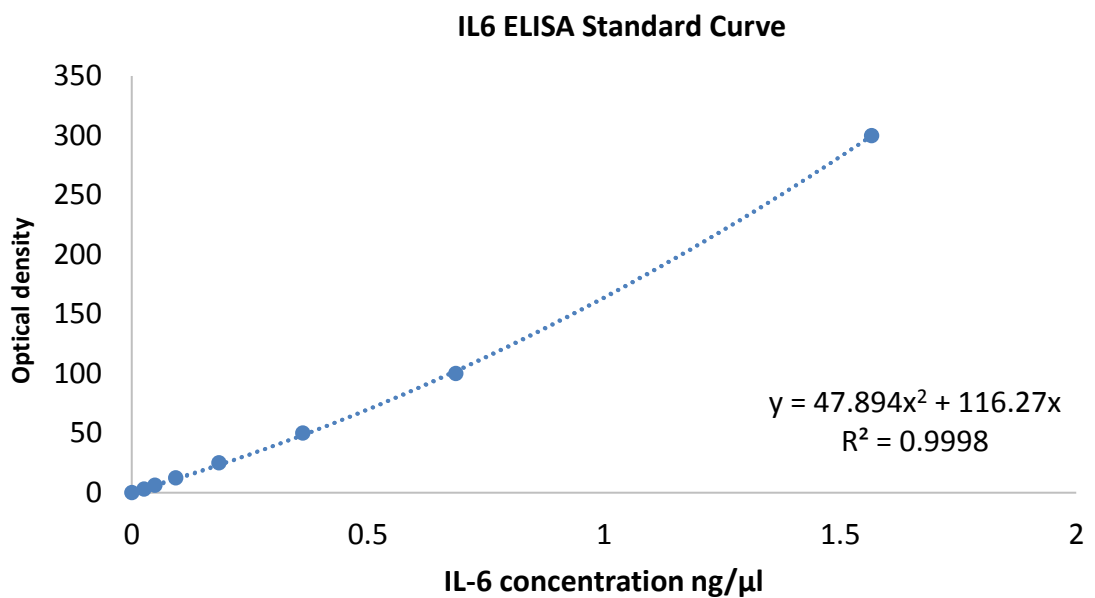


Figure 2-10 IL6 ELISA Standard Curve

CHAPTER 3

RESULTS

3.1. RP-HPLC stability indicating studies

3.1.1. Analytical Method Validation

3.1.1.1. Linearity

The Linearity data obtained is presented in Table 3-1. The linear regression showed coefficient of determination (r^2) for each analysis.

Table 3-1 Linearity Data. (n=3)

Compound		equation	Slope	Coefficient of determination (r^2)
MTX		$y = 58.87x + 4.82$	58.87	0.9993
Curcumin		$y = 76.83x - 3.97$	76.83	0.9998
Combination	MTX	$y = 56.70x - 37.76$	56.70	0.9999
	Curcumin	$y = 84.89x - 13.14$	84.89	0.9998

3.1.1.2. Limit of Detection (LOD) and Lower Limit of Quantification (LLOQ) of stability indicating method

The LOD and LLOQ values for Curcumin and MTX were found to be consistent when analysed individually and as a combination. The LOD and LLOQ values for both MTX and curcumin are presented in Table 3-2.

Table 3-2 LOD and LLOQ concentrations. (n=3)

Compound	LOD (nM)	LLOQ (nM)
MTX	77	307
Curcumin	106	424

3.1.1.3. Intraday and Interday precision for the stability indicating method

The intraday and interday evaluation established the repeatability and reproducibility of the system as the Relative Standard Deviation (RSD) obtained for both Curcumin and MTX was found to be consistent at concentrations 20 µg/ml, 50 µg/ml and 70 µg/ml as shown in Table 3-3.

Table 3-3 Intraday and Interday precision for HPLC analysis of MTX and curcumin.

Compound		Concentration (µg/ml)	Intraday (n= 3)		Interday (n=3)	
			Mean (µg/ml)	RSD	Mean (µg/ml)	RSD
MTX		20	20.45	0.35	20.20	0.89
		50	49.59	1.49	50.15	1.68
		70	70.44	0.78	69.55	1.66
Curcumin		20	20.26	0.62	20.30	1.20
		50	49.73	0.71	50.47	0.84
		70	70.36	1.29	69.63	1.32
Combination	MTX	20	20.65	1.03	20.45	1.33
		50	50.45	1.07	49.89	1.13
		70	69.98	0.55	69.53	0.88
	Curcumin	20	20.63	1.25	19.89	1.46
		50	50.10	0.65	49.73	0.85
		70	70.36	0.49	69.89	1.09

3.1.2. Forced Degradation Studies

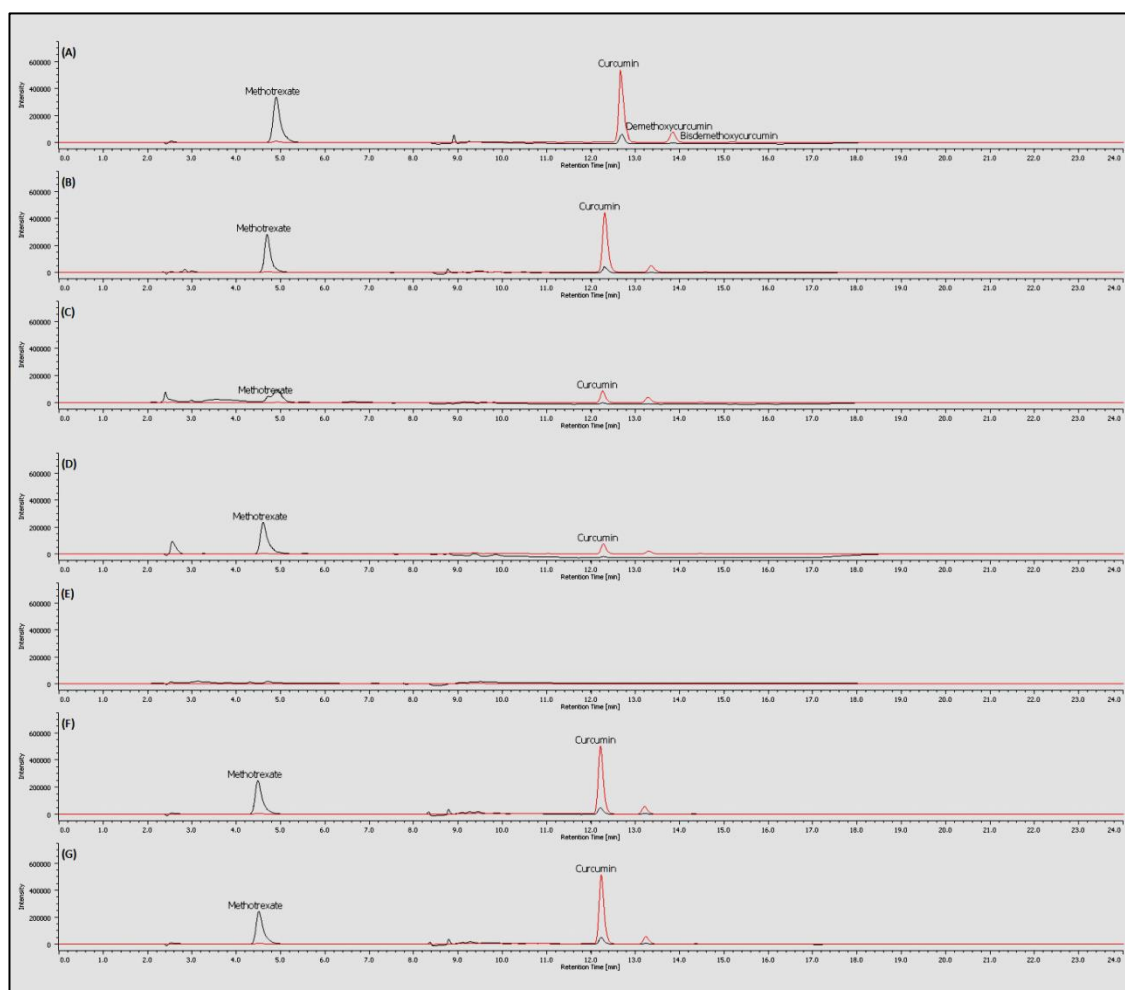


Figure 3-1 Chromatograms showing elution of 50 $\mu\text{g/ml}$ MTX (at 305 nm) and 50 $\mu\text{g/ml}$ Curcumin (at 430 nm) under different conditions. (A) Standard untreated compounds, (B) Compounds treated with 0.1 M HCL for 30 days, (C) Compounds treated with 0.1 NaOH for 5 days, (D) Compounds treated with 3% H_2O_2 for 5 days, (E) Compounds treated with UV radiation for 3 hours, (F) Compounds treated with 75% humidity at 40°C for 10 days, (G) Compounds treated with dry heat at 70°C for 10 days

3.1.2.1. Acid Degradation

The partial degradation of both compounds was observed when treated individually and as a combination. The recovery was found to be inversely proportional to the rise in temperature. All degradation products were eluted before 12.32 min. and no degradation peaks were found to interfere with the peaks corresponding to the two compounds of interest. The percent recovery obtained is shown in Table 3-4.

3.1.2.2. Base Degradation for stability indicating method

The degradation observed in both compounds was again found to increase with rise in temperature (Table 3-5). Notably, Curcumin was completely degraded after only 24 hours and 48 hours at 70°C and 40°C, respectively. The degradation products were detected before 12.32 min. with major degradation products being eluted within first 4 min. No degradation peaks were found to interfere with the peaks corresponding to the two compounds of interest.

Table 3-4 Acid Degradation for stability indicating method. (n=3)

Compound (50 µg/ml)		Temperature (°C)	% Recovery determined on days indicated						
			1	2	5	10	20	30	60
MTX		RT	97.98	96.48	97.69	96.25	96.54	95.73	94.78
		40	96.52	95.21	92.33	86.61	77.13	73.15	72.43
		70	81.13	58.16	25.11	2.93	1.95	1.61	1.60
Curcumin		RT	99.59	99.15	97.70	95.55	86.97	84.58	84.58
		40	96.82	92.39	87.16	75.58	66.87	59.92	59.92
		70	75.66	62.13	34.08	19.74	5.44	0.33	0.33
Combination	MTX	RT	95.10	94.84	93.67	94.45	94.42	92.46	91.54
		40	94.90	94.17	90.73	86.56	80.36	75.41	74.67
		70	77.34	65.37	43.74	10.26	5.95	0.40	0.39
	Curcumin	RT	98.71	96.91	95.86	95.55	90.16	84.71	80.48
		40	96.38	93.28	85.69	75.01	61.52	53.33	49.12
		70	50.10	38.19	15.88	3.70	0.53	0.52	0.00

Table 3-5 Base Degradation for stability indicating method. (n=3)

Compound (50 µg/ml)		Temperature (°C)	% Recovery determined on days indicated		
			1	2	5
MTX		RT	63.72	51.46	42.41
		40	39.95	0.00	
		70	27.98	0.00	
Curcumin		RT	78.40	60.46	20.23
		40	4.53	0.00	
		70	0.00	N/A	
Combination	MTX	RT	65.97	57.60	0.00
		40	55.28	0.00	
		70	30.15	0.00	
	Curcumin	RT	75.74	54.42	16.92
		40	3.85	0.00	
		70	0.00		

3.1.2.3. Oxidation

There was a significant decrease in peak area for curcumin and MTX over time and accelerated with increase in temperature. In combination, the decrease in peak area was accelerated due to the presence of both compounds (Table 3-6).

From the alternative oxidation method using potassium permanganate and sulphuric acid, recovery for curcumin and MTX were found to be 0.53% and 4.83% respectively, while in the combination the recovery were found to be 0.2% and 2.74% respectively.

Table 3-6 Oxidation Degradation for stability indicating method. (n=3)

Compound (50 µg/ml)		Temperature (°C)	% Recovery determined on days indicated				
			1	2	5	10	20
MTX		RT	99.85	99.67	99.41	97.51	97.02
		40	99.74	98.01	96.83	91.48	85.18
Curcumin		RT	86.84	64.83	35.22	6.54	0.68
		40	21.41	6.83	0.58	0.00	
Combination	MTX	RT	99.78	99.35	98.44	91.58	86.27
		40	94.47	91.72	85.94	84.14	84.01
	Curcumin	RT	76.14	54.39	24.16	4.60	0.65
		40	17.53	5.26	0.00		

3.1.2.4. Photolytic Degradation Data for stability indicating method. (n=3)

As shown in Table 3-7 the compounds were completely degraded after 3 h. The degradation products were eluted within first four minutes.

Table 3-7 Photolysis Data for stability indicating method. (n=3)

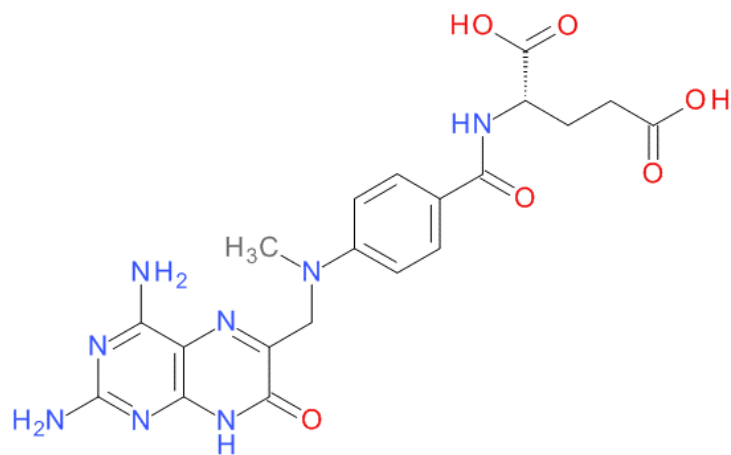
Compound (50 µg/ml)		% Recovery determined on the hours indicated		
		1 hr.	2 hrs.	3 hrs.
MTX		61.24	28.83	0.00
Curcumin		7.52	0.00	
Combination	MTX	73.54	27.95	0.00
	Curcumin	12.28	0.00	

3.1.2.5. Dry heat and Humidity

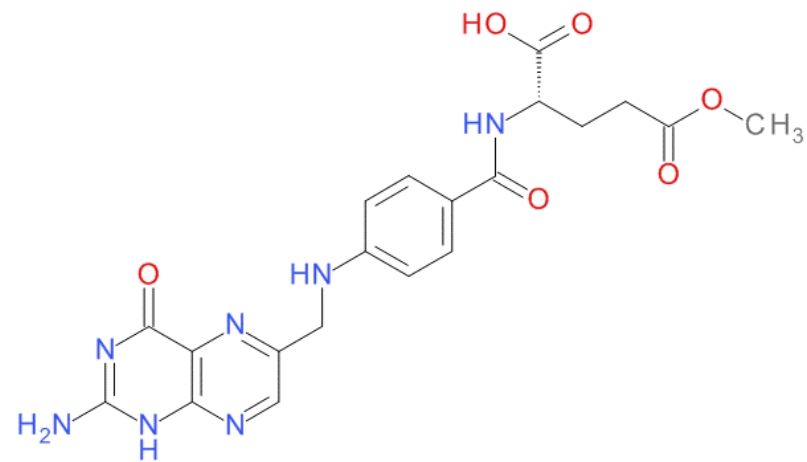
No significant degradation could be identified in first 30 days in both dry and humid conditions. The recovery for MTX and Curcumin is shown in Table 3-8. After 40 days the percentage recovery was found to be 93.77% and 90.05% when analysed individually and in combination respectively. Similarly for Curcumin, the recovery after 40 days was found to be 96.94% and 95.73% respectively.

Table 3-8 Heat/Humidity exposure Data. (n=3)

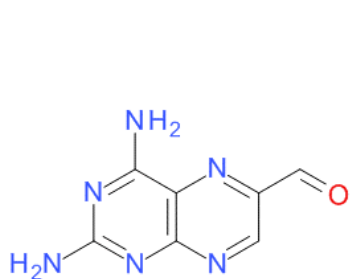
Compound (50 µg/ml)		% Recovery determined after 40 days	
		Relative humidity	Dry heat
MTX		96.45	93.77
Curcumin		97.66	96.94
Combination	MTX	95.37	90.05
	Curcumin	92.48	95.73



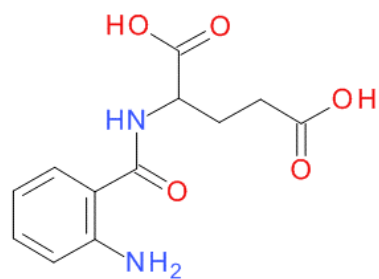
7-hydroxymethotrexate



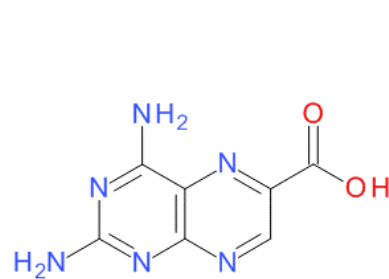
10-Methylpteroylglutamic acid



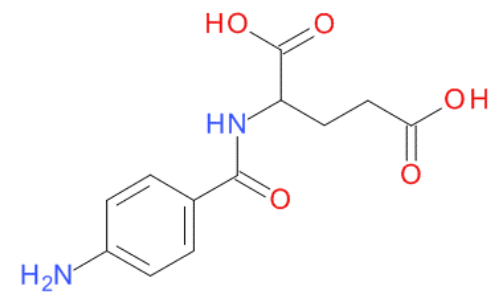
2,4-diamino-6-pteridinecarbaldehyde



Aminobenzoylglutamic acid

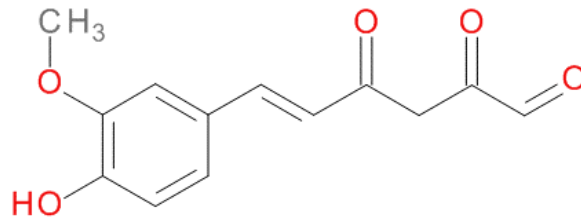


2,4-diamino-6-pteridinecarboxylic acid

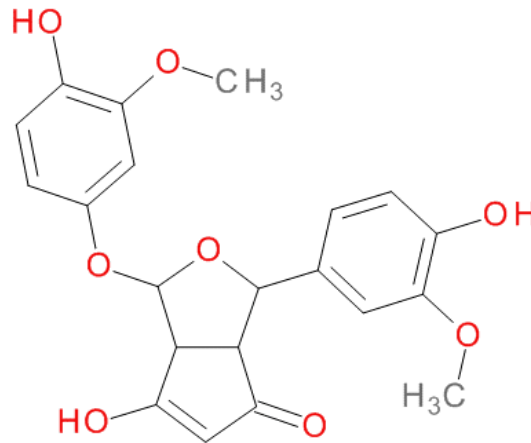


p-aminobenzoylglutamic acid

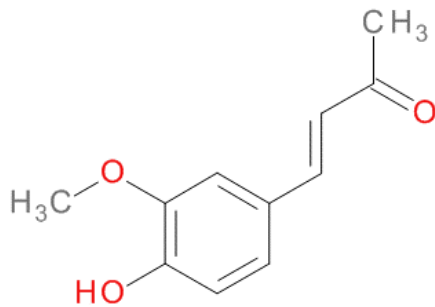
Figure 3-2 Possible degradation products of MTX



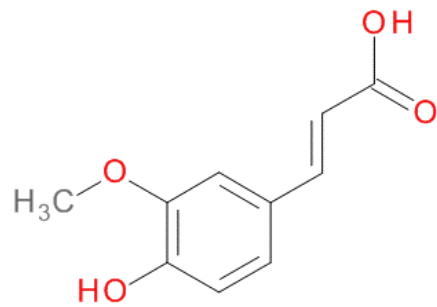
trans-6-(4-hydroxy-3-methoxyphenyl)-2,4-dioxo-5-hexenal



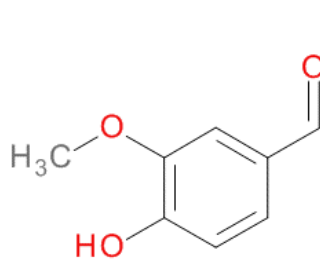
Bicyclopentadione



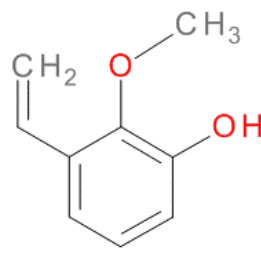
Feruloylmethane



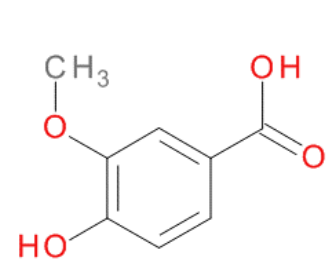
Ferulic acid



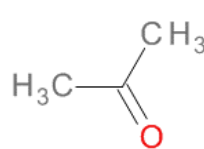
Vanillin



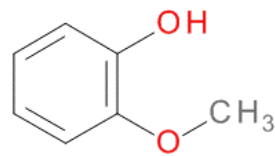
Vinyl guaiacol



Vanillic acid



Acetone



Guaiacol

Figure 3-3 Possible degradation products of curcumin

3.2. Inhibitory concentration (IC₅₀) of MTX and curcumin in HFLS-RA

The 50% inhibitory concentrations of MTX and curcumin for 48 hours were determined using HFLS-RA cells. The cells were treated with increasing concentrations of the inhibitory compounds and the cell viability was analysed using *CellTiter-Glo*[®] Luminescent cell viability assay. Figure 3-4-Figure 3-5 below show decreased cell viability with increases in the drugs dose. The 50% inhibition concentrations (IC₅₀) for MTX and curcumin in HFLS-RA cells were 53.71 nM and 15.28 μ M, respectively.

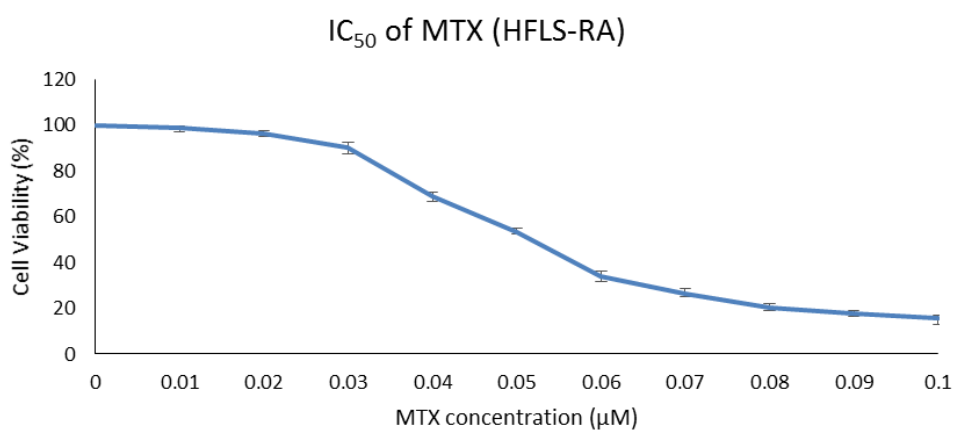


Figure 3-4 Dose-dependent inhibitory effects on cell viability employing different concentrations (0 – 0.1 μ M) of MTX on HFLS-RA cells. The data values are \pm SD, n=3.

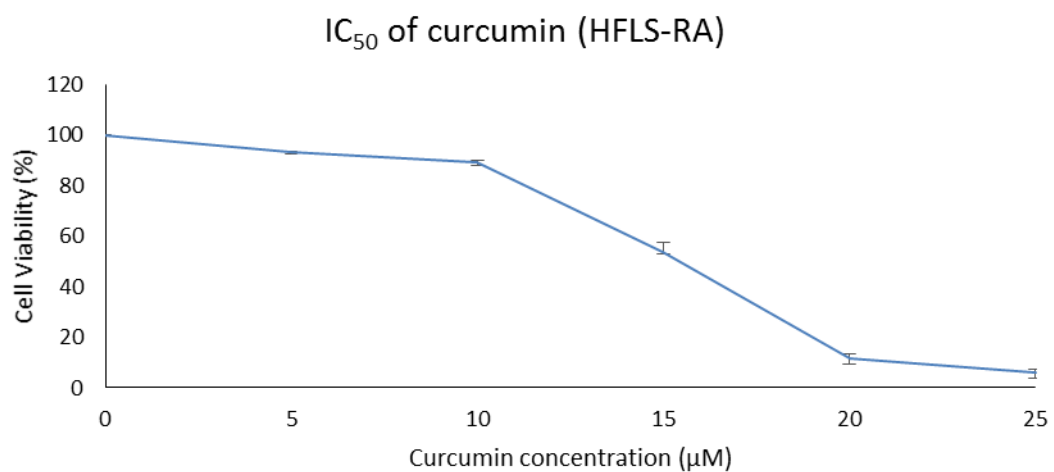


Figure 3-5 Dose-dependent inhibitory effects on cell viability employing different concentrations (0 – 25µM) of curcumin on HFLS-RA cells. The data values are ±SD, n=3.

3.3. Gene Expression Profiling

The HFLS-RA cells were used for further gene expression analysis. In order to obtain comparative analysis of effect of MTX and curcumin, individually and in combination, on HFLS-RA cells DNA microarray was carried out. The gene expression profiling was performed on four sets (including three treated and an untreated as control) each consisting of two samples. Samples were analysed on Agilent SurePrint G3 Human Gene Expression 8x60K v2 Microarray. All the procedures were carried out according to manufacturer's protocol.

3.3.1. Total RNA concentration, purity and integrity

Total RNA was isolated from the samples and concentrations at an A260/A280 ratios of each sample was determined using the NanoDrop ND-1000 instrument. RNA integrity was assessed on the Agilent 2100 Bioanalyzer. The results, shown in Table 3-9, show that RNA concentrations of all samples were found to be sufficient for microarray analysis and their purity (as indicated by the A260/A280 and A260/A230 ratios) was found to be ideal for further analysis. All total RNA samples were found to have RIN (RNA Integrity Number) values above 9.2, indicating excellent RNA quality. The electropherograms of all analysed samples along with electrophoretic gels are also shown in Figure 3-6 and Figure 3-7.

Table 3-9 Table showing quality control results for the total RNA samples for HFLS-RA cells

HFLS-RA Sample Treatment	Concentration (ng/ μ l)	A260/A280 ratio	A260/A230 ratio	RIN
Control 1	267.01	2.06	2.02	10.0
Control 2	239.55	2.08	2.04	10.0
MTX 1	286.20	2.05	1.90	10.0
MTX 2	310.58	2.07	2.14	10.0
Curcumin 1	305.11	2.05	1.94	9.2
Curcumin 2	389.16	2.04	2.14	9.6
Combination 1	445.74	2.02	2.14	9.7
Combination 2	308.05	2.04	1.72	9.6

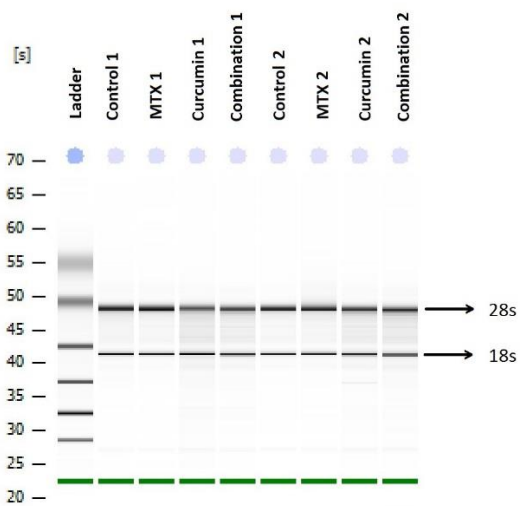


Figure 3-6 Original electrophoresis gel for assessing RNA integrity. (Co-relating with Figure 3-7)

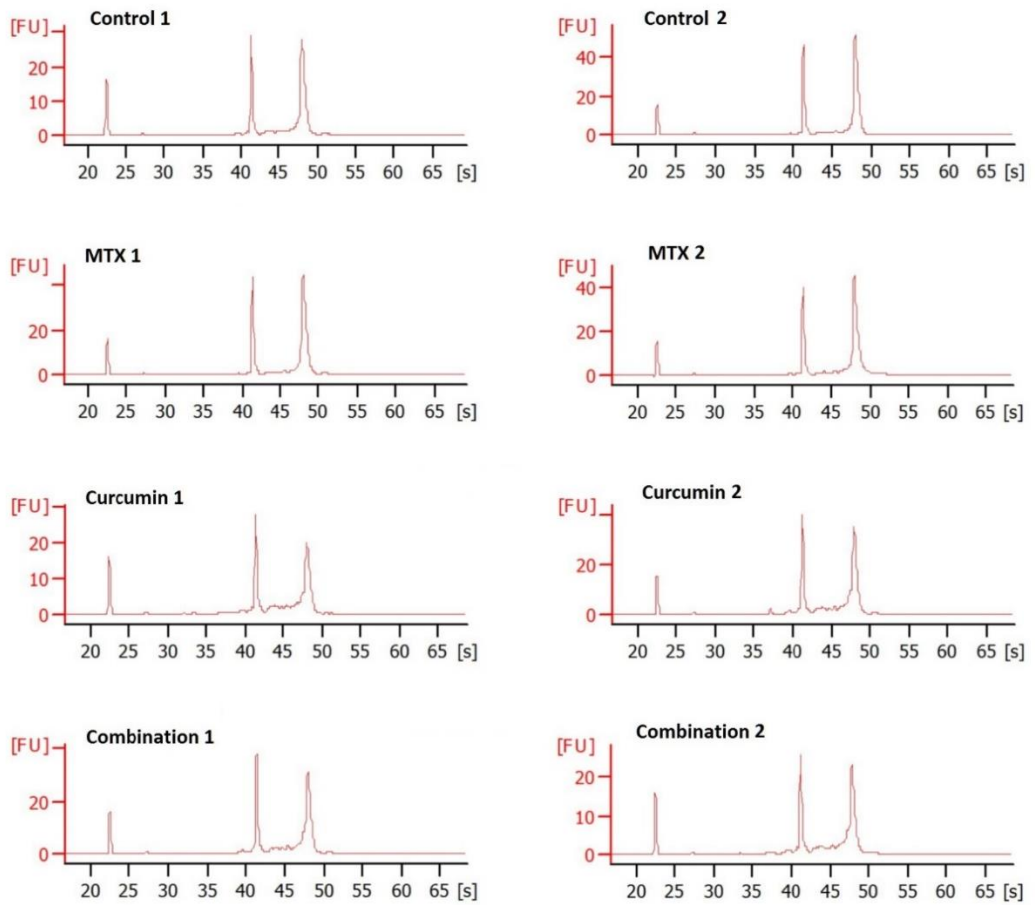


Figure 3-7 Original chart recordings showing electropherograms for RNA integrity in HFLS-RA cells

3.3.2. Quantification and quality control of labeled cRNA

After conversion into Cyanine-3-labeled cRNA, the concentration of labeled cRNA and incorporated Cyanine-3 was assessed using a NanoDrop ND-1000 spectrophotometer and the NanoDrop software. The cRNA yield (μg) and the specific activity ($\text{pmol dye}/\mu\text{g cRNA}$) are shown in Table 3-10. the cRNA yield for all samples was above the required threshold proposed by Agilent (825 ng). All samples had specific activity of more than 6.0 pmol Cyanine-3 per μg cRNA and fulfilled the quality criteria defined by Agilent Technologies. All eight samples were successfully labeled and were used for hybridization.

Table 3-10 NanoDrop ND-1000 quality control parameters for all labeled cRNA samples

HFLS-RA treatment	cRNA conc. (ng/μl)	A260/A280 ratio	Dye conc. (pmol/μl)	cRNA yield (μg)	Specific activity (pmol/μg)
Control 1	187.81	2.15	2.99	5.63	15.92
Control 2	195.52	2.24	3.20	5.87	16.37
MTX 1	207.58	2.24	3.25	6.23	15.66
MTX 2	205.51	2.26	3.25	6.17	15.81
Curcumin 1	181.11	2.26	2.79	5.43	15.41
Curcumin 2	177.01	2.20	2.82	5.31	15.93
Combination 1	172.68	2.22	2.77	5.18	16.04
Combination 2	155.25	2.24	2.37	4.66	15.27

3.3.3. Microarray quality control

The quality control analysis, performed using Feature Extraction software, were used to evaluate the array results. Visual control of the corner spots in each array confirmed automatic corner finding and the grid placement for all arrays. Analysis of the Agilent One-Color RNA Spike-In signals demonstrated equal and good performance of each single labelling and hybridisation experiment.

3.3.4. Effects of Quantile normalisation

The box plot shown in Figure 3-8 demonstrates the effect of quantile normalisation for the analysed samples. Box plots are a visualisation of the data distribution. Normally, the middle 50% of the data lie within the turquoise-coloured boxes and the horizontal line within the box indicates the median. Quantile normalisation adjusts all microarray samples to an identical data distribution in order to enable the comparison.

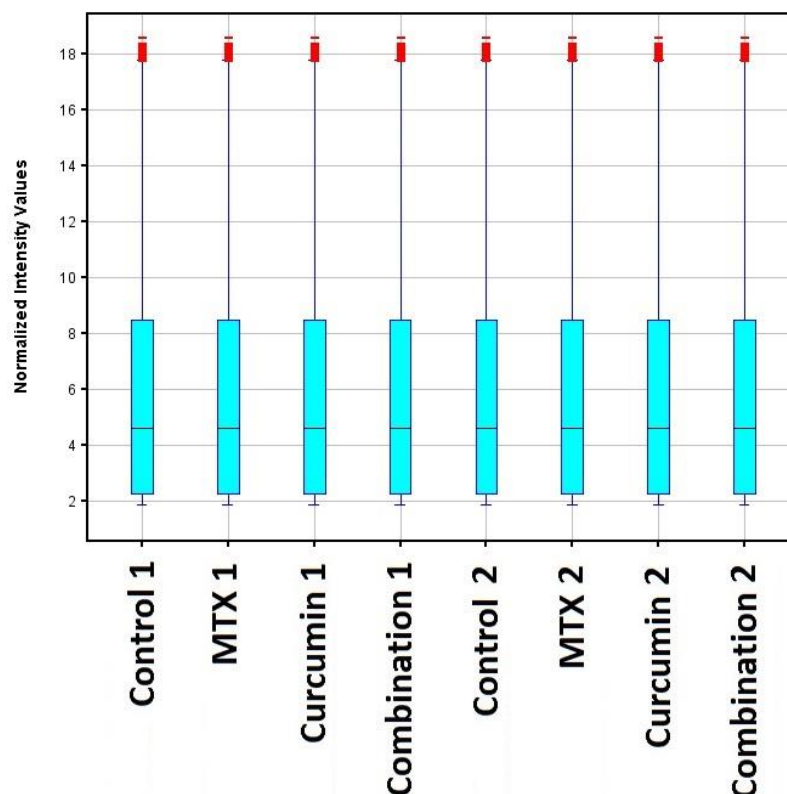


Figure 3-8 BoxWhisker plot after quantile normalisation

3.3.5. Correlation analysis

The similarities of the expression profiles of samples within and between the study groups was analysed by determining Pearson's correlation coefficient r (Table 3-11). Each microarray was analysed for quality control using standardised set of QC metrics to ensure samples can be accounted for bioinformatics analysis. The filtered flag information was applied on each array to obtain 'Detected' (D) and 'Not Detected' (ND) data. In Table 3-12, the number and % Detected is mentioned for each sample array. In total minimum of 24,928 *ProbeNames* of the 50,739 available probes were found to be detected in each sample.

Table 3-11 Correlation coefficient (r) values between and within the treatment samples with corresponding heat-map. The colour range starts at a lowest level of r=0.920 (Green) and ends at the highest level of r= 1.000 (Red) which represents high correlation

Group	Control 1	Control 2	MTX 1	MTX 2	Curcumin 1	Curcumin 2	Combination 1	Combination 2
Control 1	1.000							
Control 2	0.997	1.000						
MTX 1	0.960	0.965	1.000					
MTX 2	0.962	0.965	0.999	1.000				
Curcumin 1	0.922	0.920	0.923	0.923	1.000			
Curcumin 2	0.918	0.915	0.919	0.918	0.995	1.000		
Combination 1	0.929	0.926	0.929	0.929	0.996	0.992	1.000	
Combination 2	0.928	0.926	0.929	0.929	0.996	0.992	0.999	1.000

Table 3-12 Number and percentage of *ProbeNames* detected in each HFLS-RA sample

HFLS-RA treatment	Detected (D)	% Detected (D)
Control 1	25805	50.9
Control 2	25420	50.1
MTX 1	25874	51.0
MTX 2	25524	50.3
Curcumin 1	27522	54.2
Curcumin 2	26810	52.8
Combination 1	26554	52.3
Combination 2	24928	49.1

3.3.6. Differential gene expression

Following % detected samples, the data were filtered to obtain quantile normalisation and log₂ transformed data were averaged within biological replicates. The pair-wise comparison was carried out using untreated HFLS-RA samples as control group and gene expression of MTX treated HFLS-RA, curcumin treated HFLS-RA and HFLS-RA treated with combination of MTX and curcumin were compared to the control group.

In order to identify significantly differentially expressed genes in these pairwise comparisons, a filtering approach was applied using combination of FDR-corrected p-value [$p(\text{Corr}) \leq 0.05$] and Fold Change cut-off ($|FC| \geq 2$). The stringent filtering, when applied to the data, identified 3613 (1886 upregulated and 1727 downregulated) and 4063 (2127 upregulated and 1936 downregulated) significantly differentially expressed genes in pair wise comparison for Curcumin and combination treatment respectively while no significant differential expression was observed in case of MTX. Therefore, non-stringent filter ($p \leq 0.05$ and $|FC| \geq 2$) was applied to data which identified 74 genes (21 upregulated and 53 downregulated) with differential expression (Table 3-13).

Table 3-13 The list of genes identified to be differentially expressed in sampled treated with MTX.

Gene	MTX FC	Curcumin FC	Combination FC (MTX + curcumin)	Description
<i>ADAMTSL2</i>	-2	-20	-29	Homo sapiens ADAMTS-like 2 (<i>ADAMTSL2</i>), transcript variant 1, mRNA [NM_014694]
<i>AKD1</i>	3	5	-1	Homo sapiens cDNA FLJ16163 fis, clone BRCAN2014229. [AK131244]
<i>ANGPTL7</i>	-5	-518	-563	Homo sapiens angiopoietin-like 7 (<i>ANGPTL7</i>), mRNA [NM_021146]
<i>ANKRD1</i>	3	4	2	Homo sapiens ankyrin repeat domain 1 (cardiac muscle) (<i>ANKRD1</i>), mRNA [NM_014391]
<i>APLN</i>	-2	-28	-33	Homo sapiens apelin (<i>APLN</i>), mRNA [NM_017413]
<i>ARHGAP32</i>	-2	-4	-4	Homo sapiens Rho GTPase activating protein 32 (<i>ARHGAP32</i>), transcript variant 2, mRNA [NM_014715]
<i>BCAR4</i>	-1	99	149	Homo sapiens breast cancer anti-estrogen resistance 4 (non-protein coding) (<i>BCAR4</i>), non-coding RNA [NR_024049]
<i>CCDC81</i>	2	7	6	Homo sapiens coiled-coil domain containing 81 (<i>CCDC81</i>), transcript variant 2, mRNA [NM_021827]
<i>CCL5</i>	-3	-1	-1	Homo sapiens chemokine (C-C motif) ligand 5 (<i>CCL5</i>), mRNA [NM_002985]
<i>CCRN4L</i>	2	6	10	Homo sapiens CCR4 carbon catabolite repression 4-like (<i>S. cerevisiae</i>) (<i>CCRN4L</i>),

Gene	MTX FC	Curcumin FC	Combination FC (MTX + curcumin)	Description
				mRNA [NM_012118]
CD248	3	-22	-23	Homo sapiens CD248 molecule, endosialin (CD248), mRNA [NM_020404]
CD274	-3	75	90	Homo sapiens CD274 molecule (CD274), mRNA [NM_014143]
CD300A	2	1	-2	Homo sapiens CD300a molecule (CD300A), mRNA [NM_007261]
CH25H	-4	-58	-78	Homo sapiens cholesterol 25-hydroxylase (CH25H), mRNA [NM_003956]
CHI3L2	-3	-7	-5	Homo sapiens chitinase 3-like 2 (CHI3L2), transcript variant 3, mRNA [NM_001025199]
COL14A1	-3	-40	-33	Homo sapiens collagen, type XIV, alpha 1 (COL14A1), mRNA [NM_021110]
CP	-7	-38	-30	Homo sapiens ceruloplasmin (ferroxidase) (CP), mRNA [NM_000096]
CRHR2	-2	-3	-2	Homo sapiens corticotropin releasing hormone receptor 2 (CRHR2), transcript variant 1, mRNA [NM_001883]
CRTAC1	-2	-2	-2	Homo sapiens cartilage acidic protein 1 (CRTAC1), transcript variant 1, mRNA [NM_018058]
CRTAM	-2	-7	-14	Homo sapiens cytotoxic and regulatory T cell molecule (CRTAM), mRNA [NM_019604]
CXCL12	-3	-40	-45	Homo sapiens chemokine (C-X-C motif) ligand 12 (CXCL12), transcript variant 1,

Gene	MTX FC	Curcumin FC	Combination FC (MTX + curcumin)	Description
				mRNA [NM_199168]
<i>CYTL1</i>	-3	-26	-18	Homo sapiens cytokine-like 1 (CYTL1), mRNA [NM_018659]
<i>DDIT4L</i>	-2	-3	-3	Homo sapiens DNA-damage-inducible transcript 4-like (DDIT4L), mRNA [NM_145244]
<i>DIO2</i>	-3	-12	-13	Homo sapiens deiodinase, iodothyronine, type II (DIO2), transcript variant 1, mRNA [NM_013989]
<i>DIO3</i>	-3	-4	-5	Homo sapiens deiodinase, iodothyronine, type III (DIO3), mRNA [NM_001362]
<i>DNAH10</i>	2	9	12	Homo sapiens dynein, axonemal, heavy chain 10 (DNAH10), mRNA [NM_207437]
<i>ERVK13-1</i>	2	33	27	Homo sapiens endogenous retrovirus group K13, member 1 (ERVK13-1), non-coding RNA [NR_040023]
<i>ERVMER34-1</i>	-4	-1	-1	Homo sapiens endogenous retrovirus group MER34, member 1 (ERVMER34-1), transcript variant 1, mRNA [NM_024534]
<i>FAM20A</i>	-2	-121	-120	Homo sapiens family with sequence similarity 20, member A (FAM20A), transcript variant 1, mRNA [NM_017565]
<i>FGFBP2</i>	-3	-2	-1	Homo sapiens fibroblast growth factor binding protein 2 (FGFBP2), mRNA [NM_031950]
<i>FLJ45950</i>	-3	2	2	Homo sapiens cDNA FLJ45950 fis, clone PLACE7008136. [AK127847]

Gene	MTX FC	Curcumin FC	Combination FC (MTX + curcumin)	Description
<i>GALNTL2</i>	-2	-46	-41	Homo sapiens UDP-N-acetyl-alpha-D-galactosamine:polypeptide N-acetylgalactosaminyltransferase-like 2 (GALNTL2), mRNA [NM_054110]
<i>GJB2</i>	-4	-7	-7	Homo sapiens gap junction protein, beta 2, 26kDa (GJB2), mRNA [NM_004004]
<i>GPR88</i>	-2	-17	-17	Homo sapiens G protein-coupled receptor 88 (GPR88), mRNA [NM_022049]
<i>HEATR7B1</i>	3	-3	-3	PREDICTED: Homo sapiens HEAT repeat containing 7B1 (HEATR7B1), mRNA [XM_291007]
<i>HK2</i>	-3	-4	-2	Homo sapiens hexokinase 2 (HK2), mRNA [NM_000189]
<i>HLF</i>	4	-2	-2	Homo sapiens hepatic leukemia factor (HLF), mRNA [NM_002126]
<i>HSPA6</i>	-2	12	77	Homo sapiens heat shock 70kDa protein 6 (HSP70B') (HSPA6), mRNA [NM_002155]
<i>IFITM1</i>	-2	-15	-13	Homo sapiens interferon induced transmembrane protein 1 (9-27) (IFITM1), mRNA [NM_003641]
<i>IGFN1</i>	2	4	4	Homo sapiens immunoglobulin-like and fibronectin type III domain containing 1 (IGFN1), mRNA [NM_001164586]
<i>IL36A</i>	-2	2	3	Homo sapiens interleukin 36, alpha (IL36A), mRNA [NM_014440]
<i>IL6</i>	-2	-6	-8	Homo sapiens interleukin 6 (interferon, beta 2) (IL6), mRNA [NM_000600]
<i>IL7</i>	-3	-39	-69	Homo sapiens interleukin 7 (IL7), transcript variant 1, mRNA [NM_000880]

Gene	MTX FC	Curcumin FC	Combination FC (MTX + curcumin)	Description
LAMTOR3	-2	3	4	Homo sapiens late endosomal/lysosomal adaptor, MAPK and MTOR activator 3 (LAMTOR3), transcript variant 1, mRNA [NM_021970]
LGALS8-AS1	-2	2	3	Homo sapiens LGALS8 antisense RNA 1 (non-protein coding) (LGALS8-AS1), non-coding RNA [NR_034040]
LOC649201	2	-1	-1	PREDICTED: Homo sapiens paraneoplastic antigen like 6A-like (LOC649201), mRNA [XM_001127211]
MAFB	-2	-4	-5	Homo sapiens v-maf musculoaponeurotic fibrosarcoma oncogene homolog B (avian) (MAFB), mRNA [NM_005461]
MCHR1	-6	-16	-8	Homo sapiens melanin-concentrating hormone receptor 1 (MCHR1), mRNA [NM_005297]
MIR17HG	-3	20	23	Homo sapiens miR-17-92 cluster host gene (non-protein coding) (MIR17HG), non-coding RNA [NR_027350]
MMP1	-5	2	2	Homo sapiens matrix metalloproteinase 1 (interstitial collagenase) (MMP1), transcript variant 1, mRNA [NM_002421]
MMP13	-9	-4	-4	Homo sapiens matrix metalloproteinase 13 (collagenase 3) (MMP13), mRNA [NM_002427]
MSMP	-3	-7	-6	Homo sapiens microseminoprotein, prostate associated (MSMP), mRNA [NM_001044264]

Gene	MTX FC	Curcumin FC	Combination FC (MTX + curcumin)	Description
<i>NHLH1</i>	3	13	20	Homo sapiens nescient helix loop helix 1 (NHLH1), mRNA [NM_005598]
<i>NPPC</i>	-3	-1	1	Homo sapiens natriuretic peptide C (NPPC), mRNA [NM_024409]
<i>NR3C2</i>	2	-3	-4	Homo sapiens nuclear receptor subfamily 3, group C, member 2 (NR3C2), transcript variant 1, mRNA [NM_000901]
<i>OTP</i>	-2	56	87	Homo sapiens orthopedia homeobox (OTP), mRNA [NM_032109]
<i>PARK2</i>	-2	-3	-2	Homo sapiens parkinson protein 2, E3 ubiquitin protein ligase (parkin) (PARK2), transcript variant 1, mRNA [NM_004562]
<i>RBM47</i>	-4	-1	-1	Homo sapiens RNA binding motif protein 47 (RBM47), transcript variant 2, mRNA [NM_019027]
<i>RELT</i>	-2	9	8	Homo sapiens RELT tumor necrosis factor receptor (RELT), transcript variant 1, mRNA [NM_032871]
<i>RND1</i>	-3	7	7	Homo sapiens Rho family GTPase 1 (RND1), mRNA [NM_014470]
<i>RPGR</i>	5	3	2	Homo sapiens retinitis pigmentosa GTPase regulator (RPGR), transcript variant C, mRNA [NM_001034853]
<i>SLC2A5</i>	-2	-15	-14	Homo sapiens solute carrier family 2 (facilitated glucose/fructose transporter), member 5 (SLC2A5), transcript variant 1, mRNA [NM_003039]
<i>SNORD103A</i>	3	10	12	Homo sapiens small nucleolar RNA, C/D box 103A (SNORD103A), small nucleolar

Gene	MTX FC	Curcumin FC	Combination FC (MTX + curcumin)	Description
				RNA [NR_004054]
<i>SPDYE3</i>	3	6	20	Homo sapiens speedy homolog E3 (Xenopus laevis) (SPDYE3), mRNA [NM_001004351]
<i>TCTEX1D1</i>	4	1	10	Homo sapiens Tctex1 domain containing 1 (TCTEX1D1), mRNA [NM_152665]
<i>TLR2</i>	-4	-6	-4	Homo sapiens toll-like receptor 2 (TLR2), mRNA [NM_003264]
<i>TMCO2</i>	-2	16	27	Homo sapiens transmembrane and coiled-coil domains 2 (TMCO2), mRNA [NM_001008740]
<i>TNFSF10</i>	-5	-24	-12	Homo sapiens tumor necrosis factor (ligand) superfamily, member 10 (TNFSF10), transcript variant 1, mRNA [NM_003810]
<i>TREM1</i>	-4	-4	-3	Homo sapiens triggering receptor expressed on myeloid cells 1 (TREM1), transcript variant 1, mRNA [NM_018643]
<i>TRIML2</i>	3	7	5	Homo sapiens tripartite motif family-like 2 (TRIML2), mRNA [NM_173553]
<i>TRPA1</i>	-3	-5	-3	Homo sapiens transient receptor potential cation channel, subfamily A, member 1 (TRPA1), mRNA [NM_007332]
<i>VAV3</i>	-2	-10	-6	Homo sapiens vav 3 guanine nucleotide exchange factor (VAV3), transcript variant 1, mRNA [NM_006113]
<i>WDR33</i>	5	4	3	Homo sapiens WD repeat domain 33 (WDR33), transcript variant 1, mRNA

Gene	MTX FC	Curcumin FC	Combination FC (MTX + curcumin)	Description
				[NM_018383]
<i>WDR66</i>	2	7	8	Homo sapiens WD repeat domain 66 (WDR66), transcript variant 1, mRNA [NM_144668]

3.3.7. Analysis and validation of expression of significantly regulated Genes

The total of 13 genes were selected as the potential biomarkers out of which eight were to be upregulated in untreated HFLS-RA cells while five were downregulated. The fold change obtained from the microarray data for the same genes in pairwise comparison is presented in Table 3-14. The further qRT-PCR experiment was carried out to validate the effects of MTX and curcumin on the expression levels of these genes (Table 3-15).

Table 3-14 Fold change of the selected genes in Microarray data in pairwise comparison

Gene	MTX vs Control	Curcumin vs Control	Combination (MTX + curcumin) vs Control
<i>ANGPTL7</i>	-5	-518	-563
<i>CD248</i>	3	-22	-23
<i>CH25H</i>	-4	-58	-78
<i>CXCL12</i>	-3	-40	-45
<i>CYTL1</i>	-3	-26	-18
<i>IFITM1</i>	-2	-15	-13
<i>IL7</i>	-3	-39	-69
<i>COL14A1</i>	-3	-40	-33
<i>BCAR4</i>	-1	99	149
<i>CD274</i>	-1	75	90
<i>RELT</i>	-1	9	8
<i>HSPA6</i>	-1	12	77

OTP	-1	56	87
------------	----	----	----

Table 3-15 The copy numbers obtained from qRT-PCR validation of gene expression analysis of selected genes. (Data values are mean \pm SD, n=3).

Gene	Control	MTX	Curcumin	Combination (MTX + curcumin)
<i>ANGPTL7</i>	12432 \pm 1706	10657 \pm 1249	1436 \pm 369	171 \pm 40
<i>CD248</i>	503528 \pm 14827	373925 \pm 31655	20917 \pm 2484	23139 \pm 6152
<i>CH25H</i>	189022 \pm 8538	138965 \pm 22219	1811 \pm 132	1222 \pm 706
<i>CXCL12</i>	292320 \pm 12408	227935 \pm 11672	31868 \pm 2153	26534 \pm 1768
<i>CYTL1</i>	130485 \pm 10838	113943 \pm 26142	4270 \pm 171	4291 \pm 238
<i>IFITM1</i>	327237 \pm 12408	295525 \pm 11672	43206 \pm 2153	43262 \pm 1768
<i>IL7</i>	18304 \pm 510	13549 \pm 1596	999 \pm 680	760 \pm 481
<i>COL14A1</i>	1269247 \pm 123002	1045595 \pm 129295	112168 \pm 132235	45353 \pm 27089
<i>BCAR4</i>	5 \pm 0	7 \pm 3	416 \pm 62	591 \pm 139
<i>CD274</i>	90631 \pm 18174	141564 \pm 13983	360024 \pm 7353	1417841 \pm 64756
<i>RELT</i>	912988 \pm 30910	779414 \pm 90172	1855449 \pm 47592	833045 \pm 46630
<i>HSPA6</i>	1282 \pm 893	5330 \pm 3664	16809 \pm 11585	601754 \pm 93606
<i>OTP</i>	15 \pm 6	17 \pm 2	25 \pm 17	1358 \pm 463

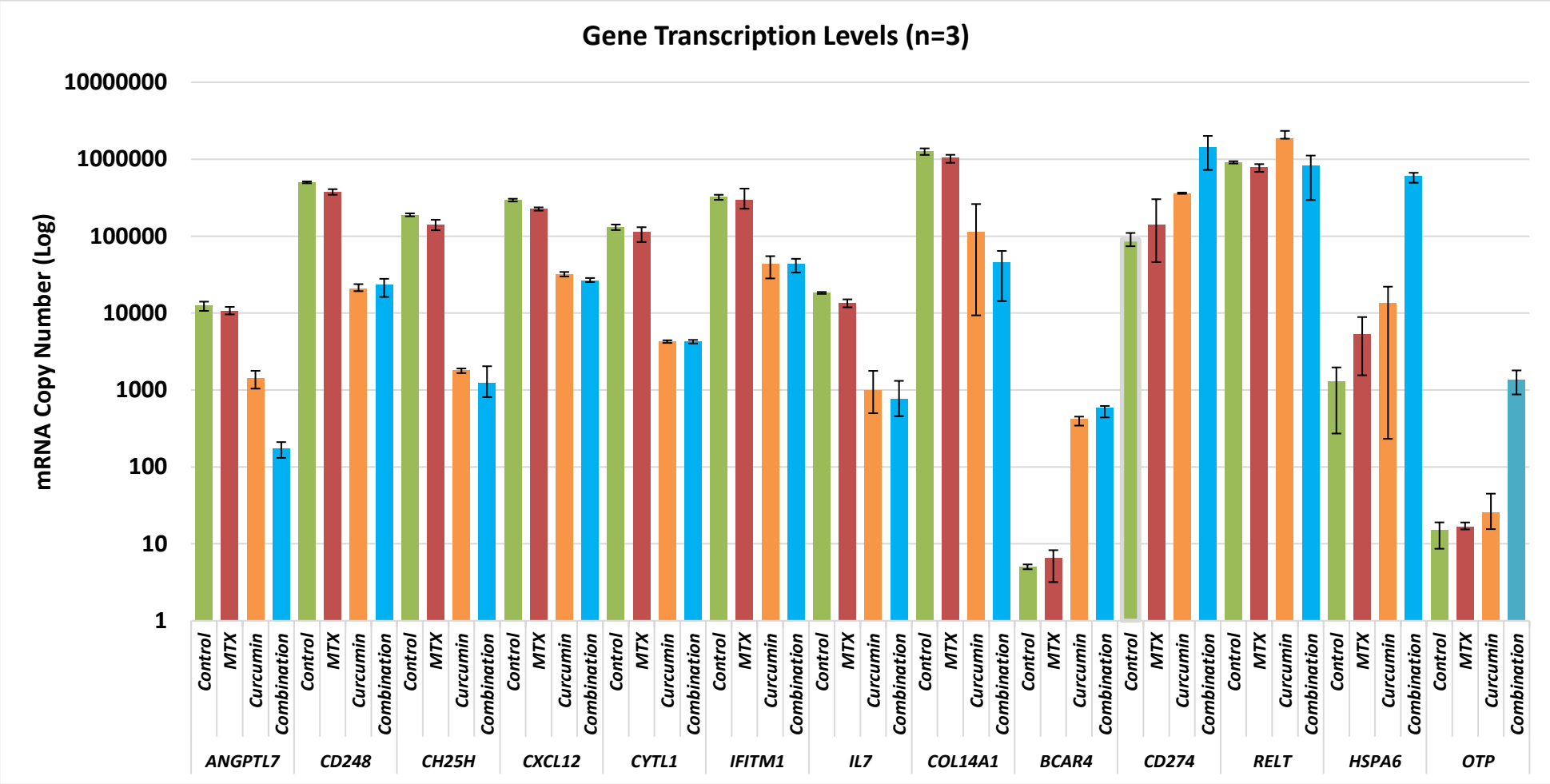


Figure 3-9 Bar charts showing Gene transcription levels of selected genes. (n=3)

3.4. Interleukin-6 (IL6) Activity

IL6 is one of the highly expressed biomarkers associated with RA. The effect of MTX and curcumin was analysed on cell secretion levels of IL6 using the Human IL6 Quantikine ELISA kit (Table 3-16). Standard curves were plotted to determine IL6 levels in treated and untreated samples. The equation in each graph was utilised to calculate the IL6 concentration in cell culture supernatant.

Table 3-16 IL6 concentration in cell culture supernatant from treated HFLS-RA cells.
(Data values are mean \pm SD, n=3)

HFLS-RA cells Treatment	IL6 concentration (ng/ μ l)
Control	1.34 \pm 0.07
MTX	1.16 \pm 0.01
Curcumin	0.90 \pm 0.02
Combination	0.82 \pm 0.05

CHAPTER 4

DISCUSSION

RA is a chronic inflammatory disorder with a genetic origin and requires a prolonged duration of treatment (Ogawa *et al.* 2003). RA is characterised by the autoimmune response that causes progressive degeneration of the cartilaginous tissues in the joints leading to inflammation, pain and loss of mobility. Primary treatments for RA focus on restricting the synovial deterioration and relieving the pain. Despite great strides in the therapeutic treatment over the past couple of decades, the effectiveness of the drugs currently used in RA treatment still remains a major concern due to the adverse effects involved.

MTX is currently used as the first line treatment due to its ability to modify the rheumatic conditions by suppressing the *de novo* synthesis of nucleic acids so that the disease progression can be prevented (Dolezalova *et al.* 2005). However, the prolonged exposure to the drug, even at doses as low as 10-20 mg/week, can lead to a wide range of adverse effects from nausea and stomatitis to hepatotoxicity and lung fibrosis. The folate deficiency caused by the inhibition of dihydrofolate reductase can lead to severe anaemia and depression. While the folate supplementation is effective in avoiding these symptoms it is counterproductive to the RA treatment (Dhanasekaran *et al.* 2013). The most glaring problem in the MTX treatment is the nonspecific mode of action which involves targeting *de novo* synthesis of the DNA. In order to improve the efficacy of the existing treatment while reducing the overall level of the side-effects, a more specific approach is required that targets the disease-related biomarkers. Curcumin is a promising alternative due to its ability to induce apoptosis and inhibit pro-inflammatory biomarkers. Therefore, it can be an ideal candidate that could be used to complement MTX in the treatment of RA.

If MTX and curcumin were to be used in combination as a therapeutic treatment, it is pertinent that the two compounds are compatible. A stability indicating method was developed and validated for monitoring the progressive degradation of the compounds while being subjected to stress conditions such as hydrolysis, oxidation and photolysis. A validated stability indicating method is defined as an accurate analytical method which can be used to quantitate the decrease in the concentration of the compounds at any given time. It can be used to detect how the stability of the drug substances and products changes over time. This involves subjecting the compounds to stress conditions and then analysing the degradation rate of the compounds. The forced degradation typically involves exposing the compounds to a range of pH values, heat, humidity and light.

An isocratic, ion-pairing mobile phase consisting of 35% (v/v) aqueous acetonitrile together with tetrabutylammonium acetate, sodium dodecyl sulphate and citric acid (pH 3.4) which was previously developed by our research group was used to perform the initial analysis (Shervington *et al.* 2005). However, due to the extreme hydrophobic nature of curcumin a gradient system was designed which allowed for elution of both compounds within 25 minutes. The gradient system consisted of two mobile phases with the concentration of acetonitrile increasing from 35% to 60% over a five minute period after injection. The method was validated for linearity, repeatability and reproducibility. As previously reported in literature, the compounds are found to be relatively stable under acidic conditions compared with alkaline conditions (Sabry *et al.* 2003). The percentage recovery of both MTX and Curcumin decreased over time under these conditions. The degradation was found to accelerate at higher temperatures and when the compounds were treated as a mixture.

Hydrolysis is one of the most common degradation reactions carried out over a wide range of pH. Hydrolytic studies under acidic and basic conditions involves catalysis of ionisable functional groups present in the molecule. Both MTX and curcumin were subjected separately as well as in combination to 0.10 M Hydrochloric acid and 0.10 M sodium hydroxide and the organic solvent DMSO was used to solubilise the curcumin.

Both compounds were found to be relatively more stable in aqueous solutions at lower pH. The hydrolysis of MTX involves the glutamic part of the molecule undergoing dissociation forming degradation products such as formaldehyde, formic acid, aminobenzoylglutamic acid, 2,4-diamino-6-pteridinecarbaldehyde and 2,4-diamino-6-pteridinecarboxylic acid (Sabry *et al.* 2003). Hydrolysis of Curcumin involves decomposition to form trans-6-(4-hydroxy-3-methoxyphenyl)-2,4-dioxo-5-hexenal as the initial degradation product. The final degradation products formed are guaiacol, vinyl guaiacol, feruloylmethane and ferulic acid. Vanillylidene acetone further splits to form vanillin and acetone (Ansari *et al.* 2005).

The rate of hydrolysis was found to increase at higher temperatures with complete degradation of both compounds observed in basic solution within five days. However, the investigation did not indicate significant change in compound stability when treated as part of a mixture. The elution times for the degradation products were found not to interfere with the compounds, thereby allowing accurate quantification of the compounds.

Hydrogen peroxide with 3% final concentration at neutral pH is usually used for oxidation of drug substances in forced degradation studies. The oxidative degradation of compounds involves an electron transfer mechanism to form reactive anions and cations (Rao *et al.* 2013). The major oxidation products of MTX is 7-

hydroxymethotrexate, however, negligible methotrexate-oxidizing activity is observed in both in vivo and in vitro experiments (Jordan *et al.* 1999). The results obtained from the validated method correlate with these findings since less than 3% degradation was observed at room temperature following 20 days exposure to 3% hydrogen peroxide. Curcumin was found to be rapidly oxidised at increased temperatures, accelerating the rate of degradation. Curcumin was found to be almost completely degraded within 20 days at room temperature and in 5 days at 40°C with major oxidation product being deoxygenated bicyclopentadione (Ketrone *et al.* 2013). The oxidation rate was found to be higher when the compounds were treated as part of a mixture, however, the chromatogram did not indicate any degradation products eluting at the same elution time as the compounds, thereby allowing an accurate quantification.

The purpose of the photo stability studies is to evaluate the intrinsic photosensitivity of the compounds to demonstrate that exposure to light does not induce degradation. In order to induce degradation both compounds in solution form were exposed to UV-C light in the range of 100 nm – 280 nm. Light stress conditions can induce photo oxidation by free radical mechanisms. Functional groups such as alkenes, weak C–H and O–H bonds present in MTX and curcumin are responsible for introducing photosensitivity. The major degradation products of MTX are 2,4-diamino-6-pteridinecarbaldehyde, 2,4-diamino-6-pteridinecarboxylic acid and p-aminobenzoylglutamic acid (Chatterji and Gallelli 1978). The major degradation products of curcumin are vanillin, ferulic aldehydes, ferulic acid and vanillic acid. When subjected to UV-C (200nm - 280nm) both compounds underwent rapid degradation within 3 h which was further accelerated when exposed to UV as mixture. The degradation products were eluted separately and did not interfere with the peaks corresponding to the compounds thus enabling an accurate quantification of the

recovered compounds.

Both MTX and curcumin are usually stored at -20°C in their solid state. When exposed to a relative humidity of 75% at 40°C as well as dry heat at 70°C, very little degradation was observed in both compounds. However, the compounds underwent rapid degradation when exposed to higher temperatures in solution. The major degradation product of MTX under thermal degradation is 10-Methylpteroylglutamic acid while curcumin is broken down into vanillin and ferulic acid (Tønnesen *et al.* 2002). The HPLC method was therefore found to be stability indicating for the simultaneous analysis of MTX and curcumin. The forced degradation analysis confirmed that the two compounds were found to be fairly stable in solution when stored at or lower than room temperature.

The pathogenesis of RA includes several cell types including T and B lymphocytes and macrophages. The human fibroblast-like synoviocytes (HFLS), present in the synovial lining, play a key role in the RA progression due to their ability to produce pro-inflammatory cytokines and proteases which at increased concentrations contribute to cartilage degeneration. The rheumatoid HFLS (HFLS-RA) phenotype also involves increased invasiveness into the extracellular matrix, thereby further accelerating joint destruction. Recent investigations have confirmed the role of HFLS in regulation of innate immune responses and intracellular signalling mechanisms (Bartok *et al.* 2010). Therefore HFLS-RA cells were chosen for the evaluation of the disease pathogenesis and to identify potential therapeutic biomarkers. The HFLS-RA cells were treated with MTX and curcumin to compare the effect of the two compounds on the expression levels of the biomarkers. The concurrent treatment with both compounds was also carried out to confirm if the compounds exhibited synergistic activity.

The HFLS-RA cells were cultured in the lab using appropriate and safe techniques as per the guidelines provided by the Cell Applications, PHE, INC. Cell growth was restricted to a range of 70-80% confluency to avoid external stress and media deprivation. The HFLS-RA cells were treated with IC₅₀ concentrations of MTX and curcumin, independently and in combination, in order to compare the effect of the compounds on the gene expression levels. The untreated HFLS-RA cells were used as the control during the investigations. There have been numerous studies carried out analysing the inhibitory effect of the two compounds on specific pro-inflammatory molecules. The anti-rheumatic activity of MTX has been well documented (Chan and Cronstein 2013). However, while the inhibitory effect of Curcumin has been demonstrated in previous studies, a clear mechanism of action involved in this process has not been identified.

The DNA microarray is an efficient high throughput method used to establish the complete expression profile of the entire genome in specific cells. Due to the accuracy and precision of the technique, coupled with the standardised statistical analysis, it was used to quantify the effect of MTX and curcumin on the HFLS-RA cells. In this study the DNA microarray was carried out on duplicate samples of MTX treated cells, curcumin treated cells and cells treated simultaneous with both MTX and curcumin. The quality of the total RNA extracted from the untreated as well as the treated HFLS-RA samples was confirmed by analysing the RNA integrity so that the total RNA used for the microarray experiments was confirmed to be of high quality. Each array was subjected to a feature extraction software in order to carry out the data normalisation. The quantile normalisation of the data enabled comparisons between gene expressions under different treatment regimes. The normalisation of the raw intensity values obtained in each array allowed for the identical data distribution as shown in

Figure 3-8. The quantile normalisation enabled the comparison within different arrays. The similarities of the expression profiles of within samples with same treatment and between differently treated samples is analysed and presented in form of Pearson's correlation coefficients in Table 3-11. The value of coefficient close to 1.000 indicated the higher correlation between the gene expressions values obtained in different arrays while decrease the in the value of coefficient indicated the differential expression of the gene within the two arrays. The value of coefficient in samples treated with curcumin was lower compared to samples treated with MTX indicating lower correlation with the untreated control samples which meant that the curcumin treatment induced higher differential expression. The further decrease in the coefficient value in samples concurrently treated with MTX and curcumin indicated increased differential gene expression. The differential gene expression was expressed in the form of fold changes, comparing the normalised treatment groups (MTX, curcumin and combination) against the control (untreated HFLS-RA cells). Each pairwise comparison group was subjected to bioinformatics analysis to establish the statistical significant fold change under stringent filtration which used a combination of false discovery rate (FDR)-corrected p-value [$p(\text{Corr}) \leq 0.05$] and Fold Change cut-off ($|\text{FC}| \geq 2$). On application of the stringent filter 3613 genes were found to be significantly differentially expressed in pairwise comparison between curcumin treated cells and untreated HFLS-RA. Out of the 3613 genes 1886 were upregulated while 1727 were downregulated. For the pair wise comparison of cells treated concurrently with both MTX and curcumin and the untreated HFLS-RA cells, 4063 genes were found to be significantly differentially expressed, of which 2127 were upregulated and 1936 were downregulated. Since no differential regulation was obtained in the cells treated with MTX under stringent filter, the non-stringent filtering, which removed the FDR

correction, was applied which identified 74 genes to be differentially expressed out of which 21 genes were upregulated while 53 genes were downregulated. A comparative analysis between the three pair-wise comparisons exhibited a higher cumulative fold change in samples treated with curcumin than MTX treated samples, indicating that the curcumin is more efficient than MTX in selectively targeting the genes involved the inflammatory and the autoimmune responses. The further increase in the fold change with the samples treated with a combination of both drugs indicates possible synergistic activity between MTX and curcumin.

Out of the 74 genes, 13 genes were selected for further analysis and validation using qRT-PCR in which untreated HFLS-RA cells were used as control. The genes were selected based on their differential expression in pair-wise comparisons in cells treated with curcumin and their potential to be established as potential therapeutic biomarkers for further research. The 13 genes have previously been identified to be involved in inflammatory and cell proliferation pathways such as Wnt5a-mediated cell signalling, JAK-STAT signalling and JNK signalling pathways. The genes such as *ANGPTL7*, *CD248*, *CD274*, *CH25H*, *CXCL12* and *IL7* have previously been confirmed to play important roles in carcinogenesis and autoimmune disorders. Earlier studies involving our research group, identified the HSP70 protein encoding gene *HSPA6* as therapeutic biomarker in Glioma (Shervington *et al.* 2015). The qRT-PCR experiments were carried out to confirm the effect of MTX and curcumin on the gene expression levels on the 13 genes in HFLS-RA cells.

The Angiopoietin-like (ANGPTL) proteins are structurally related to the angiogenic factors. Though the ANGPTLs are unable to regulate blood vessel formation (Katoh and Katoh 2006) they appear to exhibit other functions such as induction of inflammation

and regulation of lipid and glucose metabolism (Xu *et al.* 2005). The biological functions of Angiopoietin-like 7 (*ANGPTL7*) present on chromosome 1 has not been completely evaluated though it is found to be significantly over-expressed in cancer (Parri *et al.* 2014). It has been identified as a target gene in WNT/ β -catenin signalling pathway, postulating function in the promotion of cell adhesion and plays role in production of extracellular matrix protein fibronectin thus promoting cell adhesion and proliferation (Buie *et al.* 2011, Comes *et al.* 2011). In addition, another member of angiopoietin-like gene family *ANGPTL4* has been implicated in metastatic processes in cancers by modulating vascular permeability (Tanaka *et al.* 2015). It contributes to tumour growth and protects the cancer cells from anoikis (programmed cell death). *ANGPTL7* may also share similar functions in RA and cancer. In RA, Wnt5a-mediated signalling directly contributes towards the induction of pro-inflammatory chemokines such as IL6 and IL8. Therefore, as target gene, *ANGPTL7* can be used as biomarker to determine the efficacy of the treatment (de Rooy *et al.* 2013). The present data shows *ANGPTL7* downregulated 5 fold in MTX treated samples while the downregulation was significantly increased by 518 and 562 fold in samples treated with curcumin and the combination, respectively. The qRT-PCR analysis showed that the decreased expression of *ANGPTL7* in HFLS-RA samples treated with MTX and curcumin correlates with the anti-inflammatory ability of both compounds. The significantly higher fold change in samples treated with curcumin indicate a higher efficiency of the compounds in inhibiting the pro-inflammatory activities.

CD248 gene present on chromosome 11 codes for the lectin-like transmembrane protein Endosialin which in normal conditions is responsible for cell-cell adhesion and immune response to pathogens. *In vitro*, Endosialin is expressed by fibroblasts, pericytes and smooth muscle cells. The expression of the protein is strongly

upregulated in angiogenic endothelial cells. The over-expression of Endosialin is observed in glioma where it upregulates angiogenic vasculature and in arthritis where it results in increased adhesion to fibronectin and contributes to synovial hyperplasia. The downregulation of Endosialin directly results in the reduction of synovial hyperplasia and, therefore, can be concluded to be effective in anti-rheumatic treatment. The microarray data shows a 3 fold upregulation of *CD248* in MTX treated samples which correlates with established pulmonary toxicity and lung fibrosis caused due to MTX. The HFLS-RA cells treated with curcumin show a 22 fold downregulation which the concurrent treatment using MTX and curcumin, downregulated gene expression 23 fold confirming the anti-rheumatic activity of the compound. The expression of *CD248* gene has been previously shown to be upregulated in rheumatic cells as compared to normal synoviocytes (Maia *et al.* 2010). The decreased expression of the *CD248* gene in samples treated with curcumin confirm the role of curcumin in the reduction of synovial hyperplasia. The Endosialin expression was also found to be downregulated in HFLS-RA samples treated with the MTX and curcumin combination which indicates the efficiency of curcumin in reducing the severe effects of the MTX treatment.

The cholesterol 25-hydroxylase (*CH25H*) gene present on chromosome 10 encodes for the hydroxylase enzyme which metabolises cholesterol in to 25-Hydroxycholesterol in macrophages as a response to TLR activation (Bauman *et al.* 2009). The increased levels of the enzyme and the oxysterol product in RA due to increased activity of TLR receptors leads to the release of pro-inflammatory chemokines. The microarray data shows that gene expression is 4, 58 and 78 fold downregulated when treated with MTX, curcumin and the combination, respectively, which indicates reduced inflammation and a restricted auto-immune response. The expression of cholesterol

25-hydroxylase enzyme has been previously shown to be increased in neurodegenerative disorders as well as rheumatoid arthritis (Forwell *et al.* 2016, Taberner *et al.* 2005). The down regulation of this gene by both MTX and curcumin suggests the anti-rheumatic effect of both compounds, while further reduction in gene expression when treated with the combination confirms the synergistic effect of the compounds. These results were validated in the qRT-PCR data which indicated that the *CH25H* expression in RA synoviocytes was inhibited after treatment with MTX and curcumin.

The *COL14A1* gene, present on chromosome 8, encodes for collagen, type XIV, alpha-1 (CXIV) protein which is a variant of the protein Undulin (UND). Both CXIV and UND are present on collagen fibrils where they are involved in adhesion and integration of collagen bundles (Schuppan *et al.* 2001). The *COL14A1* gene has been previously identified as therapeutic biomarker in autoimmune rheumatic disorders, confirmed to be upregulated in rheumatic conditions (de la Rica *et al.* 2013). The increased expression of this gene from the family Fibril-associated collagens with interrupted helices (FACIT) leads to aggregation of fibroblasts and extracellular matrix in synovium causing inflammation and rigidity in joints. The microarray data shows downregulation of *COL14A1* by 3 and 40 folds when treated with MTX and curcumin, respectively, while gene expression was downregulated 33 fold in samples treated with MTX and curcumin simultaneously confirming the ability of the compounds to inhibit the fibrogenesis in synovial cavity. The significant difference in the fold change observed in the samples treated with MTX and curcumin indicates that curcumin is more effective in reducing fibrogenesis as compared to MTX.

The chemokine (C-X-C motif) ligand 12 (*CXCL12*) gene codes for chemokine stromal cell-derived factor 1 (SDF-1), which upon pro-inflammatory stimuli from TNF and IL, activates leukocytes. The chemokine SDF-1 primarily binds to CXC receptor 4 which induces intracellular signalling via chemotaxis and increases the gene transcription levels for the proteins required in cell survival pathways. The SDF-1/CXCR4 coupling plays a crucial role in angiogenesis and cell proliferation. The increased expression of SDF-1 in rheumatoid arthritis means it could be used as a therapeutic biomarker in the treatment of arthritis (Orimo *et al.* 2005). The gene expression data confirmed 3 fold downregulation of gene expression of samples treated with MTX while the curcumin treatment downregulated 40 fold. The expression of *CXCL12* has been confirmed to be increased in HFLS-RA cells (Pablos *et al.* 2003), therefore the downregulation of this gene following treatment with MTX and curcumin confirmed the inhibitory properties of MTX and curcumin and their ability to control the angiogenesis in RA progression. The reduced gene expression of samples treated with both MTX and curcumin (45 fold downregulation) indicates that both compounds exhibit synergistic activity in leukocyte inhibition.

The cytokine-like 1 (*CYTL1*) gene present on chromosome 4 codes for protein specifically expressed in bone marrow and mononuclear cells. It undergoes conformational changes and along with the C-C motif ligand 2 (CCL2) bind to chemokine (C-C motif) receptor (CCR2) receptor. These proteins mediate monocyte chemotaxis and promote monocyte infiltration in RA leading to chronic inflammation and cartilage destruction (Jeon *et al.* 2011, Tomczak and Pisabarro 2011). The increased expression of *CYTL1* in rheumatoid arthritis has also been confirmed to be associated with increased cardiovascular risk (Boyer *et al.* 2011). The data obtained from the microarray analysis showed downregulation of *CYTL1* by 3 and 26 fold when

treated with MTX and curcumin, respectively, while samples treated with both MTX and curcumin showed 18 fold downregulation of gene expression. The results from qRT-PCR also confirmed decrease in the expression levels of *CYTL1* gene, therefore, confirming the anti-inflammatory properties as well as potential therapeutic benefits of curcumin in cardiovascular disorders.

The interferon-induced transmembrane protein 1 (*IFITM1*) gene present on chromosome 11, also known as CD225, encodes the transmembrane protein. In normal cells this protein is involved in physiological processes of the immune response and cell maturation (Kim *et al.* 2010). The activation of interferon signalling pathways and the increased expression of *IFITM1* gene has been associated with RA progression (van Baarsen *et al.* 2010). The data from microarray analysis showed a downregulation of gene expression by 2 and 15 fold following treatment separately with MTX and curcumin, respectively, while the gene expression was found to be downregulated 13 fold in samples treated with both MTX and curcumin. The difference in the fold change observed confirmed that curcumin appears to be more efficient in modulating the interferon activity and hence, has a greater therapeutic impact compared with MTX.

The protein encoded by interleukin 7 (*IL7*) gene, present on chromosome 8, plays an important role in lymphoid cell development and homeostasis. It is involved in the activation of JAK-STAT pathway which in turn upregulates the production of pro-inflammatory molecules such as TNF and NF- κ B (van Roon *et al.* 2003, Zuvich *et al.* 2010, Puel *et al.* 1998). The induced expression of IL7 in RA cells has been associated with the production of the osteoclastogenic cytokines by T-cells leading to the maturation of osteoclasts and bone destruction. The increased circulating concentration of IL7 directly leads to chronic inflammation and joint destruction,

therefore selective inhibition of IL7 could be of therapeutic importance (Churchman *et al.* 2014). The microarray data showed that gene expression was downregulated by 3 and 40 folds when treated with MTX and curcumin, respectively, while treatment involving a combination, the downregulation was 69 fold, thereby confirming the anti-rheumatic properties and a synergistic effect of the two compounds.

The Breast Cancer Anti-estrogen Resistance 4 (*BCAR4*) is a RNA gene present on chromosome 16; comprising of a region coding for long non-coding RNAs (lncRNAs) and non-protein coding RNAs (npcRNAs). It has been associated with the BCAR1 gene and breast cancer. The expression of *BCAR4* was found to be significantly inhibited in RA cells compared to the normal synoviocytes. The lncRNAs, which in eukaryotes are almost 80% of the transcription products, serve as regulators for translation via several interrelated mechanisms. The npcRNAs code for several variations such as siRNAs, miRNAs and tRNAs that are also involved in regulation of related mRNA translation (Godinho *et al.* 2011). The primary function of *BCAR4* is to regulate the activity of Breast Cancer Anti-Estrogen Resistance 1 (BCAR1) protein which coordinates the tyrosine kinase-based signalling in cell adhesion and migration. The overexpression of BCAR1 protein is associated with increased chances of developing breast cancer. The samples treated with MTX did not indicate significant change in the gene expression level, however, *BCAR4* was upregulated 99 fold when treated with curcumin indicating the ability of the compound to indirectly modulate the interaction of related BCAR1 (Robinson *et al.* 2006). This also indicates the potential anti-carcinogenic properties of curcumin which could be a potential candidate in breast cancer treatment.

The *CD274* gene, present on chromosome 9, encodes an immune inhibitory receptor ligand called programmed death-ligand 1 (PD-L1) which is expressed on the surface of

both T and B lymphocytes. The interaction of this ligand with the receptor inhibits the T-cell activation and cytokine production. During the inflammation interaction of PD-L1 is important in order to prevent an autoimmune response. The expression of PD-L1 as well as the associated enzyme programmed death 1 (PD-1), which negatively regulates the immune response, has been found to be significantly downregulated in RA cases (Li and Schwarz 2013). The microarray data indicated that samples treated with MTX did not show significant changes in those reduced expression levels. However, *CD274* was upregulated 75 fold when treated with curcumin, therefore, confirming the capability of the compound to modulate ability of PD-L1 to bind to the PD-1 receptor present on the T-cells, thereby inhibiting the activation of IL2 production and T-cell proliferation (Lee *et al.* 2006, Al-Chaqmaqchi *et al.* 2013). The ability of curcumin to induce the expression of *CD274* indicates the potential of the compound to regulate pathogenesis and progression of RA.

The *HSPA6* gene encodes for the heat shock 70kDa protein 6 (HSP70B') which is upregulated in stress like conditions. The qRT-PCR data showed an increased expression level of *HSPA6* in RA cells which was further upregulated 12 fold when treated with curcumin. HSP70 has immunoregulatory potential such as the ability to modulate inflammatory response in arthritis models by promoting the production of anti-inflammatory cytokines. The increased expression indicates the ability of curcumin to induce immunosuppressive potential of this protein (Borges *et al.* 2012).

The Orthopedia Homeobox (*OTP*) gene, present on chromosome 5, encodes a member of homeodomain (HD) family. A homeobox is a DNA sequence found within genes that regulate anatomical developments by modulating the cell fates and has been shown to play a crucial role in breast carcinogenesis (Kim *et al.* 2012). The data obtained from

the microarray analysis shows an upregulation of *OTP* by 56 and 87 fold when treated with curcumin, individually and in combination with MTX respectively, thereby confirming the ability of the compound to induce cell death.

The *RELT* gene encodes for Tumour necrosis factor receptor superfamily member 19L (TNFRSF19). This receptor is highly expressed in embryonic developmental stages. It interacts with TNF receptor-associated factors (TRAFs) and activates the JNK signalling pathway when overexpressed, thus regulating anti-apoptotic signalling of TNF and activation of T cells. The *RELT* gene is found to be downregulated in HFLS-RA cells compared to the normal synoviocytes. The MTX treated samples did not show a significant change in the inhibited expression level; on the other hand, samples treated with curcumin and the combination showed an upregulation of the *RELT* gene by 9 and 8 fold, respectively, in microarray data which could be attributed to its ability to induce apoptosis (Tamai *et al.* 2014).

Interleukin 6 (IL6), a prominent pro-inflammatory pleiotropic cytokine involved in RA pathogenesis and plays a key role in RA by inducing the production of C-reactive protein and fibrinogen. It also modulates proliferation and differentiation to cytotoxic T-cells and Th17 cells. IL6 stimulates the proliferation of macrophages and megakaryocytes. It induces the expression of adhesion molecules at the endothelial cell surface (Schett *et al.* 2008). IL6 mediates osteoclastogenesis by increasing the release of RANK-L by bone tissue cells including osteoblasts through the STAT-3 signalling pathway (Kudo *et al.* 2003). Together with TGF β and IL1, IL6 is also involved in T-cell differentiation to Th17 cells. Th17 cells act as powerful osteoclastogenesis inducers by increasing the release of both RANK-L and IL17, which directly stimulate osteoclast differentiation (Bettelli *et al.* 2006). Along with proinflammatory cytokines

such as TNF α , IL6 is strongly associated with RA-related systemic bone loss and systemic inflammation (Walsh *et al.* 2005). Within the inflamed synovial membrane, osteoclast differentiation is activated by many cytokines such as RANK-L and TNF α whose production by synovial fibroblasts is stimulated by IL6 (Hashizume *et al.* 2008, Axmann *et al.* 2009). Both MTX and curcumin have previously been reported to inhibit production of IL6 which would support the effectiveness of both compounds in inhibition of structural joint damage and systemic bone loss in RA. The microarray data showed the downregulation of *IL6* gene by 2 and 6 fold in samples treated with MTX and curcumin, respectively, which confirmed their anti-rheumatic abilities while the 8 fold downregulation in samples treated with both MTX and curcumin indicated synergistic effect of the two compounds. These results were further confirmed by quantifying the IL6 protein present in the serum of treated cells using ELISA. The results showed decrease in the serum concentration levels of IL6 following treatment with MTX and curcumin, separately and in combination.

The mode of action for MTX, an analogue of Dihydrofolate, in the treatment of RA is primarily through the inhibition of the enzymatic activity of Dihydrofolate Reductase, therefore, preventing the inflammatory hyperplasia and development of fibrous material in synovial membrane. The folate dependant suppression of *de novo* adenosine synthesis leads to the anti-inflammatory properties through the inhibition of intercellular adhesion molecules. However, due to the non-specificity of this mechanism, prolonged MTX treatment, even at low dose levels, could results in the development of complications such as anaemia, neutropenia, lung fibrosis and hepatotoxicity. Therefore, despite the effectiveness of the MTX treatment, it is important to develop a complementary combination which could help to reduce the adversities involved.

Curcumin, the major active component of turmeric, has been associated with antioxidant, anti-inflammatory, anticancer, antiviral and antibacterial activities. From the results obtained from microarray analysis curcumin has proven to be more efficient at inhibiting pro-inflammatory cytokines in rheumatoid arthritis such as CD248, SDF-1, CD225 and IL7, while increasing the expression levels of PD-L1 which is an anti-inflammatory cytokine. While the higher fold change in expression of the genes due to curcumin could be partly attributed to the significantly higher IC₅₀ concentration of 15 μM as compared to the IC₅₀ of MTX (50 nM), curcumin could still be considered a viable candidate as first line treatment for RA due to the high safety dose levels (12 gm/day for over 3 months) over a prolonged period of time. The gene expression profiling confirms a significant increase in the fold change induced by curcumin in the expression of established therapeutic biomarkers, therefore, suggesting that curcumin could be a more effective therapeutic agent compared with MTX in specifically modulating RA progression.

However, despite exhibiting highly pleiotropic properties the development of a formulation incorporating curcumin is problematical to some extent due aqueous insolubility, relatively low bioavailability and structural instability. Over the past 30 years several advancements have been made such as the development of liposomal encapsulation and modification of compound structure which could potentially increase the bioavailability of curcumin. However, until such modifications are established, in order to achieve the required level of therapeutic effect, a large level of daily dosage of curcumin will be required to replace MTX as first line of treatment.

Therefore the most appropriate possibility in improving RA treatment would be to use curcumin as a supplement to MTX ideally reducing the level of MTX and thereby reducing the adverse effects.

CHAPTER 5

CONCLUSION AND FUTURE WORK

5.1. Conclusion

This study has developed a novel gradient system for determining stability of both MTX and curcumin simultaneously during forced degradation. Since, the compounds were found to be relatively stable, they were used further for investigating their possible combination for the treatment of the HFLS-RA cells. Untreated HFLS-RA cells were used as control to compare the effect of the two compounds on the expression level of genes involved in RA pathogenesis. In order to understand the mechanism of action of the two compounds and to compare their effects on the expression of specific genes, DNA microarray analysis was carried out and specific genes were selected for further analysis to identify novel molecular biomarkers. Gene expression profiling identified 74 genes, based on stringent and non-stringent data, out of which a total of 13 genes were identified to be potential biomarkers due to their differential expression in normal synoviocytes and HFLS-RA cells.

The results obtained from the microarray and qRT-PCR investigations confirm the ability of curcumin to selectively modulate the expression of genes involved in the RA pathogenesis. While both compounds are effective in restraining the progression of RA, the difference in their mechanisms of action determine the level of adverse effects associated with the treatment. Due to the high toxicity level of MTX and significantly low bioavailability of curcumin, neither compound can be used independently as for RA treatment for prolonged duration. Therefore, complementing the existing MTX treatment with curcumin supplement could provide a more effective treatment while especially when it comes to reducing the long term side-effects as a result of MTX treatment.

5.2. Future work

The mechanism of action for curcumin, attributed to its pleiotropic applications, still remains to be completely understood. The current data can provide insight in to these mechanisms and can be used to analyse the effect of curcumin on various inter-related signalling pathways. In depth analysis of these signalling pathways is required to better understand the curcumin activity. The stability analysis of the analogues of curcumin and comparative studies of the effects of these compounds on the RA pathogenesis would be beneficial for improvement of RA treatment. The novel disease biomarker genes identified in this study, *ANGPTL7*, *CXCL12*, *CH25H*, *IFITM1*, *COL14A1*, *RELT* and *BCAR4*, should be further investigated since the signalling pathways relating to these biomarkers would be more beneficial in helping to understand RA pathogenesis in order to further optimise the first line RA treatment.

Gene expression profiling through DNA microarray has been well developed as reliable method that involves less labour-intensive sample preparations and data analysis. However, the limitation of this technique includes fundamental design bias, limited reproducibility which means that the results obtained from the expression profiling are more qualitative in nature (Ioannidis *et al.* 2009). Therefore, while cost effective DNA microarray is an ideal method to help identify biomarkers and specific molecules of interest, in order to obtain complete analysis of the quantitative expression of specific genes, further investigations should be carried out using more advanced techniques such as Next Generation Sequencing. The therapeutic biomarkers identified in this project could be further explored in order to help understand and improve the treatment of RA.

CHAPTER 6

REFERENCES

Aggarwal, B.B. And Harikumar, K.B., 2009. Potential therapeutic effects of curcumin, the anti-inflammatory agent, against neurodegenerative, cardiovascular, pulmonary, metabolic, autoimmune and neoplastic diseases. *The international journal of biochemistry & cell biology*, **41**(1), pp. 40-59.

Ak, P. And Levine, A.J., 2010. p53 and NF- κ B: different strategies for responding to stress lead to a functional antagonism. *The FASEB Journal*, **24**(10), pp. 3643-3652.

Akhavani, M.A., Madden, L., Buyschaert, I., Sivakumar, B., Kang, N. And Paleolog, E.M., 2009. Hypoxia upregulates angiogenesis and synovial cell migration in rheumatoid arthritis. *Arthritis Res Ther*, **11**(3), pp. R64.

Al-Chaqmaqchi, H., Sadeghi, B., Abedi-Valugerdi, M., Al-Hashmi, S., Fares, M., Kuiper, R., Lundahl, J., Hassan, M. And Moshfegh, A., 2013. The Role of Programmed Cell Death Ligand-1 (PD-L1/CD274) in the Development of Graft versus Host Disease. *Plos One*, **8**(4), pp. e60367.

Aletaha, D., Neogi, T., Silman, A.J., Funovits, J., Felson, D.T., Bingham, C.O., Birnbaum, N.S., Burmester, G.R., Bykerk, V.P., Cohen, M.D., Combe, B., Costenbader, K.H., Dougados, M., Emery, P., Ferraccioli, G., Hazes, J.M.W., Hobbs, K., Huizinga, T.W.J., Kavanaugh, A., Kay, J., Kvien, T.K., Laing, T., Mease, P., Mă©Nard, H.A., Moreland, L.W., Naden, R.L., Pincus, T., Smolen, J.S., Stanislawski-Biernat, E., Symmons, D., Tak, P.P., Upchurch, K.S., Vencovsk, J., Wolfe, F. And Hawker, G., 2010. 2010 Rheumatoid arthritis classification criteria: An American College of Rheumatology/European League Against Rheumatism collaborative initiative. *Arthritis & Rheumatism*, **62**(9), pp. 2569-2581.

Anand, P., Sundaram, C., Jhurani, S., Kunnumakkara, A.B. And Aggarwal, B.B., 2008. Curcumin and cancer: An "old-age" disease with an "age-old" solution. *Cancer letters*, **267**(1), pp. 133-164.

Angeles, L.M., R, S.H., Beverley, S., Peter, T., A, W.G. And E, S.M., 2014. Methotrexate for treating rheumatoid arthritis. *Cochrane Database of Systematic Reviews*.

Ansari, M.J., Ahmad, S., Kohli, K., Ali, J. And Khar, R.K., 2005. Stability-indicating HPTLC determination of curcumin in bulk drug and pharmaceutical formulations. *Journal of pharmaceutical and biomedical analysis*, **39**(1–2), pp. 132-138.

Ashkenazi, A., Holland, P. And Eckhardt, S.G., 2008. Ligand-Based Targeting of Apoptosis in Cancer: The Potential of Recombinant Human Apoptosis Ligand 2/Tumor Necrosis Factor-Related Apoptosis-Inducing Ligand (rhApo2L/TRAIL). *Journal of Clinical Oncology*, **26**(21), pp. 3621-3630.

Axmann, R., Boehm, C., Kroenke, G., Zwerina, J., Smolen, J. And Schett, G., 2009. Inhibition of Interleukin-6 Receptor Directly Blocks Osteoclast Formation *In Vitro* and *In Vivo*. *Arthritis and Rheumatism*, **60**(9), pp. 2747-2756.

Banji, D., Pinnapureddy, J., Banji, O.J.F., Saidulu, A. And Hayath, M.S., 2011. Synergistic activity of curcumin with methotrexate in ameliorating Freund's Complete Adjuvant induced arthritis with reduced hepatotoxicity in experimental animals. *European journal of pharmacology*, **668**(1–2), pp. 293-298.

Bartok, B. And Firestein, G.S., 2010. Fibroblast-like synoviocytes: key effector cells in rheumatoid arthritis. *Immunological reviews*, **233**(1), pp. 233-255.

Bauman, D.R., Bitmansour, A.D., McDonald, J.G., Thompson, B.M., Liang, G. And Russell, D.W., 2009. 25-Hydroxycholesterol secreted by macrophages in response to Toll-like receptor activation suppresses immunoglobulin A production. *Proceedings of the National Academy of Sciences of the United States of America*, **106**(39), pp. 16764-16769.

Bettelli, E., Carrier, Y., Gao, W., Korn, T., Strom, T.B., Oukka, M., Weiner, H.L. And Kuchroo, V.K., 2006. Reciprocal developmental pathways for the generation of pathogenic effector TH17 and regulatory T cells. *Nature*, **441**(7090), pp. 235-238.

Bharti, A.C., Donato, N. And Aggarwal, B.B., 2003. Curcumin (Diferuloylmethane) Inhibits Constitutive and IL6-Inducible STAT3 Phosphorylation in Human Multiple Myeloma Cells. *The Journal of Immunology*, **171**(7), pp. 3863-3871.

Boers, M., Verhoeven, A.C., Markusse, H.M., Van De Laar, M.,A.F.J., Westhovens, R., Van Denderen, J.C., Van Zeben, D., Dijkmans, B.A.C., Peeters, A.J., Jacobs, P., Van Den Brink, H.,R., Schouten, H.J.A., Van Der Heijde, D.,M.F.M., Boonen, A. And Van, D.L., 1997. Randomised comparison of combined step-down prednisolone, methotrexate and sulphasalazine with sulphasalazine alone in early rheumatoid arthritis. *The Lancet*, **350**(9074), pp. 309-318.

Borges, T.J., Wieten, L., Van Herwijnen, M.J.C., Broere, F., Van Der Zee, R., Bonorino, C. And Van Eden, W., 2012. The anti-inflammatory mechanisms of Hsp70. *Frontiers in immunology*, **3**, pp. 95-95.

Boyer, J., Gourraud, P., Cantagrel, A., Davignon, J. And Constantin, A., 2011. Traditional cardiovascular risk factors in rheumatoid arthritis: A meta-analysis. *Joint Bone Spine*, **78**(2), pp. 179-183.

Braun, J., Kästner, P., Flaxenberg, P., Währisch, J., Hanke, P., Demary, W., Von Hinüber, U., Rockwitz, K., Heitz, W., Pichlmeier, U., Guimbal-Schmolck, C. And Brandt, A., 2007. Comparison of the clinical efficacy and safety of subcutaneous versus oral administration of methotrexate in patients with active rheumatoid arthritis: Results of a six-month, multicenter, randomized, double-blind, controlled, phase IV trial. *Arthritis Rheum*, **58**(1), pp. 73-81.

Buie, L.K., Comes, N. And Borrás, T., 2011. Angiopoietin-like 7 (ANGPTL7) Modulates DEX Induction and Fibronectin (FN1) Fibrils Formation in the Human Trabecular Meshwork (HTM). *ARVO Annual Meeting Abstract Search and Program Planner*, **2011**, pp. 4622-4622.

Bush, J.A., Cheung, K.J.J. And Li, G., 2001. Curcumin induces apoptosis in human melanoma cells through a Fas receptor/caspase-8 pathway independent of p53. *Experimental cell research*, **271**(2), pp. 305-314.

Chabner, B.A. And Roberts, T.G., 2005. Timeline: Chemotherapy and the war on cancer. *Nature Reviews Cancer*, **5**(1), pp. 65-72.

Chakravarti, N., Kadara, H., Yoon, D., Shay, J.W., Myers, J.N., Lotan, D., Sonenberg, N. And Lotan, R., 2010. Differential Inhibition of Protein Translation Machinery by Curcumin in Normal, Immortalized and Malignant Oral Epithelial Cells. *Cancer Prevention Research*, **3**(3), pp. 331-338.

Chan, E.S.L. And Cronstein, B.N., 2013. Mechanisms of action of methotrexate. *Bulletin of the Hospital for Joint Disease (2013)*, **71 Suppl 1**, pp. S5-8.

Chan, E.S.L. And Cronstein, B.N., 2010. Methotrexate-how does it really work? *Nat Rev Rheumatol*, **6(3)**, pp. 175-178.

Chatterji, D.C. And Gallelli, J.F., 1978. Thermal and photolytic decomposition of methotrexate in aqueous solutions. *Journal of pharmaceutical sciences*, **67(4)**, pp. 526-531.

Churchman, S.M., El-Jawhari, J.J., Burska, A.N., Parmar, R., Goeb, V., Conaghan, P.G., Emery, P. And Ponchel, F., 2014. Modulation of peripheral T-cell function by interleukin-7 in rheumatoid arthritis. *Arthritis Research & Therapy*, **16(6)**, pp. 511.

Comes, N., Buie, L.K. And Borrás, T., 2011. Evidence for a role of angiopoietin-like 7 (ANGPTL7) in extracellular matrix formation of the human trabecular meshwork: implications for glaucoma. *Genes to Cells*, **16(2)**, pp. 243-259.

Courvoisier, N., Dougados, M., Cantagrel, A., Goupille, P., Meyer, O., Sibilia, J., Daures, J.P. And Combe, B., 2008. Prognostic factors of 10-year radiographic outcome in early rheumatoid arthritis: a prospective study. *Arthritis Res Ther*, **10(5)**, pp. R106.

Cronstein, B.N., 2005. Low-Dose Methotrexate: A Mainstay in the Treatment of Rheumatoid Arthritis. *Pharmacological reviews*, **57(2)**, pp. 163-172.

Cronstein, B.N., 2007. Do elevated red blood cell methotrexate polyglutamate levels predict methotrexate efficacy? *Nature Clinical Practice Rheumatology*, **3(5)**, pp. 256-257.

Cronstein, B.N and Chan, E.S.L 2000. *The mechanisms of methotrexate's action in the treatment of inflammatory disease*. Springer Science + Business Media.

Dayer, J.-. And Choy, E., 2009. Therapeutic targets in rheumatoid arthritis: the interleukin-6 receptor. *Rheumatology*, **49**(1), pp. 15-24.

De Bree, A., Verschuren, W., Kromhout, D., Kluijtmans, L. and Blom, H., 2002. Homocysteine determinants and the evidence to what extent homocysteine determines the risk of coronary heart disease. *Pharmacological reviews*, **54**(4), pp. 599-618.

De La Rica, L., Urquiza, J.M., Gómez-Cabrero, D., Islam, A.B.M.M.K., López-Bigas, N., Tegnér, J., Toes, R.E.M. And Ballestar, E., 2013. Identification of novel markers in rheumatoid arthritis through integrated analysis of DNA methylation and microRNA expression. *Journal of Autoimmunity*, **41**, pp. 6-16.

De Lathouder, S., Gerards, A.H., Dijkmans, B.A.C. And Aarden, L.A., 2004. Two Inhibitors of DNA-Synthesis Lead to Inhibition of Cytokine Production via a Different Mechanism. *Nucleosides, nucleotides & nucleic acids*, **23**(8), pp. 1089-1100.

De Rooy, D.P., Yeremenko, N.G. And Wilson, A.G., 2013. Genetic studies on components of the Wnt signalling pathway and the severity of joint destruction in rheumatoid arthritis. *Annals of the Rheumatic Diseases*, **72**(1), pp. 769-775.

Descalzo, M. Á., Carbonell, J., González-Álvaro, I., Sanmartí, R., Balsa, A., Hernandez-Barrera, V., Román-Ivorra, J.A., Ivorra-Cortés, J., Lisbona, P., Alperi, M., Jiménez-García, R. And Carmona, L., 2012. Effectiveness of a clinical practice intervention in early rheumatoid arthritis. *Arthritis Care Res*, **64**(3), pp. 321-330.

Dhanasekaran, S., Biswal, B.K., Sumantran, V.N. And Verma, R.S., 2013. Augmented sensitivity to methotrexate by curcumin induced overexpression of folate receptor in KG-1 cells. *Biochimie*, **95**(8), pp. 1567-1573.

Dolezalova, P., Krijt, J., Chladek, J., Nemcova, D. And Hoza, J., 2005. Adenosine and methotrexate polyglutamate concentrations in patients with juvenile arthritis. *Rheumatology*, **44**(1), pp. 74-79.

Fielding, C.A., Mcloughlin, R.M., Mcleod, L., Colmont, C.S., Najdovska, M., Grail, D., Ernst, M., Jones, S.A., Topley, N. And Jenkins, B.J., 2008. IL6 Regulates Neutrophil Trafficking during Acute Inflammation via STAT3. *The Journal of Immunology*, **181**(3), pp. 2189-2195.

Finckh, A., Liang, M.H., Van Herckenrode, C.M. And De Pablo, P., 2006. Long-term impact of early treatment on radiographic progression in rheumatoid arthritis: A meta-analysis. *Arthritis Rheum*, **55**(6), pp. 864-872.

Firestein, G.S., 2010. 'Rac'-ing upstream to treat rheumatoid arthritis. *Arthritis Res Ther*, **12**(1), pp. 109.

Forwell, A.L., Bernales, C.Q., Ross, J.P., Yee, I.M., Encarnacion, M., Lee, J.D., Sadovnick, A.D., Trabousee, A.L. And Vilarino-Guell, C., 2016. Analysis of CH25H in multiple sclerosis and neuromyelitis optica. *Journal of neuroimmunology*, **291**, pp. 70-72.

Funovits, J., Aletaha, D., Bykerk, V., Combe, B., Dougados, M., Emery, P., Felson, D., Hawker, G., Hazes, J.M., Huizinga, T., Kay, J., Kvien, T.K., Smolen, J.S., Symmons, D., Tak, P.P. And Silman, A., 2010. The 2010 American College of Rheumatology/European League Against Rheumatism classification criteria for rheumatoid arthritis:

Methodological Report Phase I. *Annals of the Rheumatic Diseases*, **69**(9), pp. 1589-1595.

Ganz, T., 2003. Heparin, a key regulator of iron metabolism and mediator of anemia of inflammation. *Blood*, **102**(3), pp. 783-788.

Godinho, M., Meijer, D., Setyono-Han, B., Dorssers, L.C.J. And Van Agthoven, T., 2011. Characterization of BCAR4, a Novel Oncogene Causing Endocrine Resistance in Human Breast Cancer Cells. *Journal of cellular physiology*, **226**(7), pp. 1741-1749.

Guggino, G., Giardina, A., Ferrante, A., Giardina, G., Schinocca, C., Sireci, G., Dieli, F., Ciccia, F. And Triolo, G., 2014. The in vitro addition of methotrexate and/or methylprednisolone determines peripheral reduction in Th17 and expansion of conventional Treg and of IL10 producing Th17 lymphocytes in patients with early rheumatoid arthritis. *Rheumatol Int*, **35**(1), pp. 171-175.

Haidar, M.S., Razzak, M.A. And Yasin, M.M., 2013. Rheumatoid Arthritis: Pattern and Prevalence of Extra-Articular Manifestations - A Prospective Study. *J.Armed Forces Med.Coll.*, **8**(2), pp.39-46.

Hashizume, M., Hayakawa, N. And Mihara, M., 2008. IL-6 trans-signalling directly induces RANKL on fibroblast-like synovial cells and is involved in RANKL induction by TNF- α and IL-17. *Rheumatology*, **47**(11), pp. 1635-1640.

Hatcher, H., Planalp, R., Cho, J., Torti, F.M. And Torti, S.V., 2008. Curcumin: From ancient medicine to current clinical trials. *Cell.Mol.Life Sci.*, **65**(11), pp. 1631-1652.

Hayden, M.S. And Ghosh, S., 2004. Signaling to NF-kappa B. *Genes & development*, **18**(18), pp. 2195-2224.

Huarte, M., Guttman, M., Feldser, D., Garber, M., Koziol, M.J., Kenzelmann-Broz, D., Khalil, A.M., Zuk, O., Amit, I., Rabani, M., Attardi, L.D., Regev, A., Lander, E.S., Jacks, T. And Rinn, J.L., 2010. A Large Intergenic Noncoding RNA Induced by p53 Mediates Global Gene Repression in the p53 Response. *Cell*, **142**(3), pp. 409-419.

Hung, T., Wang, Y., Lin, M.F., Koegel, A.K., Kotake, Y., Grant, G.D., Horlings, H.M., Shah, N., Umbricht, C., Wang, P., Wang, Y., Kong, B., Langerã,D, A., Bã,Resen-Dale, A., Kim, S.K., Van, D.V., Sukumar, S., Whitfield, M.L., Kellis, M., Xiong, Y., Wong, D.J. And Chang, H.Y., 2011. Extensive and coordinated transcription of noncoding RNAs within cell-cycle promoters. *Nature genetics*, **43**(7), pp. 621-629.

Ioannidis, J.P.A., Allison, D.B., Ball, C.A., Coulibaly, I., Cui, X., Culhane, A.C., Falchi, M., Furlanello, C., Game, L., Jurman, G., Mangion, J., Mehta, T., Nitzberg, M., Page, G.P., Petretto, E. And Van Noort, V., 2009. Repeatability of published microarray gene expression analyses. *Nature genetics*, **41**(2), pp. 149-155.

Iwakura, Y., Ishigame, H., Saijo, S. And Nakae, S., 2011. Functional Specialization of Interleukin-17 Family Members. *Immunity*, **34**(2), pp. 149-162.

Jeon, J., Oh, H., Lee, G., Ryu, J., Rhee, J., Kim, J., Chung, K., Song, W., Chun, C. And Chun, J., 2011. Cytokine-like 1 Knock-out Mice (Cyt11(-/-)) Show Normal Cartilage and Bone Development but Exhibit Augmented Osteoarthritic Cartilage Destruction. *Journal of Biological Chemistry*, **286**(31), pp. 27206-27213.

Jiang, X., Kallberg, H., Arlestig, L., Rantapaa-Dahlqvist, S., Klareskog, L., Alfredsson, L. And Padyukov, L., 2013. OP0052 A Dense Mapping of HLA Region for Study of

Interaction with Smoking in the Development of Rheumatoid Arthritis. *Annals of the Rheumatic Diseases*, **72**, pp. A67-A67.

Johnston, A., Gudjonsson, J.E., Sigmundsdottir, H., Runar Ludviksson, B. And Valdimarsson, H., 2005. The anti-inflammatory action of methotrexate is not mediated by lymphocyte apoptosis, but by the suppression of activation and adhesion molecules. *Clinical Immunology*, **114**(2), pp. 154-163.

Jordan, C.G.M., Rashidi, M.R., Laljee, H., Clarke, S.E., Brown, J.E. And Beedham, C., 1999. Aldehyde Oxidase-catalysed Oxidation of Methotrexate in the Liver of Guinea-pig, Rabbit and Man. *Journal of Pharmacy and Pharmacology*, **51**(4), pp. 411-418.

Katoh, Y. And Katoh, M., 2006. Comparative integromics on Angiopoietin family members. *International journal of molecular medicine*, **17**(6), pp. 1145-1149.

Ketron, A.C., Gordon, O.N., Schneider, C. And Osheroff, N., 2013. Oxidative Metabolites of Curcumin Poison Human Type II Topoisomerases. *Biochemistry*, **52**(1), pp. 221-227.

Keystone, E.C., Kavanaugh, A.F., Sharp, J.T., Tannenbaum, H., Hua, Y., Teoh, L.S., Fischkoff, S.A. And Chartash, E.K., 2004. Radiographic, clinical and functional outcomes of treatment with adalimumab (a human anti-tumor necrosis factor monoclonal antibody) in patients with active rheumatoid arthritis receiving concomitant methotrexate therapy: A randomized, placebo-controlled, 52-week trial. *Arthritis & Rheumatism*, **50**(5), pp. 1400-1411.

Khan, S., Shehzad, O., Jin, H., Woo, E., Kang, S.S., Baek, S.W., Kim, J. And Kim, Y.S., 2012. Anti-inflammatory Mechanism of 15,16-Epoxy-3 alpha-hydroxylabda-

8,13(16),14-trien-7-one via Inhibition of LPS-Induced Multicellular Signaling Pathways. *Journal of natural products*, **75**(1), pp. 67-71.

Kim, J., Kim, H., Suk, K. And Lee, W., 2010. Activation of CD147 with Cyclophilin A Induces the Expression of IFITM1 through ERK and PI3K in THP-1 Cells. *Mediators of inflammation*, pp. 821-940.

Kim, J.Y., Cho, T.J., Woo, B.H., Choi, K.U., Lee, C.H., Ryu, M.H. And Park, H.R., 2012. Curcumin-induced autophagy contributes to the decreased survival of oral cancer cells. *Archives of Oral Biology*, **57**(8), pp. 1018-1025.

Kim, M.S., Lee, J., Oh, T., Moon, Y., Chang, E., Seo, K.S., Hoehn, B.D., An, S. And Lee, J., 2012. Genome-wide identification of OTP gene as a novel methylation marker of breast cancer. *Oncology reports*, **27**(5), pp. 1681-1688.

Klarenbeek, N.B., Guler-Yuksel, M., Van, D.K., Han, K.H., Runday, H.K., Kerstens, P.J.S.M., Seys, P.E.H., Huizinga, T.W.J., Dijkmans, B.A.C. And Allaart, C.F., 2011. The impact of four dynamic, goal-steered treatment strategies on the 5-year outcomes of rheumatoid arthritis patients in the BeSt study. *Annals of the Rheumatic Diseases*, **70**(6), pp. 1039-1046.

Kooloos, W.M., Wessels, J.A.M., Van, D.S., Allaart, C.F., Huizinga, T.W.J. And Guchelaar, H., 2010. Functional polymorphisms and methotrexate treatment outcome in recent-onset rheumatoid arthritis. *Pharmacogenomics*, **11**(2), pp. 163-175.

Kudo, O., Sabokbar, A., Pocock, A., Itonaga, I., Fujikawa, Y. And Athanasou, N.A., 2003. Interleukin-6 and interleukin-11 support human osteoclast formation by a RANKL-independent mechanism. *Bone*, **32**, pp. 1-7.

Lee, S.J., Jang, B.C., Lee, S.W., Yang, Y.I., Suh, S.I., Park, Y.M., Oh, S., Shin, J.G., Yao, S., Chen, L.P. And Choi, I.H., 2006. Interferon regulatory factor-1 is prerequisite to the constitutive expression and IFN-gamma-induced upregulation of B7-H1 (CD274). *FEBS letters*, **580**(3), pp. 755-762.

Levin and Almog, 2015. *Compliance with Methotrexate Treatment for Ectopic Pregnancy*. Springer Science + Business Media.

Li, P. And Schwarz, E.M., 2003. The TNF- α transgenic mouse model of inflammatory arthritis. *Springer seminars in immunopathology*, **25**(1), pp. 19-33.

Lin, 2007. *Molecular Targets Of Curcumin*. Springer Science + Business Media.

Linn-Rasker, S., Van Der Helm-Van Mil, A.H.M., Breedveld, F.C. And Huizinga, T.W.J., 2007. Arthritis of the large joints--in particular, the knee--at first presentation is predictive for a high level of radiological destruction of the small joints in rheumatoid arthritis. *Annals of the Rheumatic Diseases*, **66**(5), pp. 646-650.

Lutzky, V., Hannawi, S. And Thomas, R., 2007. Cells of the synovium in rheumatoid arthritis. Dendritic cells. *Arthritis Res Ther*, **9**(4), pp. 219.

Maia, M., De Vriese, A., Janssens, T., Moons, M., Van Landuyt, K., Tavernier, J., Lories, R.J. And Conway, E.M., 2010. CD248 and Its Cytoplasmic Domain A Therapeutic Target for Arthritis. *Arthritis and Rheumatism*, **62**(12), pp. 3595-3606.

Majithia, V. and Geraci, S.A., 2007. Rheumatoid Arthritis: Diagnosis and Management. *The American Journal of Medicine*, **120**(11), pp. 936-939.

McInnes, I.B. And Schett, G., 2011. The Pathogenesis of Rheumatoid Arthritis. *New England Journal of Medicine*, **365**(23), pp. 2205-2219.

Montesinos, M.C., Takedachi, M., Thompson, L.F., Wilder, T.F., Fernandez, P. And Cronstein, B.N., 2007. The antiinflammatory mechanism of methotrexate depends on extracellular conversion of adenine nucleotides to adenosine by ecto-5'-nucleotidase - Findings in a study of ecto-5'-nucleotidase gene-deficient mice. *Arthritis and Rheumatism*, **56**(5), pp. 1440-1445.

Nagai, T., Sato, M., Kobayashi, M., Yokoyama, M., Tani, Y. And Mochida, J., 2014. Bevacizumab, an anti-vascular endothelial growth factor antibody, inhibits osteoarthritis. *Arthritis Res Ther*, **16**(5), pp. 427.

Nakashima, T. And Takayanagi, H., 2009. Osteoimmunology: Crosstalk Between the Immune and Bone Systems. *Journal of clinical immunology*, **29**(5), pp. 555-567.

Nalbandian, A., Crispãñ, J.C. And Tsokos, G.C., 2009. Interleukin-17 and systemic lupus erythematosus: current concepts. *Clinical & Experimental Immunology*, **157**(2), pp. 209-215.

Nam, J.L., Winthrop, K.L., Van Vollenhoven, R.F., Pavelka, K., Valesini, G., Hensor, E.M.A., Worthy, G., Landewe, R., Smolen, J.S., Emery, P. And Buch, M.H., 2010. Current evidence for the management of rheumatoid arthritis with biological disease-modifying antirheumatic drugs: a systematic literature review informing the EULAR recommendations for the management of RA. *Annals of the Rheumatic Diseases*, **69**(6), pp. 976-986.

Neogi, T., Aletaha, D., Silman, A.J., Naden, R.L., Felson, D.T., Aggarwal, R., Bingham, C.O., Birnbaum, N.S., Burmester, G.R., Bykerk, V.P., Cohen, M.D., Combe, B., Costenbader, K.H., Dougados, M., Emery, P., Ferraccioli, G., Hazes, J.M.W., Hobbs, K., Huizinga, T.W.J., Kavanaugh, A., Kay, J., Khanna, D., Kvien, T.K., Laing, T., Liao, K., Mease, P., Mă©Nard, H.A., Moreland, L.W., Nair, R., Pincus, T., Ringold, S., Smolen, J.S., Stanislawska-Biernat, E., Symmons, D., Tak, P.P., Upchurch, K.S., Vencovský J., Wolfe, F. And Hawker, G., 2010. The 2010 American College of Rheumatology/European League Against Rheumatism classification criteria for rheumatoid arthritis: Phase 2 methodological report. *Arthritis & Rheumatism*, **62**(9), pp. 2582-2591.

Nesher, G., Mates, M. And Zevin, S., 2003. Effect of caffeine consumption on efficacy of methotrexate in rheumatoid arthritis. *Arthritis and Rheumatism*, **48**(2), pp. 571-572.

Nowell, M.A., Richards, P.J., Fielding, C.A., Ognjanovic, S., Topley, N., Williams, A.S., Bryant-Greenwood, G. And Jones, S.A., 2006. Regulation of pre-B cell colony-enhancing factor by STAT-3-dependent interleukin-6trans-signaling: Implications in the pathogenesis of rheumatoid arthritis. *Arthritis Rheum*, **54**(7), pp. 2084-2095.

Ogawa, Y., Ohtsuki, M., Uzuki, M., Sawai, T., Onozawa, Y., Nakayama, J., Yonemura, A., Kimura, T. And Matsuno, H., 2003. Suppression of osteoclastogenesis in rheumatoid arthritis by induction of apoptosis in activated CD4+ T cells. *Arthritis & Rheumatism*, **48**(12), pp. 3350-3358.

Orimo, A., Gupta, P.B., Sgroi, D.C., Arenzana-Seisdedos, F., Delaunay, T., Naeem, R., Carey, V.J., Richardson, A.L. And Weinberg, R.A., 2005. Stromal fibroblasts present in

invasive human breast carcinomas promote tumor growth and angiogenesis through elevated SDF-1/CXCL12 secretion. *Cell*, **121**(3), pp. 335-348.

Pablos, J.L., Santiago, B., Galindo, M., Torres, C., Brehmer, M.T., Blanco, F.J. And Garcia-Lazaro, F.J., 2003. Synoviocyte-derived CXCL12 is displayed on endothelium and induces angiogenesis in rheumatoid arthritis. *Journal of Immunology*, **170**(4), pp. 2147-2152.

Pae, H., Jeong, G., Jeong, S., Kim, H.S., Kim, S., Kim, Y., Yoo, S., Kim, H. And Chung, H., 2007. Roles of heme oxygenase-1 in curcumin-induced growth inhibition in rat smooth muscle cells. *Experimental and Molecular Medicine*, **39**(3), pp. 267-277.

Panichi, V., Migliori, M., De Pietro, S., Taccola, D. andreini, B., Metelli, M.R., Giovannini, L. And Palla, R., 2000. The link of biocompatibility to cytokine production. *Kidney Int*, **58**, pp. 96-103.

Parri, M., Pietrovito, L., Grandi, A., Campagnoli, S., De Camilli, E., Bianchini, F., Marchio, S., Bussolino, F., Jin, B., Sarmientos, P., Grandi, G., Viale, G., Pileri, P., Chiarugi, P. And Grifantini, R., 2014. Angiopoietin-like 7, a novel pro-angiogenic factor over-expressed in cancer. *Angiogenesis*, **17**(4), pp. 881-896.

Patel, A.M. And Moreland, L.W., 2009. Methotrexate versus combination methotrexate and etanercept for rheumatoid arthritis. *Curr Rheumatol Rep*, **11**(5), pp. 309-310.

Picone, P., Nuzzo, D., Caruana, L., Messina, E., Scafidi, V. And Di Carlo, M., 2014. Curcumin induces apoptosis in human neuroblastoma cells via inhibition of AKT and Foxo3a nuclear translocation. *Free Radic Res*, **48**(12), pp. 1397-1408.

Puel, A., Ziegler, S., Buckley, R. And Leonard, W., 1998. Defective IL7R expression in T-B+NK+ severe combined immunodeficiency. *Nature genetics*, **20**(4), pp. 394-397.

Quinn, M.A., Conaghan, P.G., O'connor, P.J., Karim, Z., Greenstein, A., Brown, A., Brown, C., Fraser, A., Jarret, S. And Emery, P., 2005. Very early treatment with infliximab in addition to methotrexate in early, poor-prognosis rheumatoid arthritis reduces magnetic resonance imaging evidence of synovitis and damage, with sustained benefit after infliximab withdrawal: Results from a twelve-month randomized, double-blind, placebo-controlled trial. *Arthritis Rheum*, **52**(1), pp. 27-35.

Rabe, B., Chalaris, A., Adam, N., Paliga, K., Lange, H., Laskay, T., Fielding, C.A., Waetzig, G.H., Seegert, D., Williams, A.S., Jones, S.A., Sina, C., Rose-John, S. And Scheller, J., 2008. The role of IL6-transsignaling in acute and chronic inflammation. *Cytokine*, **43**(3), pp. 244.

Ramakers, B.P., Wever, K.E., Kox, M., Van, D.B., Mbuyi, F., Rongen, G., Masereeuw, R., Van, D.H., Smits, P., Riksen, N.P. And Pickkers, P., 2012. How systemic inflammation modulates adenosine metabolism and adenosine receptor expression in humans in vivo. *Critical Care Medicine*, **40**(9), pp. 2609-2616.

Ranganathan, P. And Mcleod, H.L., 2006. Methotrexate pharmacogenetics: The first step toward individualized therapy in rheumatoid arthritis. *Arthritis Rheum*, **54**(5), pp. 1366-1377.

Rao, R.N., Naidu, C.G., Prasad, K.G., Santhakumar, B. And Saida, S., 2013. Development and validation of a stability indicating assay of doxofylline by RP-HPLC: ESI-MS/MS, 1H and 13C NMR spectroscopic characterization of degradation products and process

related impurities. *Journal of pharmaceutical and biomedical analysis*, **78–79**, pp. 92-99.

Robinson, L., Sharrow, A.C., Yaroslavskiy, B.B. And Blair, H.C., 2006. Osteoclastic differentiation of monocytes is inhibited by non-transcriptional effects of estrogen mediated by BCAR1. *Blood*, **108**(11), pp. 372A-372A.

Rosner, M.H., Ronco, C. And Okusa, M.D., 2012. The Role of Inflammation in the Cardio-Renal Syndrome: A Focus on Cytokines and Inflammatory Mediators. *Seminars in nephrology*, **32**(1), pp. 70-78.

Rustin, G.J., Booth, M., Dent, J., Salt, S., Rustin, F. And Bagshawe, K.D., 1984. Pregnancy after cytotoxic chemotherapy for gestational trophoblastic tumours. *BMJ*, **288**(6411), pp. 103-106.

Sabry, S.M., Abdel-Hady, M., Elsayed, M., Fahmy, O.T. And Maher, H.M., 2003. Study of stability of methotrexate in acidic solution Spectrofluorimetric determination of methotrexate in pharmaceutical preparations through acid-catalyzed degradation reaction. *Journal of pharmaceutical and biomedical analysis*, **32**(3), pp. 409-423.

Sattar, N., 2003. Explaining How "High-Grade" Systemic Inflammation Accelerates Vascular Risk in Rheumatoid Arthritis. *Circulation*, **108**(24), pp. 2957-2963.

Schett, G., Zwerina, J. And David, J.P., 2008. The role of Wnt proteins in arthritis. *Nature Clinical Practice Rheumatology*, **4**(9), pp. 473-480.

Schoels, M., Wong, J., Scott, D.L., Zink, A., Richards, P., Landewe, R., Smolen, J.S. And Aletaha, D., 2010. Economic aspects of treatment options in rheumatoid arthritis: a systematic literature review informing the EULAR recommendations for the

management of rheumatoid arthritis. *Annals of the Rheumatic Diseases*, **69**(6), pp. 995-1003.

Schroeder, A., Mueller, O., Stocker, S., Salowsky, R., Leiber, M., Gassmann, M., Lightfoot, S., Menzel, W., Granzow, M. And Ragg, T., 2006. The RIN: an RNA integrity number for assigning integrity values to RNA measurements. *BMC molecular biology*, **7**, pp. 3.

Schuppan, D., Ruehl, M., Somasundaram, R. And Hahn, E.G., 2001. Matrix as a modulator of hepatic fibrogenesis. *Seminars in liver disease*, **21**(3), pp. 351-372.

Shankar, S., Chen, Q., Sarva, K., Siddiqui, I. And Srivastava, R.K., 2007. Curcumin enhances the apoptosis-inducing potential of TRAIL in prostate cancer cells: molecular mechanisms of apoptosis, migration and angiogenesis. *Journal of molecular signaling*, **2**, pp. 10-10.

Shervington, L.A., Abba, M., Hussain, B. And Donnelly, J., 2005. The simultaneous separation and determination of five quinolone antibiotics using isocratic reversed-phase HPLC: Application to stability studies on an ofloxacin tablet formulation. *Journal of pharmaceutical and biomedical analysis*, **39**(3-4), pp. 769-775.

Shervington, L., Patil, H. And Shervington, A., 2015. Could the anti-chaperone ver155008 replace temozolomide for glioma treatment. *Journal of Cancer*, **6**(8), pp. 786-794.

Shin, H.K., Kim, J., Lee, E.J. And Kim, S.H., 2009. Inhibitory effect of curcumin on motility of human oral squamous carcinoma YD-10B cells via suppression of ERK and NF- κ B activations. *Phytother.Res.*,**24**(4), pp. 577-582.

Smolen, J.S., Aletaha, D., Bijlsma, J.W.J., Breedveld, F.C., Boumpas, D., Burmester, G., Combe, B., Cutolo, M., De Wit, M., Dougados, M., Emery, P., Gibofsky, A., Gomez-Reino, J., Haraoui, B., Kalden, J., Keystone, E.C., Kvien, T.K., McInnes, I., Martin-Mola, E., Montecucco, C., Schoels, M. And Van, D.H., 2010. Treating rheumatoid arthritis to target: recommendations of an international task force. *Annals of the Rheumatic Diseases*, **69**(4), pp. 631-637.

Smolen, J.S. And Aletaha, D., 2015. Rheumatoid arthritis therapy reappraisal: strategies, opportunities and challenges. *Nat Rev Rheumatol*, **11**(5), pp. 276-289.

Smolen, J.S., Nash, P., Durez, P., Hall, S., Ilivanova, E., Irazoque-Palazuelos, F., Miranda, P., Park, M., Pavelka, K., Pedersen, R., Szumski, A., Hammond, C., Koenig, A.S. And Vlahos, B., 2013. Maintenance, reduction, or withdrawal of etanercept after treatment with etanercept and methotrexate in patients with moderate rheumatoid arthritis (PRESERVE): a randomised controlled trial. *The Lancet*, **381**(9870), pp. 918-929.

Song, K., Peng, S., Sun, Z., Li, H. And Yang, R., 2011. Curcumin suppresses TGF- β signaling by inhibition of TGIF degradation in scleroderma fibroblasts. *Biochemical and biophysical research communications*, **411**(4), pp. 821-825.

Spurlock, C.F., Gass, H.M., Bryant, C.J., Wells, B.C., Olsen, N.J. And Aune, T.M., 2014. Methotrexate-mediated inhibition of nuclear factor κ B activation by distinct pathways in T cells and fibroblast-like synoviocytes. *Rheumatology*, **54**(1), pp. 178-187.

Stamp, L.K., Barclay, M.L., O'donnell, J.L., Zhang, M., Drake, J., Frampton, C. And Chapman, P.T., 2011. Effects of Changing from Oral to Subcutaneous Methotrexate on Red Blood Cell Methotrexate Polyglutamate Concentrations and Disease Activity in Patients with Rheumatoid Arthritis. *The Journal of rheumatology*, **38**(12), pp. 2540-2547.

Staud, R., 2009. The overestimation of disease activity in patients with rheumatoid arthritis and concomitant fibromyalgia. *Curr Rheumatol Rep*, **11**(6), pp. 390-391.

Strimpakos, A.S. And Sharma, R.A., 2008. Curcumin: Preventive and therapeutic properties in laboratory studies and clinical trials. *Antioxidants & Redox Signaling*, **10**(3), pp. 511-545.

Symmons, D.P.M., 2003. Environmental factors and the outcome of rheumatoid arthritis. *Best Practice & Research Clinical Rheumatology*, **17**(5), pp. 717-727.

Taberner, M., Scott, K.F., Weininger, L., Mackay, C.R. And Rolph, M.S., 2005. Overlapping gene expression profiles in rheumatoid fibroblast-like synoviocytes induced by the proinflammatory cytokines interleukin-1 β and tumor necrosis factor. *Inflammation Research*, **54**(1), pp. 10-16.

Tamai, K., Nakamura, M., Mizuma, M., Mochizuki, M., Yokoyama, M., Endo, H., Yamaguchi, K., Nakagawa, T., Shiina, M., Unno, M., Muramoto, K., Sato, I., Satoh, K., Sugamura, K. And Tanaka, N., 2014. Suppressive expression of CD274 increases tumorigenesis and cancer stem cell phenotypes in cholangiocarcinoma. *Cancer Science*, **105**(6), pp. 667-674.

Tanaka, J., Irie, T., Yamamoto, G., Yasuhara, R., Isobe, T., Hokazono, C., Tachikawa, T., Kohno, Y. And Mishima, K., 2015. ANGPTL4 regulates the metastatic potential of oral squamous cell carcinoma. *Journal of Oral Pathology & Medicine*, **44**(2), pp. 126-133.

Tapia, E., Soto, V., Mariana Ortiz-Vega, K., Zarco-Marquez, G., Molina-Jijon, E., Cristobal-Garcia, M., Santamaria, J., Ramses Garcia-Nino, W., Correa, F., Zazueta, C. And Pedraza-Chaverri, J., 2012. Curcumin Induces Nrf2 Nuclear Translocation and Prevents Glomerular Hypertension, Hyperfiltration, Oxidant Stress and the Decrease in Antioxidant Enzymes in 5/6 Nephrectomized Rats. *Oxidative Medicine and Cellular Longevity*, , pp. 269039.

Tomczak, A. And Pisabarro, M.T., 2011. Identification of CCR2-binding features in Cyt11 by a CCL2-like chemokine model. *Proteins-Structure Function and Bioinformatics*, **79**(4), pp. 1277-1292.

Tønnesen, H.H., Másson, M. And Loftsson, T., 2002. Studies of curcumin and curcuminoids. XXVII. Cyclodextrin complexation: solubility, chemical and photochemical stability. *International journal of pharmaceutics*, **244**(1–2), pp. 127-135.

Van Baarsen, L.,G.M., Wijbrandts, C.A., Rustenburg, F., Cantaert, T., Van Der Pouw Kraan, Tineke,C.T.M., Baeten, D.L., Dijkmans, B.A.C., Tak, P.P. And Verweij, C.L., 2010. Regulation of IFN response gene activity during infliximab treatment in rheumatoid arthritis is associated with clinical response to treatment. *Arthritis Research & Therapy*, **12**(1), pp. 1-10.

Van Dieren, J.M., Kuipers, E.J., Samsom, J.N., Nieuwenhuis, E.E. And Van, D.W., 2006. Revisiting the immunomodulators tacrolimus, methotrexate and mycophenolate

mofetil: Their mechanisms of action and role in the treatment of IBD. *Inflammatory bowel diseases*, **12**(4), pp. 311-327.

Van Roon, J.A.G., Glaudemans, K.A.F.M., Bijlsma, J.W.J. And Lafeber, F.P.J.G., 2003. Interleukin 7 stimulates tumour necrosis factor alpha and Th1 cytokine production in joints of patients with rheumatoid arthritis. *Annals of the Rheumatic Diseases*, **62**(2), pp. 113-119.

Walsh, N.C., Crotti, T.N., Goldring, S.R. And Gravallese, E.M., 2005. Rheumatic diseases: the effects of inflammation on bone. *Immunological reviews*, **208**, pp. 228-251.

Weinblatt, M.E., Kremer, J.M., Coblyn, J.S., Maier, A.L., Helfgott, S.M., Morrell, M., Byrne, V.M., Kaymakjian, M.V. And Strand, V., 1999. Pharmacokinetics, safety and efficacy of combination treatment with methotrexate and leflunomide in patients with active rheumatoid arthritis. *Arthritis & Rheumatism*, **42**(7), pp. 1322-1328.

Xu, A., Lam, M., Chan, K., Wang, Y., Zhang, J., Hoo, R., Xu, J., Chen, B., Chow, W., Tso, A. And Lam, K., 2005. Angiotensin-like protein 4 decreases blood glucose and improves glucose tolerance but induces hyperlipidemia and hepatic steatosis in mice. *Proceedings of the National Academy of Sciences of the United States of America*, **102**(17), pp. 6086-6091.

Yan, G., Graham, K. And Lanza-Jacoby, S., 2012. Curcumin enhances the anticancer effects of trichostatin a in breast cancer cells. *Mol.Carcinog.*, **52**(5), pp. 404-411.

Zhang, H., Ruan, Z. And Sang, W., 2011. HDAC1/NF kappa B Pathway Is Involved in Curcumin Inhibiting of Tat-Mediated Long Terminal Repeat Transactivation. *Journal of cellular physiology*, **226**(12), pp. 3385-3391.

Zuvich, R.L., Mccauley, J.L., Oksenberg, J.R., Sawcer, S.J., De Jager, P.L., Aubin, C., Cross, A.H., Piccio, L., Aggarwal, N.T., Evans, D., Hafler, D.A., Compston, A., Hauser, S.L., Pericak-Vance, M.A., Haines, J.L. And Int Multiple Sclerosis Genetics Co, 2010. Genetic variation in the IL7RA/IL7 pathway increases multiple sclerosis susceptibility. *Human genetics*, **127**(5), pp. 525-535.

CHAPTER 7

APPENDIX

Table 7-1 Primer design of *ANGPTL7* gene using PrimerBlast.

	Sequence (5'->3')	Template strand	Length	Start	Stop	Tm	GC%	Self complementarity	Self 3' complementarity
Forward primer	GTGTAGAGATGGAGGACTGGG	Plus	21	950	970	58.96	57.14	2.00	0.00
Reverse primer	ATACTGGAGGGCGTCGTTTC	Minus	19	1086	1068	59.19	57.89	3.00	2.00

Table 7-2 Primer design of *CD248* gene using PrimerBlast.

	Sequence (5'->3')	Template strand	Length	Start	Stop	Tm	GC%	Self complementarity	Self 3' complementarity
Forward primer	CCATCAAATCTCTGTGCCTGC	Plus	21	1826	1846	59.60	52.38	2.00	2.00
Reverse primer	GTCTGGTTAGTGGGGCTCTG	Minus	20	1906	1887	59.75	60.00	2.00	1.00

Table 7-3 Primer design of *CH25H* gene using PrimerBlast.

	Sequence (5'->3')	Template strand	Length	Start	Stop	Tm	GC%	Self complementarity	Self 3' complementarity
Forward primer	CACCCTGACTTCTCGCCATC	Plus	20	242	261	60.46	60.00	2.00	0.00
Reverse primer	CACGGGGAACACAAACATCAC	Minus	21	328	308	60.00	52.38	2.00	0.00

Table 7-4 Primer design of *CXCL12* gene using PrimerBlast.

	Sequence (5'->3')	Template strand	Length	Start	Stop	Tm	GC%	Self complementarity	Self 3' complementarity
Forward primer	GACAAGTGTGCATTGACCCG	Plus	20	295	314	59.76	55.00	4.00	2.00
Reverse primer	CTCATGGTTAAGGCCCCCTC	Minus	20	467	448	59.82	60.00	4.00	1.00

Table 7-5 Primer design of *CYTL1* gene using PrimerBlast.

	Sequence (5'->3')	Template strand	Length	Start	Stop	Tm	GC%	Self complementarity	Self 3' complementarity
Forward primer	AGATCACCCGCGACTTCAAC	Plus	20	135	154	60.39	55.00	4.00	1.00
Reverse primer	GTACAGCCTGGGCAGGTATC	Minus	20	211	192	59.89	60.00	6.00	2.00

Table 7-6 Primer design of *IFITM1* gene using PrimerBlast.

	Sequence (5'->3')	Template strand	Length	Start	Stop	Tm	GC%	Self complementarity	Self 3' complementarity
Forward primer	CGCCAAGTGCCTGAACATC	Plus	19	423	441	59.50	57.89	2.00	1.00
Reverse primer	GTCACAGAGCCGAATACCACT	Minus	21	509	489	59.80	52.38	3.00	2.00

Table 7-7 Primer design of *IL7* gene using PrimerBlast.

	Sequence (5'->3')	Template strand	Length	Start	Stop	Tm	GC%	Self complementarity	Self 3' complementarity
Forward primer	GTGACTATGGGCGGTGAGAG	Plus	20	529	548	59.90	60.00	3.00	0.00
Reverse primer	GCTACTGGCAACAGAACAAGG	Minus	21	669	649	59.46	52.38	3.00	0.00

Table 7-8 Primer design of *COL14A1* gene using PrimerBlast.

	Sequence (5'->3')	Template strand	Length	Start	Stop	Tm	GC%	Self complementarity	Self 3' complementarity
Forward primer	AGACGAGGTGGTGGTAGATG	Plus	20	1455	1474	58.52	55.00	2.00	0.00
Reverse primer	AGCAGTGTGGGCATAGATTG	Minus	20	1560	1541	57.95	50.00	3.00	2.00

Table 7-9 Primer design of *BCAR4* gene using PrimerBlast.

	Sequence (5'->3')	Template strand	Length	Start	Stop	Tm	GC%	Self complementarity	Self 3' complementarity
Forward primer	ACCAGTGACCTTGAGTGAAC	Plus	20	630	649	57.38	50.00	3.00	2.00
Reverse primer	CTTGGGTGGGGATAGTGATTG	Minus	21	713	693	58.06	52.38	2.00	0.00

Table 7-10 Primer design of *CD274* gene using PrimerBlast.

	Sequence (5'->3')	Template strand	Length	Start	Stop	Tm	GC%	Self complementarity	Self 3' complementarity
Forward primer	CTATGGTGGTGCCGACTACA	Plus	20	459	478	59.18	55.00	3.00	2.00
Reverse primer	AGGACTTGATGGTCACTGCT	Minus	20	632	613	58.64	50.00	3.00	1.00

Table 7-11 Primer design of *RELT* gene using PrimerBlast.

	Sequence (5'->3')	Template strand	Length	Start	Stop	Tm	GC%	Self complementarity	Self 3' complementarity
Forward primer	AACTTGCGGTGTGAGGG	Plus	17	134	150	57.01	58.82	3.00	0.00
Reverse primer	CATAAGGAAGCAGGACAGGG	Minus	20	272	253	57.66	55.00	2.00	0.00

Table 7-12 Primer design of *HSPA6* gene using PrimerBlast.

	Sequence (5'->3')	Template strand	Length	Start	Stop	Tm	GC%	Self complementarity	Self 3' complementarity
Forward primer	AATCTGTCGCCCCATCTTCTC	Plus	21	2222	2242	59.86	52.38	2.00	0.00
Reverse primer	GCCCATAGCATAGCCCTGAC	Minus	20	2395	2376	60.32	60.00	2.00	1.00

Table 7-13 Primer design of *OTP* gene using PrimerBlast.

	Sequence (5'->3')	Template strand	Length	Start	Stop	Tm	GC%	Self complementarity	Self 3' complementarity
Forward primer	CCTTGGTTGTTTTGTGGTGGTC	Plus	22	2281	2302	60.42	50.00	2.00	1.00
Reverse primer	CAGGGTTGTAGATGTCCGAGTG	Minus	22	2371	2350	60.42	54.55	3.00	0.00

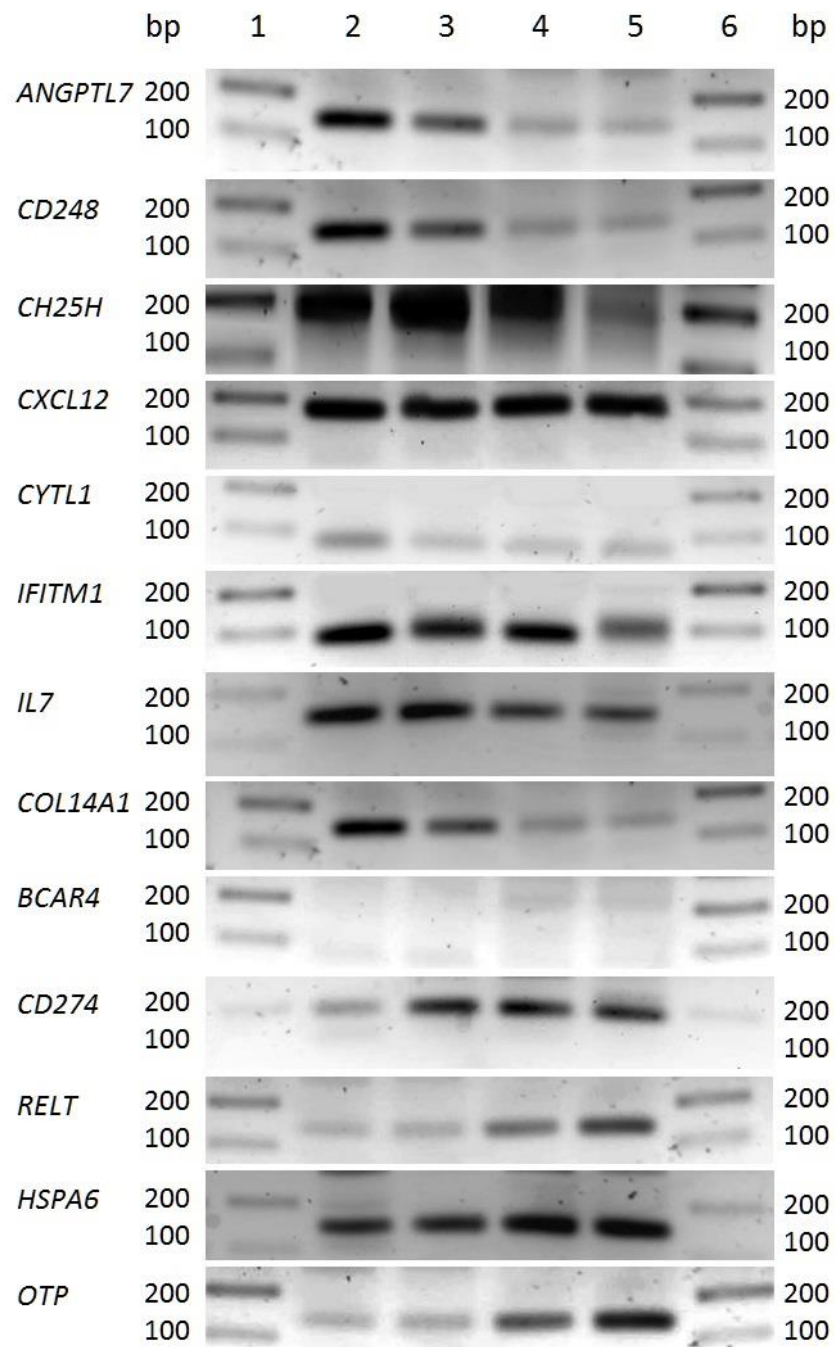


Figure 7-1 Agarose gel electrophoresis of validated 13 genes. Lane 1 and 6 represent the 100 bp molecular marker, lane 2 represents Untreated HFLS-RA cells, lane 3 represents MTX treated HFLS-RA cells, lane 4 represents curcumin treated HFLS-RA cells and lane 5 represents HFLS-RA cells treated with both MTX and curcumin.